COMMUNITY AND INFRASTUCTURE RESILIENCE PREDICTION AND MANAGEMENT IN A CHANGING CLIMATE

COMMUNITY AND INFRASTRUCTURE RESILIENCE PREDICTION AND MANAGEMENT IN A CHANGING CLIMATE

By

Moustafa Naiem Abdel-Mooty

B.Sc., M.Sc.

A Thesis Submitted to the School of Graduate Studies in Partial Fulfillment of the Requirements for the Degree

Doctor of Philosophy

Doctor of Philosophy (2023)	McMaster University
(Civil Engineering)	Hamilton, Ontario
TITLE:	Community and Infrastructure Resilience Prediction and Management in a Changing Climate
AUTHOR:	Moustafa Naiem Abdel-Mooty B.Sc., (Structural Engineering) M.Sc. (Civil Engineering) Cairo University, Egypt.
SUPERVISORS:	Dr. Wael El-Dakhakhni Dr. Paulin Coulibaly
NUMBER OF PAGES:	xxii, 283

To my wife, Merhan, my daughter, Malak

&

My parents.

Lay Abstract

Climate change poses the most pressing global challenge in recent history, with a vast impact on the functionality of the established communities in a multitude of ways, increasingly causing cascading infrastructure failures. This is aggravated by the expansive development of urban areas into exposed, hazard-prone areas, one of the costliest hazards being floods, with its increasing severity and frequency. This thesis aims at enhancing the climate-resilience of communities exposed to climate change-induced hazards, with a focus on flood risk, to develop realistic, proactive, resilience-informed risk management strategies. The thesis applies *i*) machine learning and data analytics to understand, quantify, and eventually predict the impact of climate change-induced flood risk, *ii*) descriptive analytics techniques to identify community and infrastructure vulnerabilities and exposure, *iii*) predictive analytics to predict future changes of community resilience until the year 2050. To operationalize its findings, the thesis also investigates and enhance the climate resilience of individual critical infrastructure systems and improve its risk management plans.

Abstract

Climate change poses the most pressing global challenge in recent history. The risks associated with climate change do not only pertain to the rise in temperature, but the accompanying changes in the meteorological and hydrological properties of the planet. Climate change's impact on the established communities is vast and visible, affecting the functionality of societies on a multitude of ways, and increasingly causing cascading failures and systemic risks (i.e., failures resulting from the interdependent nature of our society systems). This is aggravated by the expansive development of urban areas into exposed, hazard-prone regions. One of the costliest and most frequent hazards resulting from climate change is flood hazard, with its increasing severity and frequency due to the coupling of the aforementioned reasons. This thesis aims at enhancing the resilience of the exposed communities to climate change-induced hazards, with a focus on flood risk, to develop pertinent realistic, proactive, resilience-informed risk management plans. The thesis applies machine learning and data analytics to understand, quantify, and eventually predict climate change-induced flood risk. Descriptive analytics techniques were employed to understand the extent of flood risk on urban communities, resulting in a categorization of the different community responses to flood risk. This categorization is subsequently employed in developing predictive analysis, where global climate models are utilized to predict the changes of the resilience of the

exposed communities until the year 2050. Said studies, while revolutionary in nature, serve as a steppingstone in developing a comprehensive, proactive, global disaster management plan. Finally, the thesis narrows its scope by focusing on operationalizing the developed climate resilience methodology considering a single critical infrastructure network and enhances the climate resilience of its risk management plan, set, and operated by its asset owners and decision makers. The approaches developed herein were applied on different datasets for vulnerability identification, loss and resilience prediction, and policy improvement resulting in an overall climate resilience-informed enhancement of the current risk management practices.

Acknowledgement

Qur'an Ya-Sin 36:83 {So glory be to the One in Whose Hands is the authority over all things, and to Whom ˹alone˺ you will ˹all˺ be returned.}

First, I am grateful to Allah, the Almighty, the Most Gracious, and the Most Merciful for His blessing given to me during my study and in completing this thesis. Secondly, I would like to thank my main supervisor Prof. Wael El-Dakhakhni, I was lucky enough to be supervised by such an expert, I am indebted to him for his continuous support and guidance. I am extremely thankful for the kind of mentorship and friendship we have— empowering and enabling me to pursue my ideas, crazy as they may seem, with such dedicated support and enablement. His willingness to indulge my dreams are something I will always be grateful for. I am grateful for all I learned from him, and for the relationship that will, hopefully, last for years to come.

To my co-supervisor, Prof. Paulin Coulibaly, I am thankful for all your support, academic and otherwise, and the advice you have generously provided me over the years, supporting my research and providing valuable insights to steer me in the right direction. I would like to express my sincere gratitude to my committee members, Prof. Elkafi Hassini, and Prof. Michael Tait for their continuous guidance throughout the course of my doctoral degree. I would also like to acknowledge Dr. Ahmed Yosri and Dr. May Haggag for their help throughout my doctoral studies, their assistance with my research.

A special thanks goes to my friend, Dr. Eric Goforth, our conversations together since the beginning of this degree, and throughout the life-changing pandemic we experienced kept me grounded. Our weekly chats and updates kept me sane, and your pasta was a shining light in one of my darkest hours. Thank you. I am also grateful to all my friends here at McMaster, and in Egypt, for their continuous support which drove me to where I am today.

I am grateful to the Natural Science and Research Council of Canada (NSERC) for the financial support through the Vanier Canada Graduate Scholarship (Vanier – CGS), and the Michael Smith Foreign Study Supplement (MSFSS – CGS). I would also like to thank Mitacs for their funding through the Globalink program (Mitacs Globalink – UK Research and Innovation grant). A special thanks to my

second research group, the one I met and built a lasting relationship with at the University of Cambridge, through my stay at the Institute for Manufacturing, my Supervisor Prof. Ajith Kumar Parlikad, my friends and colleagues, the research associates' team: Dr. Manu Sasidharan, Dr. Manuel Herrera, Dr. Gocken Yilmaz, Dr. Nicola Moretta, and Dr. Mahrashi Dhada, and Yaniv Proselkov.

My Parents, Prof. Azza Saied, and Prof. Mohamed Abdel-Mooty, everything that I am, I am because of you, and everything that I ever hoped to be, is for you. You have given me a purpose in life, and everything that I accomplished, I accomplished for you, and because of you. You have shown me how to be a good person, despite my failures, and you have shown me how to become a better parent, a more capable researcher, and a better son. I owe my life to you. Thank you for your sacrifices. To my sisters, Sarah Naiem, and Yosra Naiem, without your support and bickering, I wouldn't have been where I am today. You helped shape me to the person I am today, so thank you, and may we always have each others' backs. To my brother-in-law, Dr. Ramy Fakhry, thank you for being there when I needed you, and for always supporting and cheering for me throughout the course of our degrees.

Finally, and most importantly, to my wife, *Merhan Radwan*. Words cannot begin to express how thankful I am for you, and for everything you have sacrificed, and for being there despite all my many failures. I would not be where I am without you. Your love and support throughout all the ups and downs have pushed me to continue this Ph.D., and to build a life together. Everything that I achieved; I did for you. Everything that God has given me, it was given to me for you. I am thankful for your partnership, and for every single second I got to spend with you, building our life, and our family. I love you beyond my capacity to express. Lastly, my daughter, *Malak Naiem Abdel-Mooty*, you are now the reason of my existence. I love you, and live for you now, and forever.

Table of Content

List of Figures

List of Tables

Declaration of Academic Achievement

This dissertation was prepared in accordance with the guidelines set by the school of graduate studies at McMaster University for sandwich thesis. The main chapters (chapter 2 through chapter 5) contain scholarly work that is either published, submitted, or currently in final preparation stages for submission. The work presented in this thesis in its entirety is carried out by the main author, Moustafa Naiem Abdel-Mooty, with the guidance and supervision of Prof. Wael El-Dakhakhni, and Prof. Paulin Coulibaly, with further editorial comments in Chapter 2 provided by Dr. Ahmed Yosri. Distinctly, Chapter 5 was prepared in partnership with the Asset Management team at the Institute for Manufacturing at the University of Cambridge, but the main work, modeling, draft preparation was conducted by the main author, Moustafa Naiem Abdel-Mooty. The original contributions of each author to each chapter is outlined herein:

Chapter 2 is based on published work in June 2021 in the International Journal of Disaster Risk Reduction:

Abdel-Mooty, Moustafa Naiem., Yosri, Ahmed, Coulibaly, Paulin, and El-dakhakhni, Wael. 2021. "Community Flood Resilience Categorization Framework." *Int. J. Disaster Risk Reduct.*, 61: 102349. Elsevier Ltd. https://doi.org/10.1016/j.ijdrr.2021.102349.

The main concept, analysis, modeling, visualization, and writing was conducted by Moustafa Naiem Abdel-Mooty. Dr. Ahmed Yosri and Dr. Wael El-

Dakhakhni refined the quality of the manuscript and provided editorial and conceptual guidance. Dr. Paulin Coulibaly provided technical feedback and editorial advice.

Chapter 3 is based on published work in July 2022 in the MDPI Water (Switzerland) journal:

Abdel-mooty, Moustafa Naiem, Coulibaly, Paulin, and El-dakhakhni, Wael. 2022. "Data-Driven Community Flood Resilience Prediction." *Water (Switzerland)*, 14 (13): 2120. https://doi.org/10.3390/w14132120.

The main concept, analysis, modeling, visualization, and writing was conducted by Moustafa Naiem Abdel-Mooty. Dr. Wael El-Dakhakhni refined the quality of the manuscript and provided editorial and conceptual guidance. Dr. Paulin Coulibaly provided technical feedback and editorial advice.

Chapter 4 is based on Submitted work in August 2022 in the "Nature Communications" journal, currently (as of January 2023) in second round of peer review:

Abdel-mooty, Moustafa Naiem; Coulibaly, Paulin; El-dakhakhni, Wael. "Interpretable Spatio-temporal Climate Change Impact on Flood Resilience" *Nature Communications*, Submitted Under Review: Submission: NCOMMS-22-35434

The main concept, analysis, modeling, visualization, and writing was

conducted by Moustafa Naiem Abdel-Mooty. Dr. Wael El-Dakhakhni refined the quality of the manuscript and provided editorial and conceptual guidance. Dr. Paulin Coulibaly provided technical feedback and editorial advice.

Chapter 5 is currently in final stages of preparation for submission (as of January 2023):

Abdel-mooty, Moustafa Naiem; Sasidharan, Manu; Herrera, Manuel; Parlikad, Ajith Kumar; Schooling, Jennifer; Coulibaly, Paulin and El-Dakhakhni, Wael. "Multi-Level Analysis for Bridge Management System Under Climate Induced Scour Risk"

The main concept, analysis, modeling, visualization, and writing was conducted by Moustafa Naiem Abdel-Mooty. Dr. Manu Sasidharan offered technical guidance and assisted in preparing the final draft, Dr. Manuel Herrera offered advise and editorial feedback, Dr. Jennifer Schooling, and Dr. Ajith Kumar Parlikad offered access to datasets and partners and provided guidance and feedback on the study. Dr Wael El-Dakhakhni refined the quality of the manuscript and provided editorial guidance. Dr. Paulin Coulibaly provided feedback and editorial advice.

Chapter 1 Introduction

1.1. MOTIVATION

In recent decades, flood events have increased to become (one of) the most frequent hydrological hazard (Lian et al. 2017; Wilby et al. 2007), causing the most damage to the livelihood of the residents of the exposed communities. As urbanization now increases towards flood-prone areas, it is also expected to increase the exposed communities by the year 2050, where 70% of the world's population will live in urban environments by then (NOAA 2019; da Silva et al. 2012). This increased flood exposure has steered the research community to adopt a more proactive approach to flood risk management. Over the span of the past three decades, the United States of America and Canada have witnessed a continuous increase in the frequency and magnitude of climate change-induced natural disasters. In 2016, the induced damage was estimated to be $8.6B in Canada, while the United States of America have suffered from flood events, as it is becoming one of the costliest and highest in occurrence of all climate change induced hazards, reaching an annual average of $8B (Gillet et al. 2019; Natural Resources Canada 2017; NOAA 2017, 2019). It is now evident that the effect of climate change is rapidly increasing, and costing billions of dollars annually, at an increasing rate (National Working Group

on Financial Risk of Flooding 2019). However, most physics-based categorization and analysis efforts have been focused on the hydraulic features of the flood hazard, considering aspects such as inundation depth, event duration, flow rate, and peak flow duration. These efforts tend to overlook the exposed community's natural response to these hazards, and its resilience when exposed to systemic system-level/interdependent climate-change induced risk.

To that end, understanding how different communities react to the imposed flood risk is imperative, leading to the development of tools to assess, quantify, and predict the changes of the communities' response to flood risk. In this chapter, a brief introduction on the concept of community resilience is presented, and how it ties with critical infrastructure climate resilience, and the applicability of data-driven methods within community resilience studies.

1.2. COMMUNITY RESILIENCE

The resilience of communities facing climatological hazards has been gaining a lot of attention in the research community over the past years. Since the gradual increase in the rate and magnitude of climate-change induced hazard, traditional risk management studies have been falling short in dealing with the increased impact, losses, and disruption to livelihoods of nations, ultimately driving the research community towards resilience-informed risk management studies, and the birth of what is now known as the field of "Community Resilience" (National

Institute of Standards and Technology 2020). While there has been numerous definitions of resilience in different fields, within the context of this thesis, Community Resilience defines the capacity of the system (i.e., community) to adapt to future hazards, quickly recover from disturbances back to a predefined state, albeit its original state, or a state of higher functionality (National Institute of Standards and Technology 2020). Resilience is also defined as the ability of a certain system to absorb external shock while maintaining functionality (i.e., avoid global failure) (Cimellaro et al. 2009; Murdock 2017). To understand, and therefore be able to quantify resilience, this thesis will look at resilience by its two characteristics; *Robustness and Rapidity*, enabled by its two means; *Redundancy, and Resourcefulness* (Bruneau et al. 2003). To that end, *Robustness* is the capacity of a system to absorb external shock while maintaining functionality. *Rapidity* is a measure of the system's ability to quickly recover to the predefined functionality state. These two characteristics are achieved through the system's tools to handle external disturbance (i.e., the two means of resilience), where: *Redundancy* is the system's inherent capacity to function by having replacement components to replace the failed ones, or components that are multi-functional and act as temporary replacement. Finally, *Resourcefulness* is the availability of different resource that aid in detecting disruptions and failures, and quickly acquire the necessary replacements to maintain functionality (Bruneau et al. 2003; Minsker et al. 2015; Murdock 2017).

To understand how these components act together to quantify resilience, Bruneau et al. and Holmes (Bruneau et al. 2003; Holmes 2011) introduced the concept shown in Figure 1-1. In this concept, a relationship between performance and functionality loss is introduced, where the area within the graph is inversely proportionate to the overall resilience of the system under investigation. The operationalization of this concept, and its utility in quantifying and understanding the resilience given different variables, is explained in more detail in chapters 2 and 3, where this concept was the steppingstone to the development of the resilience categories in face of flood hazard.

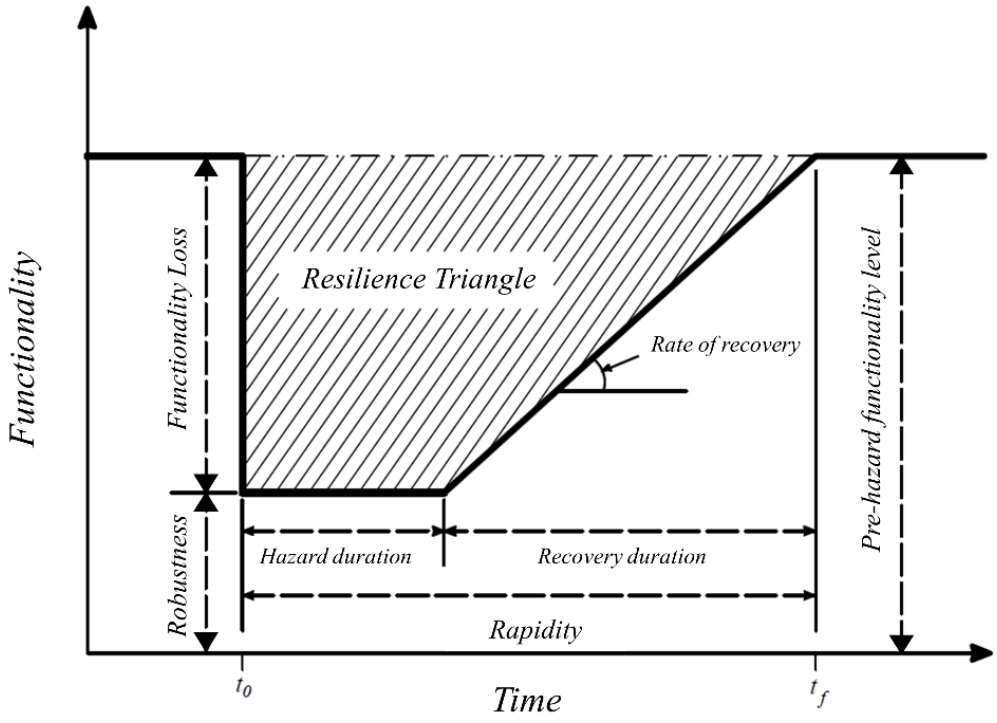

Figure 1-1: Simplified Resilience Graph.

1.3. DATA-DRIVEN RESILIENCE

Data-driven modelling is the utilization and analysis of real-life recorded data to develop meaningful insights. This can be done through numerous techniques through Descriptive analytics, or Predictive analytics (Abdel-mooty et al. 2022; Abdel-Mooty et al. 2021). While there have been numerous efforts in achieving the same objective with physics-based methods, the computational cost is too expensive that it renders said modeling almost impossible to achieve with the same output accuracy given the current computational capabilities. As such, in this thesis, data-driven methods have been adopted to bypass the complexity of physics-based methods to quantify and predict the different communities' resilience in face of climate change-induced risks. Over the years, numerous industries have been changing their strategies to incorporate data-driven methodologies into their decision-making, leveraging on data analytics to achieve said goals (Goforth et al. 2022b; a).

Machine Learning is a powerful tool that learns autonomously from the dataset presented to it, mimicking the human-based learning process, thus its name (Rodrigues and De la Riva 2014). Machine learning is usually divided into two types of learning: Supervised, and Unsupervised learning. While unsupervised learning deals with unlabelled data to discover and identify inherent patterns and features in the dataset (e.g., clustering algorithms) (Otterbach et al. 2017),

Supervised learning on the other hand, deals with the labeled dataset to develop patterns to classify and predict new input data (e.g., prediction algorithms) (Khalaf et al. 2018; Mosavi et al. 2018). Further details on the methodology, development, and utilization of both algorithms are provided in later chapters within this thesis.

1.4. THESIS ORGANIZATION

The thesis is written in the form of a "sandwich" thesis. As such, each chapter represents a stand-alone research article, with its own components (i.e., literature review, methodology, modelling, and references). To that end, it should be expected that chapters would share some of the references and literature background, since some articles complement each other to achieve an overarching research objective. As presented in later sections, Chapter 2 paves the way, and provides the cornerstone component to be used in the development of the framework presented in Chapter 3. While Chapter 4 builds on its predecessors by adding multiple layers to the frameworks, it acts as the culmination (i.e., complete picture) of the work presented in Chapters 2 and 3. Naturally, Chapters 2 and 3 share close discussions on solving a common challenge, which is predicting the effect of climate change on the exposed community's resilience. This discussion is further built upon in Chapter 4, where the employed methodology provides a solution for the problem, and multiple insights and discussions were presented.

Furthermore, all chapters fall under the general umbrella of evaluating climate change impact on community resilience. As presented in detail in upcoming sections, communities are formed by the operationalized interconnected, and interdependent, critical infrastructure networks. Hence, to operationalize the framework and methodology developed to achieve the research objective, the same train-of-thought was applied on individual critical infrastructure network to investigate, and enhance, its climate resilience. Specifically, this framework was applied on Railway Bridges on the Southeast of England, and the developed methodology and findings are presented in Chapter 5.

This section gives an overview of the content of the six chapters of the dissertation, and how the research objectives were achieved sequentially through each chapter.

Chapter 1

The Introduction chapter identifies the research scope, general background on the topic, and identifies the real-life challenges this dissertation is tackling through achieving the research objectives. It also provides an overview of the thesis organization.

Chapter 2

Chapter 2 presents an overview community flood resilience. It starts by identifying resilience, flood risk, and present a background on the current research trajectory.

The chapter attempts to understand and quantify the communities' response to flood risk, in an effort to realize the resilience of the built-environment in face of climate-change induced flood risk. This chapter introduces the necessary background on flood hazard, community resilience, and how to quantify it using data-driven and physics-based methods. The chapter then introduces a data-driven framework using multiple unsupervised Machine Learning models to capture the communities' response to flood hazard and enable the identification of vulnerabilities within the built environment, utilizing the different resilience means and goals to achieve the objective. The framework presented in this chapter was then applied to the disaster records provided by the National Weather Service for all recorded flood events in the United States, ultimately developing a 5-category based categorization that explains the different aspects of the communities' response to flood risk. These categories were then applied to develop a comparative spatial analysis for vulnerability identification, to aid the stakeholders in making resource allocation decisions.

Chapter 3

While understanding flood risk and its impact on community resilience is of pivotal importance, there has yet to be a methodology to enable a proactive disaster management plan by predicting the impact of climate-change induced flood hazard. To that end, this chapter introduces a step towards that goal. The chapter introduces

a multi-stage prediction framework that links the developed categories in Chapter 2 with climate information (i.e., Maximum Temperature, Minimum Temperature, Precipitation, etc.) to facilitate the understanding of how climate-related information, and subsequently climate change, affect the community's response to flood risk. This developed multi-stage framework uses supervised Machine Learning techniques (e.g., Naïve Bayes' classification, Decision Trees, and Random Forest). To demonstrate the utility of the proposed framework in flood resilience management studies, and test its applicability, it was deployed using the historical disaster records used in the development of the categorization, synchronized with the corresponding climate information at the time and location of the flood events. The applicability was confirmed by producing acceptable prediction accuracy, and the ability to predict future spatial and temporal changes in the flood resilience categories of the study area.

Chapter 4

This chapter serves as the culmination of the previous two chapters, where both frameworks were used as cornerstones for a comprehensive methodology that fully incorporates the effect of climate change on community flood resilience. In this chapter, different global climate models were explored for different emission scenarios set by the Intergovernmental Panel on Climate Change, where each scenario is dictated by the volume of greenhouse gas emissions, and the global

intervention measures to steer the global emissions. For this chapter, the state of Texas was used as a case study, on a county-based spatial resolution. Climate indicators for future projections until the year 2050 resulting from the global climate models were used to predict the change in the flood resilience categories developed in Chapter 2 for the study area. The predicted categories were then used to develop a Spatio-temporal analysis, investigating the change in categories in different locations across the years. The predicted categories were then reverted to its original components (i.e., monetary damage, injuries, fatalities, duration, etc.) to quantify the climate-change impact on the study area. Multiple interpretability techniques were employed in this chapter to investigate and understand how changes in the climatological information can influence the resilience of the exposed communities, ultimately nullifying the black-box nature of Machine Learning models, transforming it into a fully interpretable model. This data-driven methodology, given appropriate data, variability and quantity, can be applicable globally, on different spatial resolutions. This potentially paves the way for a climate-change ready nation, where the climate indicators can be automatically updated and synchronized, acting as an early-warning system, and a decision support tool for decision makers, and can be applicable within flood resilience management studies for climate-proofing our communities.

Chapter 5

As climate change-induced flood hazards is the focus of this thesis, along with its impact on community resilience, the compound effect of this hazard on individual critical infrastructure is yet to be addressed. This chapter serves as the operationalization of the methodology presented in the thesis, starting by enhancing the climate resilience at the infrastructure networks-scale, in an effort to the eventual betterment of the overall community resilience.

As the frequency of flood events increase due to climate change, regardless of the magnitude of said flood events, it still causes a multitude of problems to existing infrastructure. This study focuses on the scour risk on transport infrastructure networks, specifically railway bridges, associated with increased flood events' frequency. The chapter introduces a high-order multi-layer framework for resilience-informed scour risk management that accounts for the interactions between the different components of environment, the structure, and the impact of climate change. The framework presented in this chapter was applied on all railway bridges in Southeast England to assess its utilization and compare it to the established methodologies that authorities use to assess the risk on their infrastructure assets. The application proved that incorporating such information impacted the way assets were prioritized in their maintenance, ultimately prioritizing the elements more at risk of climate-induced scour risk.

Chapter 6

This chapter includes a summary of this research, overall contributions, concluding remarks, research limitations, as well as suggested future research directions and recommendations of areas to explore further.

1.5. REFERENCES

Abdel-mooty, M. N., W. El-dakhakhni, and P. Coulibaly. 2022. "Data-Driven Community Flood Resilience Prediction." Water (Switzerland), 14 (13): 2120. https://doi.org/10.3390/w14132120.

Abdel-Mooty, M. N., W. El-Dakhakhni, and P. Coulibaly. 2023. "Community Resilience Classification Under Climate Change Challenges." 227–237. Springer, Singapore. https://doi.org/10.1007/978-981-19-0507-0_21.

Abdel-Mooty, M. N., A. Yosri, W. El-Dakhakhni, and P. Coulibaly. 2021. "Community Flood Resilience Categorization Framework." Int. J. Disaster Risk Reduct., 61 (November 2020): 102349. Elsevier Ltd. https://doi.org/10.1016/j.ijdrr.2021.102349.

Bruneau, M., S. E. Chang, R. T. Eguchi, G. C. Lee, T. D. O'Rourke, A. M. Reinhorn, M. Shinozuka, K. Tierney, W. A. Wallace, and D. Von Winterfeldt. 2003. "A Framework to Quantitatively Assess and Enhance the Seismic Resilience of Communities." Earthq. Spectra, 19 (4): 733–752.

https://doi.org/10.1193/1.1623497.

Cimellaro, G. P., C. Fumo, A. M. Reinhorn, and M. Bruneau. 2009. Quantification of Disaster Resilience of Health Care Facilities. Mceer-09-0009.

Gillet, N., G. Flato, X. Zhang, C. Derksen, B. Bonsal, B. Greenan, E. Bush, M. Shepherd, D. Peters, and D. Gilbert. 2019. Canada's Changing Climate Report; Government of Canada.

Goforth, E., W. El-Dakhakhni, and L. Wiebe. 2022a. "Network Analytics for Infrastructure Asset Management Systemic Risk Assessment." J. Infrastruct. Syst., 28 (2): 1–17. https://doi.org/10.1061/(asce)is.1943-555x.0000667.

Goforth, E., A. Yosri, W. El-Dakhakhni, and L. Wiebe. 2022b. "Rapidity Prediction of Power Infrastructure Forced Outages: Data-Driven Approach for Resilience Planning." J. Energy Eng., 148 (3): 1–13. https://doi.org/10.1061/(asce)ey.1943-7897.0000836.

Holmes, W. 2011. National Earthquake Resilience. Natl. Earthq. Resil.

Khalaf, M., A. J. Hussain, D. Al-Jumeily, T. Baker, R. Keight, P. Lisboa, P. Fergus, and A. S. Al Kafri. 2018. "A Data Science Methodology Based on Machine Learning Algorithms for Flood Severity Prediction." 2018 IEEE Congr. Evol. Comput. CEC 2018 - Proc., 1–8. IEEE. https://doi.org/10.1109/CEC.2018.8477904.

Lian, J., H. Xu, K. Xu, and C. Ma. 2017. "Optimal management of the flooding risk caused by the joint occurrence of extreme rainfall and high tide level in a coastal city." Nat. Hazards, 89 (1): 183–200. Springer Netherlands. https://doi.org/10.1007/s11069-017-2958-4.

Minsker, B., L. Baldwin, J. Crittenden, K. Kabbes, M. Karamouz, K. Lansey, P. Malinowski, E. Nzewi, A. Pandit, J. Parker, S. Rivera, C. Surbeck, W. A. Wallace, and J. Williams. 2015. "Progress and recommendations for advancing performance-based sustainable and resilient infrastructure design." J. Water Resour. Plan. Manag., 141 (12). https://doi.org/10.1061/(ASCE)WR.1943-5452.0000521.

Mosavi, A., P. Ozturk, and K. W. Chau. 2018. "Flood prediction using machine learning models: Literature review." Water (Switzerland), 10 (11): 1–40. https://doi.org/10.3390/w10111536.

Murdock, H. J. 2017. "Resilience of Critical Infrastructure to Flooding: Quantifying the resilience of critical infrastructure to flooding in Toronto, Canada."

National Institute of Standards and Technology. 2020. COMMUNITY RESILIENCE PLANNING GUIDE FOR BUILDINGS AND INFRASTRUCTURE SYSTEMS: A Playbook. Gaithersburg, MD.

National Working Group on Financial Risk of Flooding. 2019. "Options for Managing Flood Costs of Canada's Highest Risk Residential Properties."

Insur. Bur. Canada, (June).

Natural Resources Canada. 2017. “Canadian Guidelines and Database of Flood Vulnerability Functions.” (March).

NOAA. 2017. Summary of natural hazard statistics for 2017 in the United States. Statistics (Ber).

NOAA. 2019. “National Climate Report - Annual 2018 | State of the Climate | National Centers for Environmental Information (NCEI).” Accessed May 5, 2020. https://www.ncdc.noaa.gov/sotc/national/201813#over.

Otterbach, J. S., R. Manenti, N. Alidoust, A. Bestwick, M. Block, B. Bloom, S. Caldwell, N. Didier, E. S. Fried, S. Hong, P. Karalekas, C. B. Osborn, A. Papageorge, E. C. Peterson, G. Prawiroatmodjo, N. Rubin, C. A. Ryan, D. Scarabelli, M. Scheer, E. A. Sete, P. Sivarajah, R. S. Smith, A. Staley, N. Tezak, W. J. Zeng, A. Hudson, B. R. Johnson, M. Reagor, M. P. Da Silva, and C. Rigetti. 2017. Unsupervised Machine Learning on a Hybrid Quantum Computer.

Rodrigues, M., and J. De la Riva. 2014. “An insight into machine-learning algorithms to model human-caused wildfire occurrence.” Environ. Model. Softw., 57: 192–201. Elsevier Ltd. https://doi.org/10.1016/j.envsoft.2014.03.003.

da Silva, J., S. Kernaghan, and A. Luque. 2012. “A systems approach to meeting the challenges of urban climate change.” Int. J. Urban Sustain. Dev., 4 (2): 125–145. https://doi.org/10.1080/19463138.2012.718279.

Wilby, R. L., K. J. Beven, and N. S. Reynard. 2007. “Climate change and fluvial flood risk in the UK: more of the same?” Hydrol. Process., 2309 (December 2007): 2300–2309. https://doi.org/10.1002/hyp.

Witten, I. H., E. Frank, M. A. Hall, and C. J. Pal. 2017. Data Mining Practical Machine Learning Tools and Techniques Fourth Edition.

Chapter 2

COMMUNITY FLOOD-RESILIENCE CATEGORIZATION FRAMEWORK

ABSTRACT

Coupled with climate change, the expansive developments of urban areas are causing a significant increase in flood-related disasters worldwide. However, most flood risk analysis and categorization efforts have been focused on the hydrologic features of flood hazards (e.g., inundation depth, extent, and duration), rarely considering the resulting long-term losses and recovery time (i.e., the community's flood resilience). This paper aims at developing a data-driven community flood resilience categorization framework that can be utilized for the development of realistic disaster management strategies and proactive risk mitigation measures to better protect urban centers from future catastrophic flood events. This approach considers key resilience metrics such as the robustness of the exposed community and its recovery rapidity. Such categorization that focuses on two resilience goals, namely resourcefulness and redundancy, can empower decision makers to learn from past events and guide future resilience strategies. To demonstrate the applicability of the developed framework, a data-driven framework was applied on historical mainland flood disaster records collected by the US National Weather Services between 1996 and 2019. Descriptive analysis was conducted to identify the features of this dataset as well as the interdependence between the different variables considered. To further demonstrate the utilization of the developed framework, a spatial analysis was conducted to quantify community flood resilience across different counties within the affected states. Beyond the work

presented in this study, the developed framework lays the foundation to adopt data driven approaches for disasters prediction to guide proactive risk mitigation measures and develop community resilience management insights.

KEYWORDS: Resilience; Robustness; Risk Classification; Unsupervised Machine Learning; Cluster Analysis; Flood Hazard; Flood Risk.

The work in this chapter appears in the Manuscript published in the International Journal of Disaster Risk Reduction. Minor modifications were made to improve the clarity of this work within the context of the thesis. The following is the citation of the published article:

Abdel-Mooty, M. N., A. Yosri, W. El-Dakhakhni, and P. Coulibaly. 2021. "Community Flood Resilience Categorization Framework." *Int. J. Disaster Risk Reduct.*, 61 (November 2020): 102349. Elsevier Ltd. https://doi.org/10.1016/j.ijdrr.2021.102349.

2.1. INTRODUCTION

Flood events have been the most frequent hydrological hazards over the past three decades (Lian et al. 2017; Wilby et al. 2007), and are among the most impactful disasters affecting the livelihood and society (Dawod et al. 2014). Historical disaster records since 1996 indicate that, similar to other regions across the globe, North America has been experiencing extreme rainfall (i.e., rainfall exceeding 100 mm in 24 hours) and increased flood frequency in urban areas (Bertilsson et al. 2019). In 2017, floods caused a total damage of approximately $60 billion in the United States, which dwarfs the recorded flood-related damages since 1980 (NOAA 2017). This increase in flood-related losses is in part due to the expansive urbanization into flood-prone areas, that were previously deserted, leading to an increase in flood-related disasters (NOAA 2019). Urban environments nowadays host about half of the world's population and are expected to host 70% of the global population by 2050 (da Silva et al. 2012). The aforementioned increase in flood-related losses led the flood management stakeholders to shift their strategies towards *proactive* risk-mitigation rather than *reactive* disaster-response approaches (de Moel and Aerts 2011; World Economic Forum 2019a). Monetary flood-related losses can be divided into (Baird 2007) direct losses that include the structural and physical damage caused by the physical contact with the flooding water; and indirect losses which include the lost opportunity of profit as well as

evacuation, unemployment, and administrative costs (Natural Resources Canada 2017).

To efficiently assess flood damage and enhance the resilience of exposed communities, flood risk needs to be evaluated first. In this respect, flood risk can be defined as the expected damages from a hazard's probabilities of occurrence, combined with the characteristics of the vulnerable and exposed elements at risk (Kron 2005; Nofal and van de Lindt 2020), considering different sources of uncertainties (Salem et al. 2020a). Flood hazard reflects potential flood events with specific characteristics (e.g., magnitude, frequency, depth, duration, and degree of severity) at a given location, and is typically characterized by its probability of occurrence. Flood vulnerability on the other hand is a measure of the community's susceptibility, and ability to adapt, to a specific flood hazard (Jabareen 2012). Community exposure refers to people and/or infrastructure located within areas prone to flood hazards (Nofal and van de Lindt, 2020). It should be noted that severe flood hazard events may not necessarily result in high risks. For example, a severe flood might occur in an uninhabited region. The flood hazard is thus high, while the potential impacts is essentially insignificant. Risk analysis is generally concerned with assessing the exposed system's vulnerability and susceptibility to damage, and its expected consequences when exposed to a hazard (ElSayed et al. 2015; Netherton and Stewart 2016; Salem et al. 2020a). While on the other end, Resilience analysis focuses more on the extended functionality reduction and recovery

trajectory of the exposed system as a function of time, while studying the system's pre-hazard history and previous restoration costs (Linkov et al. 2014; Salem et al. 2020a).

The notion of *community resilience* has been gaining researchers' attention in recent years attributed to the increase of climate-induced hazards. Within the context of this study, a community is defined by NIST as "A place designated by geographical boundaries that function under the jurisdiction of a governance structure (e.g. town, city, or county)" (National Institute of Standards and Technology 2020). Community Resilience as a concept is defined as the capacity of a community to predict, and adapt to future hazards, and rapidly recover from disruptions back to their original state in a timely manner (National Institute of Standards and Technology 2020). ***Resilience*** can be defined as: *"the ability to recover from, or resist being affected by, some shock or disturbance"* (Cimellaro et al. 2009), or the degree to which a system absorbs disturbances while continuing to function (Murdock 2017). Resilience in the context of the current study can be characterized by its two goals: *Robustness* and *Rapidity*, enabled by the two means: *Resourcefulness* and *Redundancy* (Bruneau et al. 2003). In this respect, *Robustness* can be defined as the ability of a system to withstand a certain level of demand or stress; *Redundancy* as a measure of the built-in sustainability of the system, or the availability of replacements within the system; *Resourcefulness* as the availability of resources that aid in detecting, measuring, and surviving the hazard; and finally,

Rapidity as a measure of the time needed for the system to go back to the state before the disruption takes place, taking into account the duration of the hazard's realization (Minsker et al. 2015). To facilitate resilience quantification, researchers (Bruneau et al. 2003; Holmes 2011) have introduced the concept shown in Figure 2-1, relating performance/functionality-loss, as a result of the disruption that took place, to the time needed for full recovery (Holmes 2011). The time needed for full recovery include both the hazard duration, where a flood event may take a few days, as well as the recovery and repair time. As such, the more the time the hazard takes, the longer the total rapidity (i.e., the larger the shaded area in Figure 2-1) resulting in a lower overall resilience.

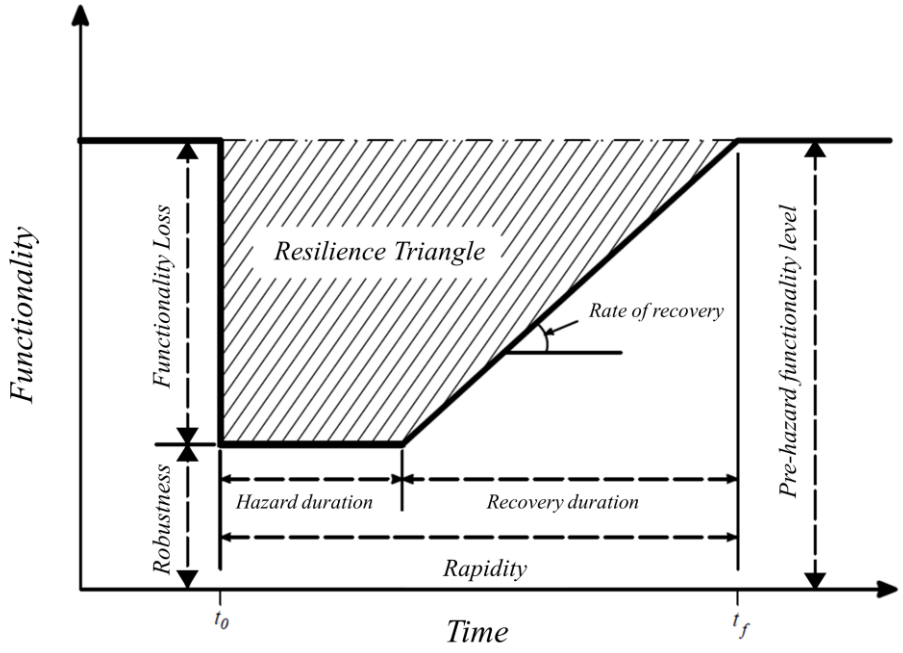

Figure 2-1: Resilience triangle and loss-time function

As such, it is imperative to categorize communities in a way that comprehensively capture the impacts of flood disasters on said communities rather than only the hazard characteristics. However, reliable information and data are key to incorporate such impacts within a resilience-based flood categorization (Downton and Pielke 2005). Integrating flood hazard, system vulnerability and flood exposure yields both short-term potential direct and indirect impacts (risk) of the flood event (i.e., through robustness assessment) as well as long-term ones (i.e., through rapidity evaluation). Numerous flood categorizations have been suggested (Australian Institute for Disaster Resilience, 2017; FEMA, 2012; Ragini, Anand, & Bhaskar, 2018; Turkington, Breinl, Ettema, Alkema, & Jetten, 2016), most notably that by the Federal Emergency Management Agency (FEMA), to facilitate the assessment of flood damages. However, all such categorizations focused on the hazard properties (i.e., categorizing floods based on magnitude, duration, and degree of severity), and to a much lesser extent, on the consequence/risk, without considering a key community resilience goal— rapidity (i.e., the time taken to recovery from both short- and long-term impacts).

2.2. COMMUNITY FLOOD-RESILIENCE CATEGORIZATION

2.2.1. CATEGORIZATION FRAMEWORK LAYOUT

The objective of the present study is to introduce a flood resilience community categorization framework that accounts for the potential/resulting

impacts of floods on exposed community. Such categorization serves as a step towards developing a fully data-driven approach for future disasters impact predictions, which will subsequently aid in developing resilience-guided flood risk management strategies considering the four resilience attributes. Data-driven models usually necessitate the availability of a large quantity of diverse data of good quality, which is often very challenging. To address this, numerous alternatives are available to account for missing data within datasets including: i) removing data points with missing variables from the dataset, ii) taking the average readings from alternate, nearby, sources and stations and take their average, and iii) utilizing unsupervised machine learning models to create clusters and generate the missing values for said datapoints (Haggag et al. 2021b; Patil et al. 2010; Yagci et al. 2018).

As can be seen in Figure 2-2, the framework can be divided into *three* main stages*:*

Stage i) Data Preprocessing and visualization: The developed data-driven approach starts by compiling a comprehensive dataset which includes the variables needed to quantify the resilience attributes. After dataset selection, data preprocessing and cleaning commences for ensuring that it is comprehensive enough for an insightful analysis. The subsequent step involves data visualization where the attributes and correlation of the variables within the dataset is assessed,

this will aid in choosing the appropriate technique for the next stage in the framework.

Stage ii) Machine Learning Model Selection: Machine Learning (ML) tools may be considered as the evolution of Statistical Learning models (Witten et al. 2017) and have thus become indispensable in applications such as image recognition, social networks, targeted advertisement, as well as engineering, biology, and medicine in general (Bose and Mahapatra 2001; Goos et al. 2006; King et al. 1992; Mckinney et al. 2006). In such applications, ML identifies patterns, discovers trends and behaviors from large datasets and have the ability to continuously learn from adapt to new data to improve its performance. ML models are also able to deal with large datasets with complex interdependent attributes and identify the hidden behaviors (Hastie et al. 2009). ML is broadly divided into Supervised (Classification), and Unsupervised (Clustering) algorithms, with the latter being the one adopted in the current study. However, both types of algorithms are used in analyzing large datasets with multiple variables (Gentleman et al. 2008; Hastie et al. 2009).

Stage iii) Clusters' features analysis: In this stage, the output of the ML algorithm is analyzed to develop the features of each category (cluster). Subsequently, guided by the developed categories, a spatial analysis is conducted to identify relative vulnerable communities. This way, unbiased insights can be drawn, facilitating the decision-making process for how to employ, or introduce,

resilience means (i.e., Resourcefulness and Redundancies) to the most vulnerable communities, maximizing use of the available resources. Such categorization framework can also enable decision makers to translate predicted flood hazards and risks into actionable plans, minimize the expected damages due to flood events (increase robustness), and develop effective policies and resilience-focused disaster mitigation strategies.

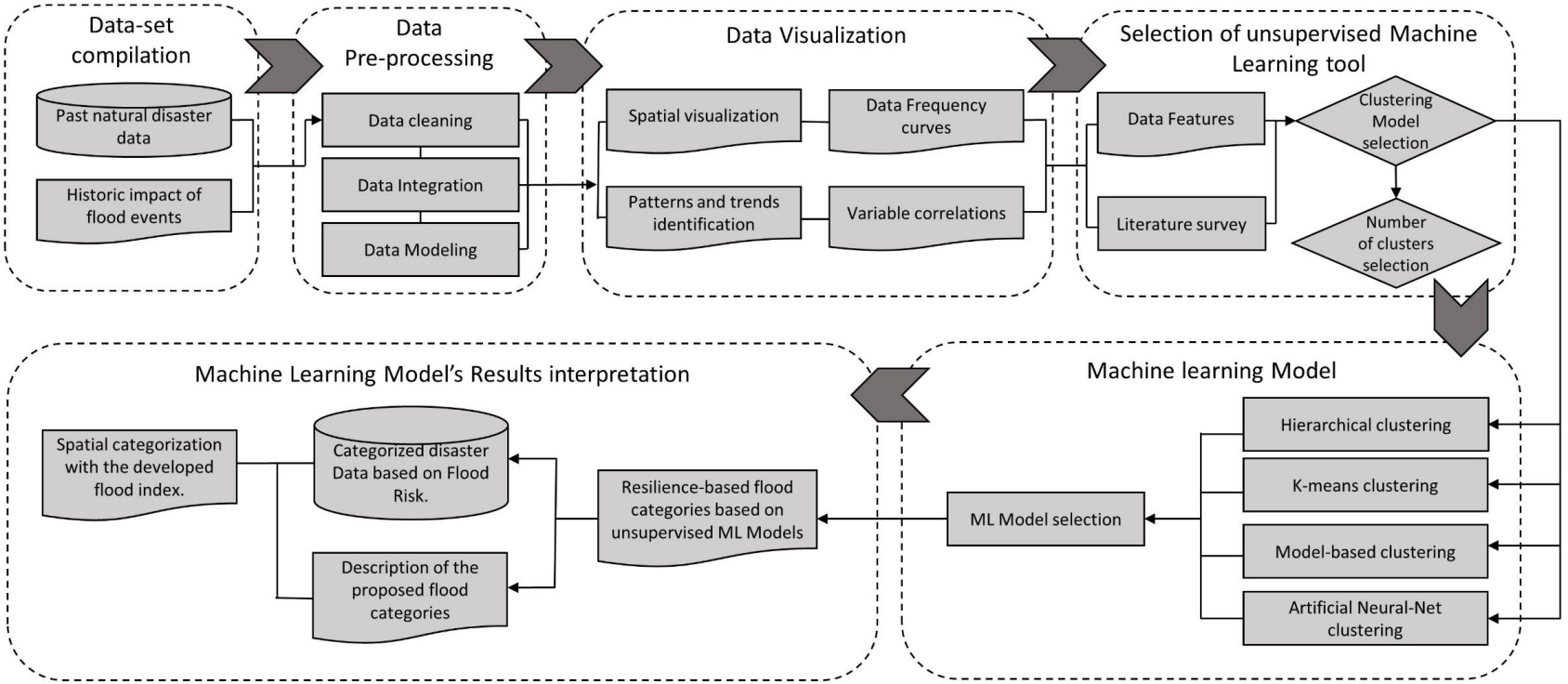

Figure 2-2: Resilience-based flood categorization proposed framework

2.2.1. METHODOLOGY

Cluster analysis uses partitioning algorithms to group observations based on similarity in an unsupervised learning fashion. Observations are assigned labels, and those with common features (i.e., similar or nearly similar) are allocated to the same cluster (Otterbach et al. 2017). This process is unguided, with observations grouped based on inherent characteristics without any specific end goal in mind, hence the term "Unsupervised". Similarity is assessed through measuring the distance between the different observations. Two observations are considered similar when the distance between them is significantly negligible. Observations allocated to the same cluster should be closer to each other than to observations in other clusters. Different similarity and distance measures have been proposed including: Euclidean distance, Hamming distance, Cosine similarity, Manhattan distance, and Gower Distance (Jain et al. 2000). Gower distance within a Partitioning Around Medoids (PAM) algorithm was explored in this study to check its applicability with the available mixed type data. However, the dissimilarity matrix developed from the dataset presented a skewness in the model, resulting in a clustering based on seasons, instead of the resilience metrics. This issue was later rectified using the alternative distance measures explored in this study (Budiaji and Leisch 2019). Euclidean distance therefore is preferred over other similarity measures as it evaluates the weighted proximity (Jain et al. 2000) of different objects in a three-dimensional space, and is thus employed in the present study (Jain

et al. 2000; Seyed Shirkhorshidi et al. 2015). However, it should be noted that other approaches can also be adopted (e.g., creating binary indicator variables for each category in a categorical data variable). In this study, three clustering algorithms were employed for the development of the new flood risk categorization and the best algorithm was chosen based on the performance of the corresponding model. The algorithms considered are: Model-based clustering, K-means clustering, and Self-Organizing Maps neural network (SOM-ANN).

MODEL-BASED CLUSTERING

Model-Based clustering depends on grouping observations based on a finite mixture model, in which each cluster is a unimodal component (Mcnicholas 2016). In this model, a random variable ***X*** follows a parametric mixture distribution with a density $f(x|\vartheta)$ expressed as (Mcnicholas 2016):

$$f(x|\vartheta) = \sum_{g=1}^{G} \pi_g f_g(x|\theta_g) \qquad (2\text{-}1)$$

where $\vartheta = (\pi, \theta_1, \ldots, \theta_G)$ is the vector of parameters characterizing the model, G is number of components mixed, $\pi_g = (\pi_1, \ldots, \pi_G)$ is the mixing proportions, and $f_g(x|\theta_g)$ is the density of the g^{th} component of the mixture. It is noteworthy that in model-based clustering, $f_g(x|\theta_g)$ is typically assumed to be the same for all components ($g = 1, \ldots, G$). In the present study, a Gaussian Parsimonious Clustering

Model (GPCM) with up to 14 components was employed (Celeux and Govaert 1995), and the model parameters were determined using an expectation-maximization algorithm (Vrbik and McNicholas 2014). Gaussian Mixture models are probabilistic models in which the data points are assumed to be generated from a mixture of a finite number of gaussian distributions (Mcnicholas 2016). To estimate how well a model fits a dataset, and to determine the complexity of such model, statistical approaches can be used. Among the most widely used approaches are the Akaike Information Criterion (AIC), and the Bayesian Information Criterion (BIC) (Bishop 2006). The AIC model measures the likelihood of a model, which measures the fitness of a model, using a penalty function that penalizes the model based on its size. The smaller the value of the AIC, the better the fitness of the model. Similarly, the BIC also uses the same approach, however, BIC differs from the AIC on the definition of the penalty. While the AIC's penalty function is a linear function, the BIC's penalty function is a logarithmic function (penalty function = k.p; k in AIC is 2, while k in BIC is log(n)). As such, AIC penalty is lower when the model is more complex, compared to BIC, indicating that BIC will prefer a less complex model in the analysis than the AIC (Hastie et al. 2009). For the study presented herein, the BIC was chosen as a sufficient method for determining the better model to be used, as the data is already complex with multiple interdependent variables (Bishop 2006; Hastie et al. 2009). The reader is referred to the study by

Mcnicholas (2016) for a detailed description of the model-based clustering and related applications.

K-MEANS CLUSTERING

K-means clustering is one of the most widely used clustering algorithms (MacQueen 1967) through which observations are partitioned into a predefined number of clusters (*K*). Multiple *K* values are assumed, and the optimal value corresponds to the minimum intra-cluster variation (defined herein as the total within-cluster variation (*WSS*)). In the present study, *WSS* is estimated as the summation of the squared Euclidean distance between observations and the respective cluster centroid (Alsabti et al. 1997; Hartigan and Wong 1979; Wagstaff et al. 2001):

$$WSS = \sum_{k=1}^{K} \sum_{x_i \in C_K} (X_i - \mu_k)^2 \qquad (2\text{-}2)$$

where X_i is an observation belonging to the cluster *k*, and μ_k is the mean of the observations allocated to the same cluster. Several methods have been developed to estimate the optimum *K* value based on *WSS*, including: *i*) the elbow method, in which *WSS* is estimated for multiple models (each with a different *K* value) and the optimum *K* value corresponds to the point where the slope of the *K*-*WSS* relationship decreases without a significant change in *WSS*; and, *ii*) the silhouette method, in which each observation is assigned a score based in its distance to the

neighboring clusters (Zumel and Mount 2020) and the optimum *K* value is at the maximum average silhouette score. It is important to note that the silhouette score ranges between -1 and 1, where: a value closer to 1 indicate that the observation is too far from the neighboring clusters and is thus allocated to the right cluster, a value of zero shows that the observation is on the boundary of two neighboring clusters, and negative values indicate that the observation is allocated to the wrong cluster.

SELF-ORGANIZING MAPS (SOM) NEURAL NETWORKS

ANN is an artificial intelligence-based technique that can be used to uncover complex interrelationships through automatic learning based on patterns in the data (Mitra et al. 2016; Park 2000). This is similar to a human brain translating signals, albeit in a simpler way and with artificial neurons. Several types of ANN have been developed to date (e.g., feed-forward back-propagation neural network, recurrent neural network, convolution neural network, and self-organizing map), each of which is suitable for specific applications. ANN has been widely employed to develop predictive models (e.g., Khajwal & Noshadravan, 2020; Kwayu, Kwigizile, Zhang, & Oh, 2020; Mitra et al., 2016) and to solve complex pattern recognition problems (e.g., (Gnanaprakkasam and Ganapathy 2019; King et al. 1992; Park 2000; Turkington et al. 2016). It is noteworthy that pattern recognition (e.g., cluster analysis) problems are most often challenging due to the unstructured

nature of the data employed, and particularly when the variables associated with the data are interdependent. As such, ANN-based clustering is preferred over other techniques (e.g., model-based and K-means clustering) as it typically converges to a global, rather than a local, optimal solution (Li 2011; Mitra et al. 2016; Park 2000)

A self-organizing map (SOM) is a type of ANN that is trained in an unsupervised manner to discretize data into groups (i.e., cluster analysis). Input data are thus organized according to a pre-set topology of neurons (the number of neurons and inputs are not necessarily the same), each of which is connected to a certain number of inputs (i.e., observations). Initial weights are assigned to each neuron, and the whole weight space is adjusted iteratively to match the correlation and patterns present in the input space. In the present study, SOM was applied using the Deep Learning toolbox in MATLAB based on the Kohonen rule (Park 2000). According to this rule, a winning neuron ($\underline{i}^*$) is identified based on the degree of similarity between the associated weights and connected inputs. Weights associated with i^* are adjusted iteratively such that i^* is most likely to win in the following iterations. As such, if the weights associated with $\underline{i}^*$ are close to the optimum values, they will become closer during the following iterations. The reader is referred to the study by Park (2000) for more details about the application of Kohonen rule.

To demonstrate its applicability, the developed categorization framework was applied on a dataset from the National Weather Service (NWS) database to: *i*) identify the different factors controlling the at-risk communities' vulnerability to floods using descriptive data analysis; *ii*) identify the key features of the variables included in the dataset as well as possible interdependence between them using descriptive and correlation analyses; and, *iii*) categorize the community's resilience to flood by using events in the dataset that are based on the flood characteristics (i.e., duration) and impacts (i.e., damages, number of people affected and duration of flood event) and resilience metrics (i.e. robustness and rapidity).

2.3. DEMONSTRATION APPLICATION

2.3.1. DATASET

The dataset provided by the NWS—one of the longest run organizations to record annual flood damages in the United States (Downton et al. 2005), is employed in the present study. The data in the dataset is gathered by third party organizations and subsequently compiled into the NWS database. The data gathering agencies follow the guidelines set by the NWS, however the quality, quantity and diversity of the data is highly dependent on the available resources and time constraints of said agencies (Murphy 2018). This dataset contains records of the flood events occurred across the United States between 1996 and 2019, with a

total of 49,775 records. For each event, start and end time, geographical center of the affected area, month, year, and related damages are recorded. The start and end time were used to estimate the event duration, which was subsequently used as an additional event attribute. The season when an event occurred was inferred from the corresponding month and was also included in the analysis. Seasons were defined as: winter commencing in December, spring commencing in March, summer commencing in June, and fall commencing in September (Jaagus and Ahas 2000). Event-related losses include: property and crop damages due to the physical contact with the flooding water as well as direct/indirect injuries and fatalities. In the present dataset, the term "Flood event" refers to the flood component of any natural disaster. For example, a Hurricane's impact is a result of multiple components (e.g., wind pressure, debris (airborne and otherwise), or inland flooding), only the impacts (monetary and otherwise) resulting from the "Flood" component of the event were recorded in this dataset (Murphy 2018). Despite the limitations of the NWS dataset (i.e., not incorporating the indirect economic damage resulting from the flood events, the people displaced, or the time taken to full recovery), it is generally accepted that this dataset represents the best available alternative that can be used for flood damage assessment in the United States (Downton et al. 2005).

Direct and indirect injuries/fatalities, as well as property and crop damages, were summed up in the present study to investigate the total impact of the

corresponding flood event. Property and crop damages were adjusted using the Customer Price Index from the Bureau of Labor Statistics to accommodate the inflation over the years (FRED 2020). Seasons were converted into numerical values to have consistent numerical, rather than categorical, attributes (Zumel and Mount 2020). As the objective of this study is to develop a new flood categorization based on flood characteristics and impacts, only the events that posed an actual risk were considered. As such, flood events causing no damage, injuries, and fatalities were excluded from the dataset since it will induce bias within the dataset, and it will produce no resilience metrics to be measured. Although the developed framework presented herein can be applied to different communities, and similar to other data-driven models, the numerical results are influenced by the input data quality and diversity. As such, to draw reliable managerial insights from the results of the proposed framework, the pertinent dataset needs to be comprehensive enough— including most/all relevant variables (e.g., flood type, type of area, flood impact, flood cause, recovery time, monetary losses, evacuated people, injuries, fatalities, etc.) and enough data points (observations) over many years to avoid biases. However, within the dataset used herein, although flood type is not explicitly listed for each affected community, such information is implicitly considered as the common spatio-temporal flood type affecting different communities. Since event attributes (i.e., duration, season, related damages, injuries, and fatalities) are measured in different units, these quantities were scaled

such that each has a mean of zero and a standard deviation of 1.0 (Zumel and Mount 2020). A state-based descriptive analysis was subsequently adopted, where the variables considered include: i) event duration, related damages, injuries, and fatalities as risk indicators (referred to herein as risk variables); ii) the season (instead of the month and year) to indicate when the event occurred; and, iii) states containing the geographical center of the affected area. However, for the Unsupervised ML algorithm, only the Risk variables (i.e., Event duration, Related Damages, injuries, and fatalities) and the season are included in the clustering algorithm, omitting the state variables to avoid geographical clustering of the data. This way the algorithm would implicitly account for the respective prevailing natural hazards of each community

2.3.2. DESCRIPTIVE ANALYSIS

The analysis shows that most of the flood events occurred during the summer (41%), followed by the spring (28%), the fall (17.5%), and the winter (13.2%), as shown in Figure 2-3(a). This is also supported by the temporal distribution of floods between 1996 and 2019 shown in Figure 2-3(b). The higher number of floods occurring in the summer is because most of the regions across the United States experience high precipitation during the summer followed by the spring. In urban environments, this high precipitation might increase the water level in the rivers which can lead to significant losses (NOAA 2019). Figure 2-3(c) shows the total

damage caused by floods in the different states, where colors were used to indicate the number of flood events causing that damage. The largest number of events and the largest damage occurred in Texas. This might be attributed to the increased heat content over the western Gulf of Mexico, which can result in a higher temperature and humidity. The heat increase is directly proportional to the amount of precipitation that a storm can produce (Trenberth et al. 2018). In addition, Texas falls within a tropical weather region where a large number of hurricanes and extreme rainfall events are likely to occur, and an increasing urbanization rate (FEMA 2012). Example of such events include a record of 60.6 inch of precipitation during Hurricane Harvey in 2017, and 43.39 inch of precipitation during the Tropical Storm Imelda in 2019 (Hayhoe et al. 2018; Trenberth et al. 2018). Such events have significantly impacted the infrastructures and properties in Texas, causing a damage of approximately $52 Billion.

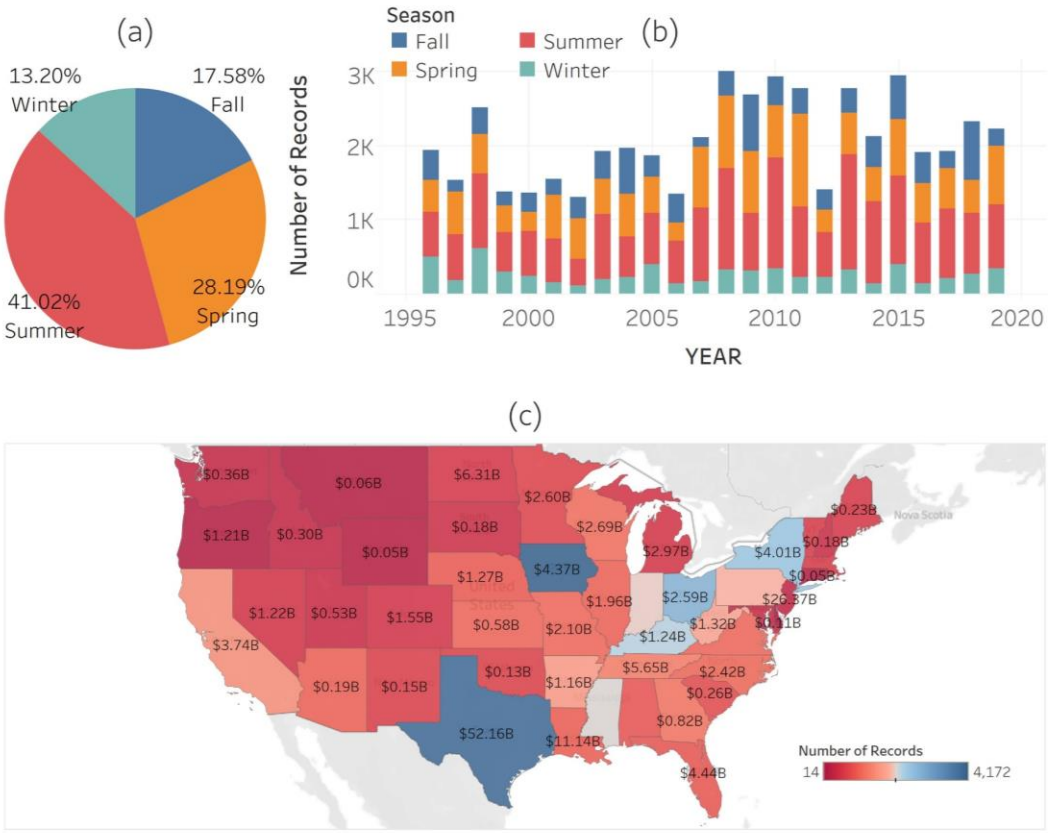

Figure 2-3: Descriptive analysis where (a) is the percentage of flood events occurred in each season, (b) is the annual number of flood events occurred between 1996 and 2019, and (c) is the total damage over the different states in Billion USD due to floods

An exploratory data analysis was conducted to investigate the properties of the different variables within the dataset and the correlation between them, as shown in Figure 2-4. This figure can be treated as a 7 × 7 matrix, in which variables were labeled on both the rows and columns. This matrix represents 4 distinct information groups: *i*) frequency curves, where the first column is the frequency curves distinguished by seasons and the diagonal is the smoothed frequency curves

(or histograms); *ii*) the frequency scatter plots located at the lower triangle of the matrix, excluding the first column; *iii*) the correlation coefficient between each variable pair at the upper triangle of the matrix, excluding the top row; *iv*) the box plots of the different variables at the top row of the matrix. It should be noted that events were divided into four groups depending on the season in which they occurred. Figure 2-4 can therefore be used to investigate the statistical behavior and seasonality of each individual variables, as well as the interdependence between the different variables.

The box plots in Figure 2-4 show that, for all variables, the distributions overlap over the different seasons. This indicates that these variables are extremely interdependent and cannot be clustered based on the season. The risk variables (i.e., duration, related damage, injuries, and fatalities) are characterized by heavy-tailed distributions with a significant number of outliers in all seasons. This is attributed to that a small portion of the flood events caused a significant impact (damages, injuries, fatalities) compared to that caused by majority of the events. In contrast, event duration has a more prominent range with more outliers in the spring followed by the winter. This can be attributed to the spring floods which typically occur when the warmer weather following the winter causes heavy rain, spring thaw, and flash floods that remain for longer periods of time and can cause additional damages (FEMA 2018a). Values of the correlation coefficient shown in Figure 2-4 support the interdependence between multiple variables rather than the direct interrelation

between variable pairs, as all values are significantly low. As such, Machine Learning, as discussed earlier, presents a powerful tool to represent the variability, and handle complexity and interdependence, in this dataset.

Figure 2-4: Results of the exploratory and sensitivity data analysis of the Season, State, and the risk variables as defined in this study

2.3.1. MODEL-BASED CLUSTERING

Model-based clustering was applied for several clusters (i.e., *K*) ranging between one and nine, and the corresponding BIC values were estimated (Figure 2-5). Based on BIC values, the recommended model was VII (a spherical model with variable volume) with nine clusters. This number of clusters is, in fact, very large considering the purpose of this study. Therefore, further investigations of the

recommended model, a classification plot was developed (Figure 2-6), where the relationships between variable pairs are investigated within each cluster. This classification plot indicates that the model-based clustering is not suitable for the purpose of the present study due to lack of separation between the clusters, inexistence of density centers, the high dimensionality, and its inability to capture the interdependence between the variables existing in the dataset.

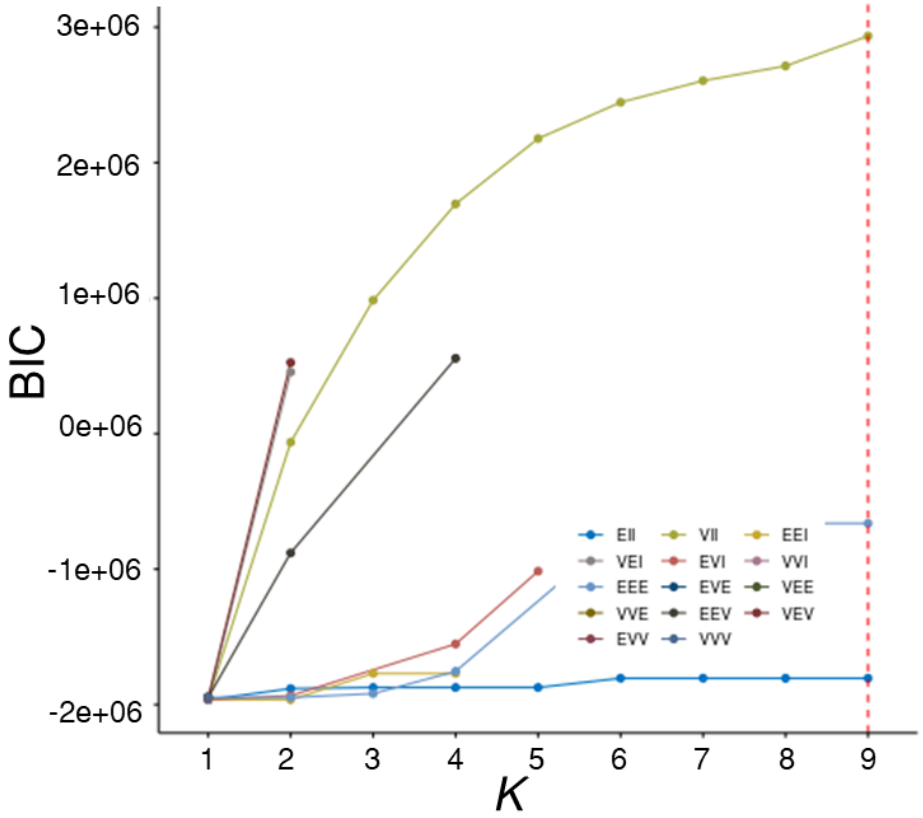

Figure 2-5: BIC Values for different GPCM Models

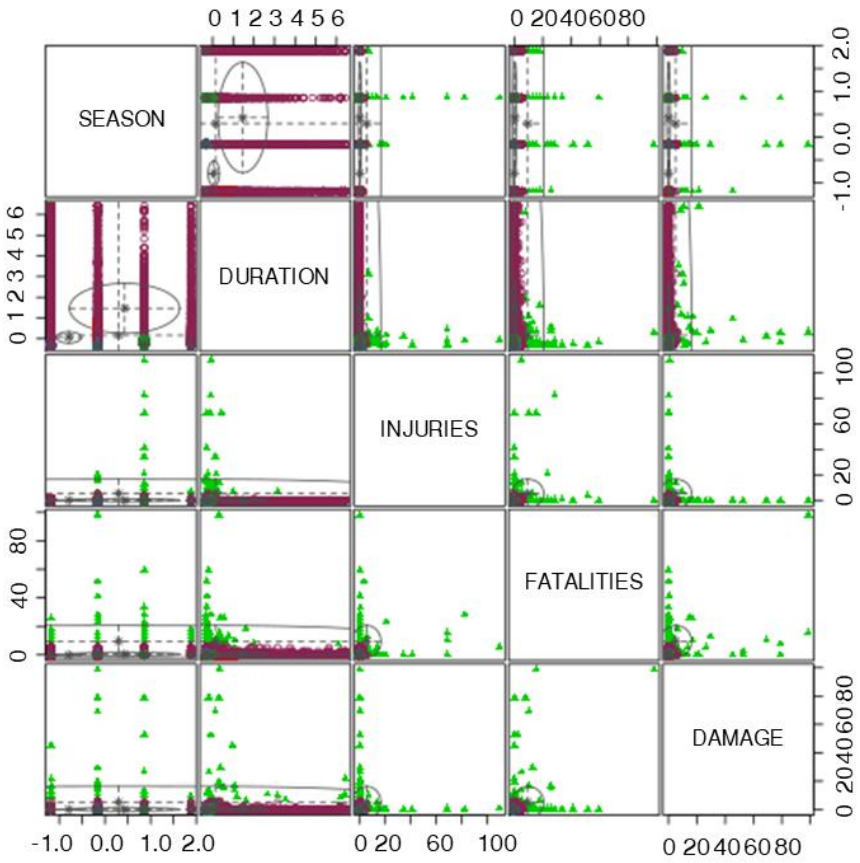

Figure 2-6: Classification plot for the VII model with nine clusters, where observations allocated to each cluster are represented by color and symbol

2.3.2. K-MEANS CLUSTERING ALGORITHM

As explained earlier, the application of K-means clustering requires a suggestion of the *K* value prior to the analysis. Therefore, *K* was varied between one and eight, and both the elbow and silhouette methods were used to estimate the optimum *K* value. Figure 2-7(a) shows the *K-WSS* relationship that was used to determine the optimum *K* value using the elbow method. It can be observed that six clusters correspond to the point where the slope of the relationship decreases

without a significant decrease in *WSS* (i.e., the optimum number of clusters is six). On the other hand, Figure 2-7(b) indicates that nine clusters are needed based on the silhouette method. However, Figure 2-7(b) also shows that: *i*) the average silhouette score increased significantly between two and six clusters compared to that beyond six clusters; and *ii*) the average silhouette score at six clusters is 0.73 which represents 91% of the corresponding maximum obtained (i.e., 0.8). As such, a *K* value of six was chosen as the optimum number of clusters based on the K-means clustering.

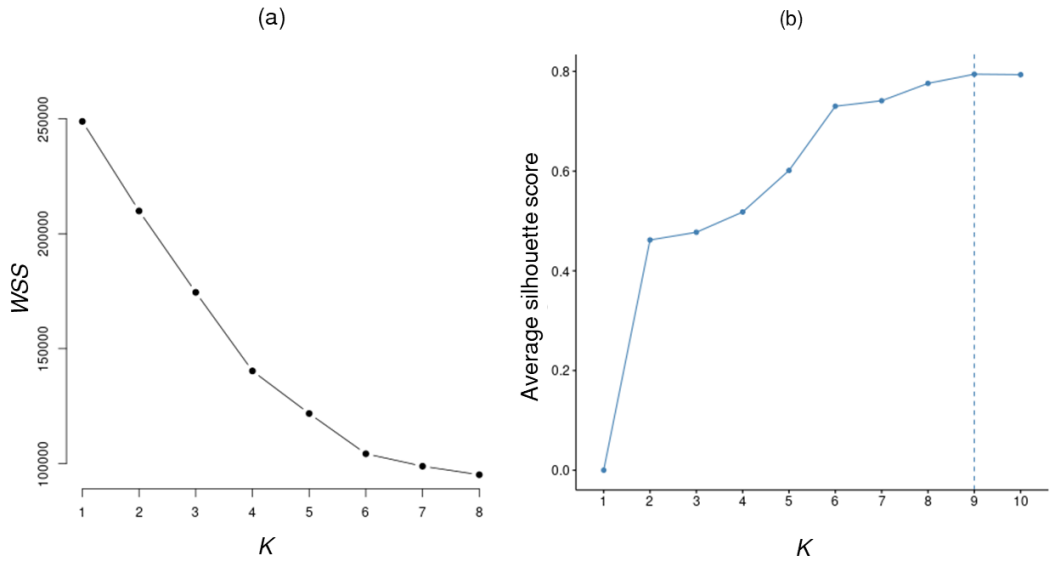

Figure 2-7: Evaluation of K where (a) is the K-WSS relationship and (b) is the average silhouette score at different K values

To effectively visualize the results of the K-means clustering, two variables are introduced. These variables are scaled and centered so that the mean of all variables is zero, and the standard deviation is one (Zumel and Mount 2020). These

variables are the: *i*) scaled affected people, which is the centered and scaled summation of fatalities and injuries; and *ii*) scaled event impact, which is the centered and scaled summation of damages, injuries, and fatalities. These variables were developed to relate to the resilience goals, namely robustness and rapidity, where the affected people and the damage variables represent the robustness, while the duration of event represent the rapidity. Figures 2-8(a) through 2-8(c) show the scaled and centered affected people-event duration-damage, affected people-season-damage, and season-event duration-event impact relationships, respectively. It should be noted that different colors were assigned to each cluster for visual distinction. Figure 2-8 shows six distinct clusters based on the different visualization variables. From Figure 2-8(a), it can be noticed that events resulting in larger damages and higher number of affected people were separated from other events in a single cluster, and those with higher down time values, and hence rapidity, were also separated in another cluster. However, most of the events were entangled, due to the high degree of interdependence between the different variables in the dataset. The three plots in figure 8 needs to be examined together to capture the different attributes the separates the categories from one another.

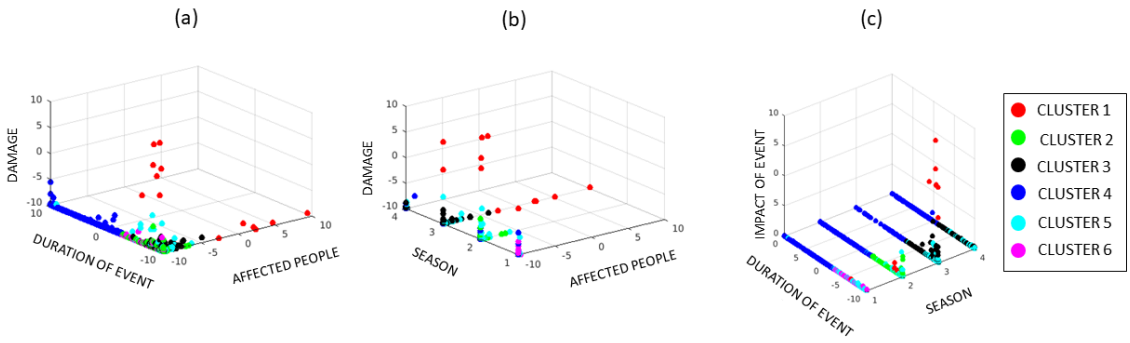

Figure 2-8: Cluster visualization for the k-means clustered data, (a) the relationship between the scaled duration of event, damage, and affected people, (b) the relationship between the Season, and the scaled affected people, and damage, and (c) the relationship between the scaled duration of event, impact of event, and season based on the results of the K-means clustering

2.3.3. SELF-ORGANIZING MAPS (SOM) NEURAL NETWORK MODEL

As discussed above, the application of ANN for cluster analysis requires predetermining the value of *K* and the number of neurons. The value of *K* was therefore varied between two and eight, and the corresponding *WSS* was calculated according to Equation 5. The *WSS* for multiple number of clusters were investigated (ranging between *K*=1 and *K*=9), and the minimum *WSS* value encountered when using four and six clusters; therefore, both models were further investigated. Figure 2-9 show the relative contribution of the different variables to each neuron/cluster within the SOM, where: negative contribution is shown as black, zero contribution is represented as red, contribution increases as the color gets lighter, and contribution decreases as the color becomes darker. Figure 2-9 supports that certain

variables heavily affect some clusters, which indicates a good separation between the different clusters within the model.

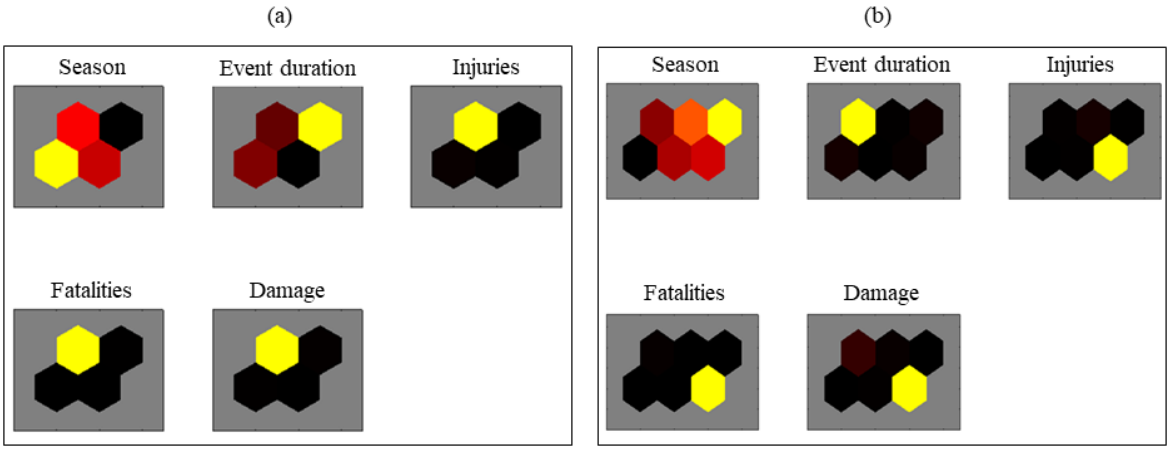

Figure 2-9: The contribution of the different variables to the different neurons (clusters) of the SOM for a (a) four-clusters model, and (b) six-clusters model

Similar to Figure 2-8, Figures 2-10(a) through 10(c) show the following relationships: affected people-event duration-damage, affected people-season-damage, and season-event duration-event impact. Similar to the results of the K-means clustering, it can be observed that the clusters are distinguishable based on the different variables. Observations with high damage and large number of affected people are included in the same cluster whereas events with high duration were clustered together. This highlights that the flood risk does not depend on the hazard's characteristics only, but also on the robustness and vulnerability of the exposed community. Therefore, categorizing flood events based on the exposed components rather than event characteristics is essential.

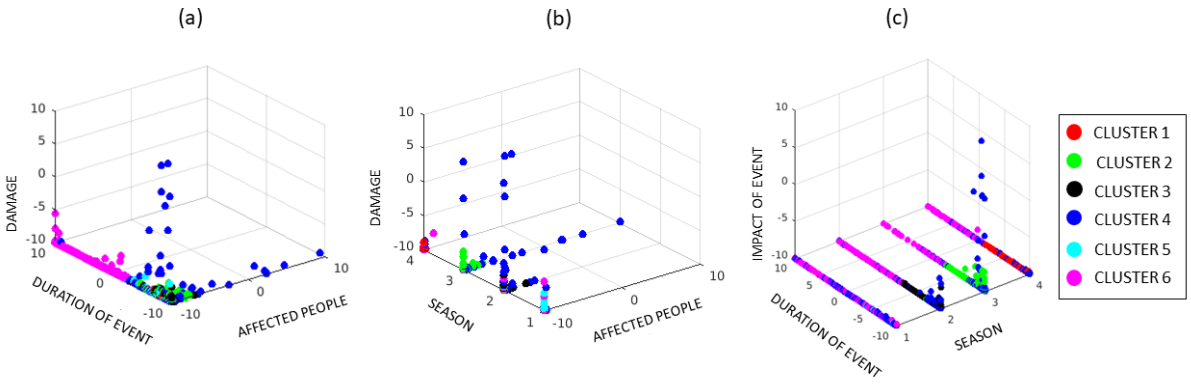

Figure 2-10: Cluster visualization for SOM clustered data, (a) the relationship between the scaled duration of event, damage, and affected people, (b) the relationship between the Season, and the scaled affected people, and damage, and (c) the relationship between the scaled duration of event, impact of event, and season based on the results of the SOM.

2.3.1. RESULTS ANALYSIS AND INSIGHTS

An appropriate number of clusters is that which strikes a balance between explaining the variance within the dataset and maximizing the distance between different clusters (Patil and Baidari 2019). The number of categories is then adopted from the number of clusters, while ensuring that the resulting number of categories is employable in practical Resilience guided studies. The choice of the number of clusters depends on the dataset and the distribution of the data withing its space. If left uncontrolled, without a penalty, the clustering algorithm will reduce the clustering error to the maximum by having the greatest number of clusters possible, ultimately reaching the total number of observations of the dataset (Patil and Baidari 2019). As such, BIC was employed in Model Based Clustering, while WSS

and Silhouette methods were employed in k-means and the SOM ANN model. The results from the three clustering algorithms employed in the present demonstration study show that: i) the model-based clustering did not provide a viable model due to the high complexity of the dataset used in this study; *ii*) K-means and ANN-based clustering algorithms have nearly similar performances; and, *iii*) a model with six clusters is suitable to meet the objective of the current study. Further investigations showed that two clusters exhibit similar features, albeit only distinguished based on the season. These two clusters were therefore merged, which resulted in having a total of only five clusters (categories), which is compatible with the goal of the framework presented herein. It is noteworthy that: *i*) most of the flood events occurring in the spring were divided into two groups, one contains the events of a greater impact and the other contains those of a lesser impact; *ii*) flood events that lasted for more than 11 days were clustered together, indicating a correlation between the impact of the flood event on the exposed environment and duration of the event; and, *iii*) all events that resulted in loss of human lives were separated together in a single cluster. Figure 2-11 show the characteristics of each category in terms of the number of records together with the average number of affected people, duration, and damage. Events falling in Categories 1, 2 and 4 are more common than those in Category 3 and 5, as shown in Figure 2-11(a). However, events designated as Category 5 are of more impact in terms of the average number of people affected and average damage (Figures 2-11(b) and 2-

11(c), respectively). Resilience is multidimensional, and within this categorization framework more emphasis was put on human lives than on monetary damage. Henceforth, even though Category 3 follows Category 5 in terms of the average damage, Category 4 follows Category 5 in terms of the average number of people affected which is why it was assigned to a higher Category. It is noteworthy that there is no significant correlation between event duration and impact, highlighting the importance of including both the event characteristics and the expected consequences for the development of an effective categorization. It should be recalled that the event's duration considered herein refers to the hazard's duration, from the moment of the flood starts, until the water level goes back to its original state before the start of recovery. Hence, larger flood duration translates to a less robust infrastructure (drainage) system to accommodate for such flood and effectively drain it in a timely manner. Subsequently, the longer the flood duration, the longer the total time until full recovery (rapidity), resulting in a lower overall community flood resilience.

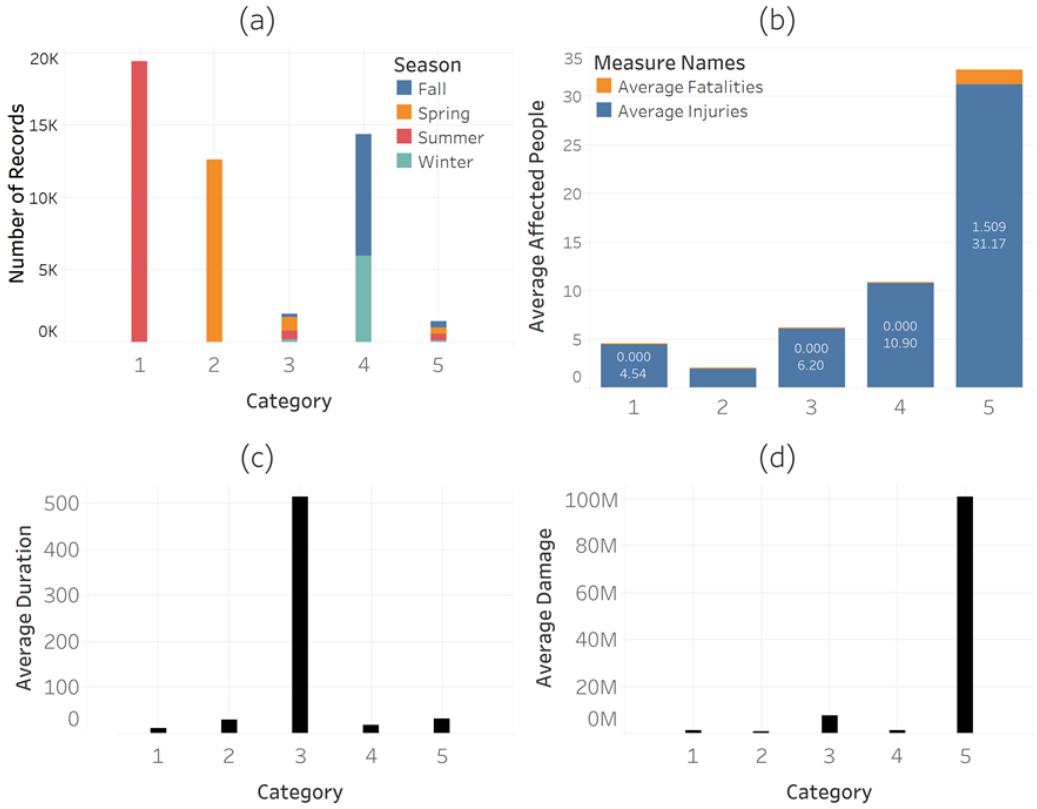

Figure 2-11: Frequency curves where (a) is the number of records per cluster, (b) is the average number of affected people per cluster, (c) is the average duration per cluster, and (d) is the average damage per cluster

In the context of this study, performance characteristics attributed to each of the developed categories were drawn by adopting the data-driven approach. In contrast to performance based seismic design, where performance measures are concluded by surveys and interviews with stakeholders (FEMA 2018b; National Research Council 1996). Based on the previous discussion, the categories presented in table 2-1 were developed. Each of these categories was assigned a flood resilience index (FRI) that increases as the functionality loss of the exposed

community increases. As such, communities exposed to flood events with impacts falling under Category *j* are more resilient than those falling under Category *j+1*, with *j* ranging between 1 and 4. Category 1 includes flood events that cause disturbance for an average of 10.6 hours (and less than 11 days) in the summer, cause an average damage of $1.36M (and less than $2.5B), with an average of 5 (and less than 250) injuries, and no fatalities. Category 2 contains flood events the cause disturbance for an average of 30 hours in the spring and cause an average damage of $1.3M (and less than $1.5B), an average of 3 injuries (and less than 20), and no fatalities. It is noteworthy that events occurring in spring are allocated to a separate category of a lower impact due to the frequency of spring floods (spring floods usually take up more time, on average, compared to those occur in other seasons (FEMA 2018a). Statistically, most flood events occurring in the spring are caused by spring floods, and those occurring in the summer are due to flash floods caused by extreme rainfall (FEMA 2018a). Category 3 encompasses flood events that cause disturbance for an average of 514 hours (and more than 11 days) during any season, regardless of the monetary damage, and an average of 7 injuries (and less than 250), and no fatalities. The last two categories are those of higher resilience loss, as shown in Figures 2-11(b) and 2-11(d). Category 4 include flood events that cause disturbance for an average of 18 hours (less than 11 days) in the fall or winter, cause an average damage of $1.51M (and less than $2.5B), with an average of 11 injuries (and less than 250), and no fatalities. Category 5 entails any

event that cause the loss of human life and/or damage more than $2.5B with an average damage of $101M.

Table 2-1: The developed community flood resilience categorization

Community Flood Resilience Category	Category description
1	Communities exposed to events that that occur in the summer, causing disturbance less than 264 hours (11 days) and/or causes up to 250 injuries, and damage less than $2.5B without fatalities
2	Communities exposed to events that occur in the spring, causing any disturbance duration, causes up to 20 injuries, and damage up to $1.5B without fatalities
3	Communities exposed to events occurring in any season, causing disturbance more than 264 hours (11 days), and causing up to 250 injuries with any damage value, and without fatalities
4	Communities exposed to events that occur in winter or fall, causing disturbance less than 264 hours (11 days) causes up to 250 injuries and damage up to $2.5B without fatalities
5	Communities exposed to events occurring in any season, causing any disturbance duration that results in more than 250 injuries, causing damage more than $2.5B, with fatalities. And Communities exposed to events occurring in the spring that are not under Category 2.

Within the context of the manuscript, the clusters are related to the community resilience metrics in response to flood disasters. Hence, a community can be placed in different category each time a disaster befalls it. However, by taking the average of the resilience indices corresponding to all recorded flood disasters, an average index can place a community in a certain category,

representing the resilience of said community in a comprehensive way that accounts for all previous disasters. A comparative spatial analysis is conducted where the average FRI can be calculated nation-wide on a state level— as per our dataset, as shown in Figure 2-12. The average FRI of a state was calculated by identifying the FRI of each individual event (according to Table 2-1). High average FRI values indicate that the corresponding state is relatively less resilient to flood events, indicating the need of measures to increase the state's resilience. It is noteworthy that when the average FRI of a state is between two categories, a roundup would be more appropriate as a conservative approach.

It is concluded from the spatial analysis that the state of Oregon has the highest Flood Resilience Index of all the states. Most of the state of Oregon falls within the Pacific Northwest region, where excessive precipitation is typically expected (Oregon Instute for Water and Watersheds 2012). This region is also characterized by a maritime climate with majority of the annual precipitation occurring between October and March (Cooley and Chang 2017). Oregon state is also known for some catastrophic flood events (e.g., the Williamette River Flooding of 1996 that disrupted the livelihood of the population of Portland and had a huge impact on the city's infrastructure, frequent flash floods due to intensive rainfall) (Michelson and Chang 2019; US Department of Commerce, NOAA 2019).

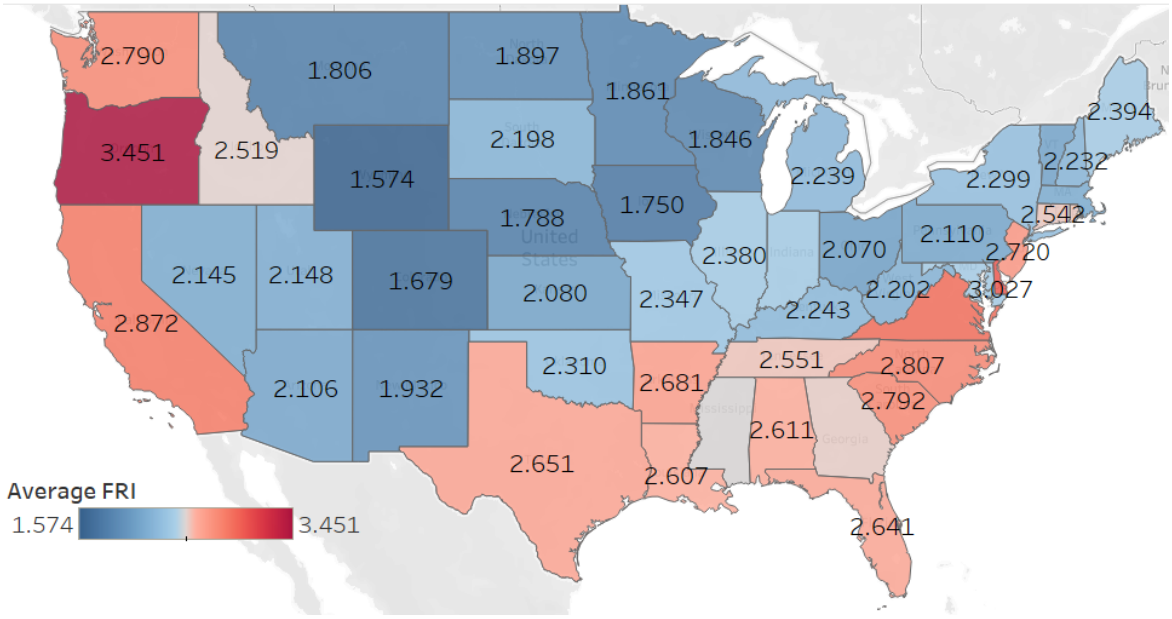

Figure 2-12: The spatial distribution of the average FRI over the different states

2.4. CONCLUSION

As the reports by the Insurance Information Institute and the World Economic Forum indicate, the damaging effect of flood events seem to increase over time, with no sign of a decreasing rate (Insurance Information Institute 2019; World Economic Forum 2019a). As such, flood damage assessment has been gaining more attention over the past decades. Several flood categorizations have therefore been developed in an effort to design effective preparedness plans under flood events. However, such categorizations incorporate the features of the flood hazard without considering the nature or resilience of the exposed system/community. In the current work, a new *community flood resilience-based* categorization framework was developed using an unsupervised machine learning

technique based on the different resilience metrics (i.e., the robustness and potential impacts on the exposed environment, and rapidity). The framework developed herein using unsupervised Machine Learning (ML) techniques, and is developed into three stages: *i) Data Preprocessing and visualization* where the available dataset is inspected and studied to determine its applicability within the proposed framework, *ii) ML Model Selection* where the appropriate ML model is selected that would yield the most applicability in this study, and finally *iii) Clusters' features analysis* to analyze the developed clusters, and define the features of the categories, upon which, actionable guidelines can be developed. To demonstrate the applicability of the proposed framework, it was applied on Flood disaster records collected by the NWS across the United States between 1996 and 2019 were adopted in the demonstration of the applicability of the proposed framework. The dataset includes direct property and crop damages, direct/indirect injuries and fatalities, duration of the flood event, and time of occurrence. A descriptive analysis was conducted and showed that the risk variables (i.e., duration, related damage, injuries, and fatalities) are highly interdependent. These risk variables are also characterized by heavy-tailed distributions with a significant number of extremes in all seasons. In contrast, event duration has a more prominent range with more extremes in the spring followed by the winter. Texas was found to sustain the most

damage, since it falls under a tropical weather region where numerous hurricanes and extreme rainfall events are likely to occur.

Three unsupervised machine learning techniques were subsequently utilized to develop the resilience-based flood risk categorization, including: Model-Based clustering, K-Means clustering, and SOM-ANN. Only the K-means and SOM-ANN-based clustering techniques were able to capture the variability within the dataset, enabling the development of a clear separation between different clusters. Accordingly, five community resilience-based flood categories were identified. The developed approach integrates the different components of resilience instead of the flood hazard characteristics as considered in earlier studies and regulations. A comparative spatial analysis was further conducted to assess the robustness of the different states to flood events. An average FRI was calculated for each state, Oregon was found to have the highest index, indicating its high susceptibility to damaging floods.

Overall, the framework developed in this study paves the way for a data-driven resilience based-categorization. It is worth noting that data-driven models typically cannot explain the physics and reasoning behind the results. Instead, data-driven models may generate more realistic and accurate and time-efficient predictions compared to physics-based models. To achieve the same level of accuracy using physics-based models, the modeling should account for different levels of complexity, especially those pertaining to interdependence, while also

accounting for the probabilistic nature of the hazard and the built community. As such, Machine Learning and Data-driven models have been gradually gaining more traction in resilience research (Haggag et al. 2020, 2021b). The data-driven categorization framework developed herein is expected to aid decision makers develop preparedness plans by identifying the most vulnerable communities through conduction a spatio-temporal comparative analysis and develop strategies to increase their resilience given available resources. The categorization can also facilitate the development of a prediction framework where, for example, climate indices act as predictors, ultimately aiding in the development of preparedness plans and policies to mitigate the risk of future hazards. This way, a model classifying the resilience of a community, based on its resilience metrics, can be developed, and validated. Further research can be implemented to advance this framework through 1) Incorporating more comprehensive variables within the dataset, giving more details to the type of flood, or vulnerable area. 2) Utilizing other Clustering techniques to account for mixed type data, and 3) Applying the framework while incorporating future flood projections to predict the expected change in the resilience of a certain community.

2.5. DATA AVAILABILITY STATEMENT

All the data and models developed herein or analyzed during the study are available from the corresponding author upon request.

2.6. ACKNOWLEDGMENT

The work presented herein is supported by the Vanier Canada Graduate Scholarship (Vanier-CGS), and the Natural Science and Engineering Research Council (NSERC) through the CaNRisk— Collaborative Research and Training Experience (CREATE) program. Additional support through the INViSiONLab and the INTERFACE Institute at McMaster University is also acknowledged.

2.7. REFERENCES

Abdel-Mooty, M. N., A. Yosri, W. El-Dakhakhni, and P. Coulibaly. 2021. "Community Flood Resilience Categorization Framework." Int. J. Disaster Risk Reduct., 61 (November 2020): 102349. Elsevier Ltd. https://doi.org/10.1016/j.ijdrr.2021.102349.

Alsabti, K., S. Ranka, and V. Singh. 1997. An efficient k-means clustering algorithm. Syracuse, Italy.

Ashari, A. 2013. "Performance Comparison between Naïve Bayes, Decision Tree and k-Nearest Neighbor in Searching Alternative Design in an Energy Simulation Tool." Int. J. Adv. Comput. Sci. Appl., 4 (11): 33–39.

Australian Institute for Disaster Resilience. 2017. Flood Emergency Response: Classification of the Floodplain. Guideline 7-2.

Baird, W. F. 2007. Flood damage estimation guide 2007 update and software guide.

Bertilsson, L., K. Wiklund, I. de Moura Tebaldi, O. M. Rezende, A. P. Veról, and M. G. Miguez. 2019. "Urban flood resilience – A multi-criteria index to integrate flood resilience into urban planning." J. Hydrol., 573 (February 2016): 970–982. Elsevier. https://doi.org/10.1016/j.jhydrol.2018.06.052.

Bishop, C. M. 2006. Pattern Recognition and Machine Learning. Springer. Springer US.

Boehmke, B., and B. M. Greenwell. 2019. Hands-On Machine Learning with R. Taylor & Francis.

Bose, I., and R. K. Mahapatra. 2001. "Business data mining - a machine learning perspective." Inf. Manag.

Breiman, L. 1996. Bagging Predictors.

Breiman, L., J. H. Friedman, R. A. Olshen, and C. J. Stone. 1984. Classification And Regression Trees. Routledge.

Brownlee, J. 2016. "Bagging and Random Forest Ensemble Algorithms for Machine Learning." Accessed May 12, 2021. https://machinelearningmastery.com/bagging-and-random-forest-ensemble-

algorithms-for-machine-learning/.

Brownlee, J. 2020. “How to Calculate Precision, Recall, and F-Measure for Imbalanced Classification.” Accessed June 16, 2021. https://machinelearningmastery.com/precision-recall-and-f-measure-for-imbalanced-classification/.

Bruneau, M., S. E. Chang, R. T. Eguchi, G. C. Lee, T. D. O’Rourke, A. M. Reinhorn, M. Shinozuka, K. Tierney, W. A. Wallace, and D. Von Winterfeldt. 2003. “A Framework to Quantitatively Assess and Enhance the Seismic Resilience of Communities.” Earthq. Spectra, 19 (4): 733–752. https://doi.org/10.1193/1.1623497.

Budiaji, W., and F. Leisch. 2019. “Simple K-Medoids Partitioning Algorithm for Mixed Variable Data.” Algorithms, 1–15. https://doi.org/10.3390/a12090177.

Celeux, G., and G. Govaert. 1995. “Gaussian parsimonious mixture models.” Pattern Recognit., 28 (5): 781–793.

Cimellaro, G. P., C. Fumo, A. M. Reinhorn, and M. Bruneau. 2009. Quantification of Disaster Resilience of Health Care Facilities. Mceer-09-0009.

Cooley, A., and H. Chang. 2017. “Precipitation intensity trend detection using hourly and daily observations in Portland, Oregon.” Climate, 5 (1). https://doi.org/10.3390/cli5010010.

Dawod, G. M., M. N. Mirza, K. A. Al-Ghamdi, and R. A. Elzahrany. 2014. "Projected impacts of land use and road network changes on increasing flood hazards using a 4D GIS: A case study in Makkah metropolitan area, Saudi Arabia." Arab. J. Geosci., 7 (3): 1139–1156. https://doi.org/10.1007/s12517-013-0876-7.

Downton, M. W., J. Z. B. Miller, and R. A. Pielke. 2005. "Reanalysis of U.S. National Weather Service flood loss database." Nat. Hazards Rev., 6 (1): 13–22. https://doi.org/10.1061/(ASCE)1527-6988(2005)6:1(13).

Downton, M. W., and R. A. Pielke. 2005. "How accurate are disaster loss data? The case of U.S. flood damage." Nat. Hazards, 35 (2): 211–228. https://doi.org/10.1007/s11069-004-4808-4.

Efron, B., and R. Tibshirani. 1986. "Bootstrap Methods for Standard Errors, Confidence Intervals, and Other Measures of Statistical Accuracy." Stat. Sci., 1 (1): 54–75.

ElSayed, M., M. Campidelli, W. El-Dakhakhni, and M. Tait. 2015. "Simplified Framework for Blast-Risk-Based Cost-Benefit Analysis for Reinforced Concrete-Block Buildings." J. Perform. Constr. Facil., 30 (4): 04015077. https://doi.org/10.1061/(asce)cf.1943-5509.0000767.

Ezzeldin, M., and W. E. El-Dakhakhni. 2019. "Robustness of Ontario power network under systemic risks." Sustain. Resilient Infrastruct., 1–20. Taylor &

Francis. https://doi.org/10.1080/23789689.2019.1666340.

FEMA. 2012. “Definitions of FEMA Flood Zone Designations.” 1–2.

FEMA. 2018a. Spring Flooding: Risks and Protection.

FEMA. 2018b. FEMA P-58-1: Seismic Performance Assessment of Buildings. Volume 1 – Methodology. Fema P-58.

Feofilovs, M., and F. Romagnoli. 2017. “Resilience of critical infrastructures: Probabilistic case study of a district heating pipeline network in municipality of Latvia.” Energy Procedia, 128: 17–23. Elsevier B.V. https://doi.org/10.1016/j.egypro.2017.09.007.

Fielding, A. H. 2006. “Introduction to classification.” Clust. Classif. Tech. Biosci., 78–96. Cambridge: Cambridge University Press.

FRED, F. R. B. of S. L. 2020. “U.S. Bureau of Labor Statistics, Consumer Price Index for All Urban Consumers: All Items in U.S. City Average [CPIAUCSL].” Accessed May 5, 2020. https://fred.stlouisfed.org/series/CPIAUCSL.

Ganguli, P., D. Paprotny, M. Hasan, A. Güntner, and B. Merz. 2020. “Projected Changes in Compound Flood Hazard From Riverine and Coastal Floods in Northwestern Europe.” Earth’s Futur., 8 (11). https://doi.org/10.1029/2020EF001752.

Ganguly, K. K., N. Nahar, and B. M. Hossain. 2019. “A machine learning-based prediction and analysis of flood affected households: A case study of floods in Bangladesh.” Int. J. Disaster Risk Reduct., 34 (March 2018): 283–294. Elsevier Ltd. https://doi.org/10.1016/j.ijdrr.2018.12.002.

Gentleman, R., K. Hornik, and G. Parmigiani. 2008. Bicondutor Case Studies.

Gnanaprakkasam, S., and G. P. Ganapathy. 2019. “Evaluation of regional flood quantiles at ungauged sites by employing nonlinearity-based clustering approaches.” Environ. Sci. Pollut. Res., 22856–22877. Environmental Science and Pollution Research. https://doi.org/10.1007/s11356-019-05473-8.

Goforth, E., M. Ezzeldin, W. El-Dakhakhni, L. Wiebe, and M. Mohamed. 2020. “Network-of-Networks Framework for Multimodal Hazmat Transportation Risk Mitigation: Application to Used Nuclear Fuel in Canada.” J. Hazardous, Toxic, Radioact. Waste, 24 (3). https://doi.org/10.1061/(ASCE)HZ.2153-5515.0000493.

Gondia, A., A. Siam, W. El-Dakhakhni, and A. H. Nassar. 2020. “Machine Learning Algorithms for Construction Projects Delay Risk Prediction.” J. Constr. Eng. Manag., 146 (1): 1–16. https://doi.org/10.1061/(ASCE)CO.1943-7862.0001736.

Gong, J., C. H. Caldas, and C. Gordon. 2011. “Learning and classifying actions of construction workers and equipment using Bag-of-Video-Feature-Words and

Bayesian network models." Adv. Eng. Informatics, 25 (4): 771–782. Elsevier Ltd. https://doi.org/10.1016/j.aei.2011.06.002.

Goos, G., J. Hartmanis, J. Van, L. E. Board, D. Hutchison, T. Kanade, J. Kittler, J. M. Kleinberg, F. Mattern, E. Zurich, J. C. Mitchell, M. Naor, O. Nierstrasz, B. Steffen, M. Sudan, D. Terzopoulos, D. Tygar, M. Y. Vardi, and G. Weikum. 2006. Computer Vision.

Haggag, M., M. Ezzeldin, W. El-dakhakhni, E. Hassini, and M. Haggag. 2020. "Resilient cities critical infrastructure interdependence: a meta-research." Sustain. Resilient Infrastruct., 00 (00): 1–22. Taylor & Francis. https://doi.org/10.1080/23789689.2020.1795571.

Haggag, M., A. S. Siam, W. El-Dakhakhni, P. Coulibaly, and E. Hassini. 2021a. "A deep learning model for predicting climate-induced disasters." Nat. Hazards, (0123456789). Springer Netherlands. https://doi.org/10.1007/s11069-021-04620-0.

Haggag, M., A. Yorsi, W. El-dakhakhni, and E. Hassini. 2021b. "Infrastructure performance prediction under Climate-Induced Disasters using data analytics." Int. J. Disaster Risk Reduct., 56 (February): 102121. Elsevier Ltd. https://doi.org/10.1016/j.ijdrr.2021.102121.

Hanewinkel, M., W. Zhou, and C. Schill. 2004. "A neural network approach to identify forest stands susceptible to wind damage." For. Ecol. Manage., 196

(2–3): 227–243. https://doi.org/10.1016/j.foreco.2004.02.056.

Hartigan, J. A., and M. A. Wong. 1979. “A K-means Clustering Algorithm.” J. R. Stat. Soc. Ser. C (Applied Stat., 28 (1): 100–108.

Hasan, R., L. Xu, and D. E. Grierson. 2002. “Push-over analysis for performance-based seismic design.” Comput. Struct., 80 (31): 2483–2493. https://doi.org/10.1016/S0045-7949(02)00212-2.

Hastie, T., R. Tibshirani, and J. Friedman. 2009. The Elements of Statistical Learning: Data Mining, Inference, and Prediction. Springer Ser. Stat. Springer US.

Hayhoe, K., D. J. Wuebbles, D. R. Easterling, D. W. Fahey, S. Doherty, J. Kossin, W. Sweet, R. Vose, and M. Wehner. 2018. “Our Changing Climate. In Impacts, Risks, and Adaptation in the United States: Fourth National Climate Assessment, Volume II.” Impacts, Risks, Adapt. United States Fourth Natl. Clim. Assessment, Vol. II, 72–144.

Hemmati, M., B. R. Ellingwood, and H. N. Mahmoud. 2020. “The Role of Urban Growth in Resilience of Communities Under Flood Risk.” Earth’s Futur., 8 (3). https://doi.org/10.1029/2019EF001382.

Holmes, W. 2011. National Earthquake Resilience. Natl. Earthq. Resil.

Insurance Information Institute. 2019. “Facts and Statistics: Global Catastrophes.”

Insur. Inf. Inst. Accessed October 17, 2019. https://www.iii.org/fact-statistic/facts-statistics-global-catastrophes.

Jaagus, J., and R. Ahas. 2000. “Space-time variations of climatic seasons and their correlation with the phenological development of nature in Estonia.” Clim. Res., 15 (3): 207–219. https://doi.org/10.3354/cr015207.

Jabareen, Y. 2012. “Planning the resilient city: Concepts and strategies for coping with climate change and environmental risk.” Int. J. Urban Policy Plan., (31): 220–229.

Jain, A. K., M. N. Murty, and P. J. Flynn. 2000. Data Clustering: A Review.

Khajwal, A. B., and A. Noshadravan. 2020. “Probabilistic Hurricane Wind-Induced Loss Model for Risk Assessment on a Regional Scale.” ASCE-ASME J. Risk Uncertain. Eng. Syst. Part A Civ. Eng., 6 (2): 1–9. https://doi.org/10.1061/AJRUA6.0001062.

Khalaf, M., A. J. Hussain, D. Al-Jumeily, T. Baker, R. Keight, P. Lisboa, P. Fergus, and A. S. Al Kafri. 2018. “A Data Science Methodology Based on Machine Learning Algorithms for Flood Severity Prediction.” 2018 IEEE Congr. Evol. Comput. CEC 2018 - Proc., 1–8. IEEE. https://doi.org/10.1109/CEC.2018.8477904.

King, R. D., S. Muggletont, R. A. Lewiso, and M. J. E. Sternberg. 1992. Drug

design by machine learning: The use of inductive logic programming to model the structure-activity relationships of trimethoprim analogues binding to dihydrofolate reductase (arfcl integence/ee acv/prote l/active sites). Biophysics (Oxf).

Kron, W. 2005. "Flood risk = hazard • values • vulnerability." Water Int., 30 (1): 58–68. https://doi.org/10.1080/02508060508691837.

Kwayu, K. M., V. Kwigizile, J. Zhang, and J. S. Oh. 2020. "Semantic N-Gram Feature Analysis and Machine Learning-Based Classification of Drivers' Hazardous Actions at Signal-Controlled Intersections." J. Comput. Civ. Eng., 34 (4). https://doi.org/10.1061/(ASCE)CP.1943-5487.0000895.

Li, Q. 2011. "A study on a new method for the analysis of flood risk assessment based on artificial neural network." Commun. Comput. Inf. Sci., 218 CCIS (PART 5): 262–266. https://doi.org/10.1007/978-3-642-23357-9_47.

Lian, J., H. Xu, K. Xu, and C. Ma. 2017. "Optimal management of the flooding risk caused by the joint occurrence of extreme rainfall and high tide level in a coastal city." Nat. Hazards, 89 (1): 183–200. Springer Netherlands. https://doi.org/10.1007/s11069-017-2958-4.

Liaw, A., and M. Wiener. 2002. Classification and Regression by RandomForest.

Linkov, I., T. Bridges, F. Creutzig, J. Decker, C. Fox-Lent, W. Kröger, J. H.

Lambert, A. Levermann, B. Montreuil, J. Nathwani, R. Nyer, O. Renn, B. Scharte, A. Scheffler, M. Schreurs, and T. Thiel-Clemen. 2014. "Changing the resilience paradigm." Nat. Clim. Chang., 4 (6): 407–409. Nature Publishing Group. https://doi.org/10.1038/nclimate2227.

MacQueen, J. 1967. "Some Methods for Classification and Analysis of Multivariate Observations." Proc. 5th Berkeley Symp. Math. Stat. Probab., 281–297.

Mccallum, A., and K. Nigam. 1998. A Comparison of Event Models for Naive Bayes Text Classification.

Mckinney, B. A., D. M. Reif, M. D. Ritchie, and J. H. Moore. 2006. BIOMEDICAL GENOMICS AND PROTEOMICS Machine Learning for Detecting Gene-Gene Interactions A Review. Appl Bioinforma.

Mcnicholas, P. D. 2016. "Model-Based Clustering." J. Classif., 373 (November): 331–373. https://doi.org/10.1007/s0035.

Menne, M. J., I. Durre, R. S. Vose, B. E. Gleason, and T. G. Houston. 2012. "An overview of the global historical climatology network-daily database." J. Atmos. Ocean. Technol., 29 (7): 897–910. https://doi.org/10.1175/JTECH-D-11-00103.1.

Menne, M. J., I. Durre, R. S. Vose, B. E. Gleason, and T. G. Houston. 2021. "Global Historical Climatology Network - Daily (GHCN-Daily), Version 3." NOAA

Natl. Clim. Data Cent. Accessed June 10, 2021. https://www.ncei.noaa.gov/access/metadata/landing-page/bin/iso?id=gov.noaa.ncdc:C00861.

Michelson, K., and H. Chang. 2019. "Spatial characteristics and frequency of citizen-observed pluvial flooding events in relation to storm size in Portland, Oregon." Urban Clim., 29 (May): 100487. Elsevier. https://doi.org/10.1016/j.uclim.2019.100487.

Minsker, B., L. Baldwin, J. Crittenden, K. Kabbes, M. Karamouz, K. Lansey, P. Malinowski, E. Nzewi, A. Pandit, J. Parker, S. Rivera, C. Surbeck, W. A. Wallace, and J. Williams. 2015. "Progress and recommendations for advancing performance-based sustainable and resilient infrastructure design." J. Water Resour. Plan. Manag., 141 (12). https://doi.org/10.1061/(ASCE)WR.1943-5452.0000521.

Mitra, P., R. Ray, R. Chatterjee, R. Basu, P. Saha, S. Raha, R. Barman, S. Patra, S. S. Biswas, and S. Saha. 2016. "Flood forecasting using Internet of things and artificial neural networks." 7th IEEE Annu. Inf. Technol. Electron. Mob. Commun. Conf. IEEE IEMCON 2016, 1–5. IEEE.

de Moel, H., and J. C. J. H. Aerts. 2011. "Effect of uncertainty in land use, damage models and inundation depth on flood damage estimates." Nat. Hazards, 58 (1): 407–425. https://doi.org/10.1007/s11069-010-9675-6.

Mojaddadi, H., B. Pradhan, H. Nampak, N. Ahmad, and A. H. bin Ghazali. 2017. "Ensemble machine-learning-based geospatial approach for flood risk assessment using multi-sensor remote-sensing data and GIS." Geomatics, Nat. Hazards Risk, 8 (2): 1080–1102. Taylor & Francis. https://doi.org/10.1080/19475705.2017.1294113.

Mosavi, A., P. Ozturk, and K. W. Chau. 2018. "Flood prediction using machine learning models: Literature review." Water (Switzerland), 10 (11): 1–40. https://doi.org/10.3390/w10111536.

Murdock, H. J. 2017. "Resilience of Critical Infrastructure to Flooding: Quantifying the resilience of critical infrastructure to flooding in Toronto, Canada."

Murnane, R. J., J. E. Daniell, A. M. Schäfer, P. J. Ward, H. C. Winsemius, A. Simpson, A. Tijssen, and J. Toro. 2017. "Future scenarios for earthquake and flood risk in Eastern Europe and Central Asia." Earth's Futur., 5 (7): 693–714. https://doi.org/10.1002/2016EF000481.

Murphy, J. D. 2018. NWSI 10-1605, Storm Data Preparation.

Nagpal, A. 2017. "Decision Tree Ensembles- Bagging and Boosting | by Anuja Nagpal | Towards Data Science." Accessed May 12, 2021. https://towardsdatascience.com/decision-tree-ensembles-bagging-and-boosting-266a8ba60fd9.

National Institute of Standards and Technology. 2020. COMMUNITY RESILIENCE PLANNING GUIDE FOR BUILDINGS AND INFRASTRUCTURE SYSTEMS: A Playbook. Gaithersburg, MD.

National Research Council. 1996. Measuring and Improving Infrastructure Performance. Meas. Improv. Infrastruct. Perform. Washington, DC: The National Academies Press.

Natural Resources Canada. 2017. "Canadian Guidelines and Database of Flood Vulnerability Functions." (March).

Netherton, M. D., and M. G. Stewart. 2016. "Risk-based blast-load modelling: Techniques, models and benefits." Int. J. Prot. Struct., 7 (3): 430–451. https://doi.org/10.1177/2041419616666455.

NOAA. 2017. Summary of natural hazard statistics for 2017 in the United States. Statistics (Ber).

NOAA. 2019. "National Climate Report - Annual 2018 | State of the Climate | National Centers for Environmental Information (NCEI)." Accessed May 5, 2020. https://www.ncdc.noaa.gov/sotc/national/201813#over.

NOAA. 2020. "U.S. high-tide flooding continues to increase | National Oceanic and Atmospheric Administration." Accessed June 10, 2021. https://www.noaa.gov/media-release/us-high-tide-flooding-continues-to-

increase.

NOAA Office for Coastal Management. 2021. “Texas.” Accessed June 10, 2021. https://coast.noaa.gov/states/texas.html.

Nofal, O. M., and J. W. van de Lindt. 2020. “Understanding flood risk in the context of community resilience modeling for the built environment: research needs and trends.” Sustain. Resilient Infrastruct., 00 (00): 1–17. Taylor & Francis. https://doi.org/10.1080/23789689.2020.1722546.

Nofal, O. M., J. W. van de Lindt, and T. Q. Do. 2020. “Multi-variate and single-variable flood fragility and loss approaches for buildings.” Reliab. Eng. Syst. Saf., 202 (March): 106971. Elsevier Ltd. https://doi.org/10.1016/j.ress.2020.106971.

Oregon Instute for Water and Watersheds. 2012. “Water and Climate in the Pacific Northwest.” 1–11.

Otterbach, J. S., R. Manenti, N. Alidoust, A. Bestwick, M. Block, B. Bloom, S. Caldwell, N. Didier, E. S. Fried, S. Hong, P. Karalekas, C. B. Osborn, A. Papageorge, E. C. Peterson, G. Prawiroatmodjo, N. Rubin, C. A. Ryan, D. Scarabelli, M. Scheer, E. A. Sete, P. Sivarajah, R. S. Smith, A. Staley, N. Tezak, W. J. Zeng, A. Hudson, B. R. Johnson, M. Reagor, M. P. Da Silva, and C. Rigetti. 2017. Unsupervised Machine Learning on a Hybrid Quantum Computer.

Park, D. C. 2000. “Centroid neural network for unsupervised competitive learning.” IEEE Trans. Neural Networks, 11 (2): 520–528. https://doi.org/10.1109/72.839021.

Patil, B. M., R. C. Joshi, and D. Toshniwal. 2010. “Missing Value Imputation Based on K-Mean Clustering with Weighted Distance.” 600–609.

Patil, C., and I. Baidari. 2019. “Estimating the Optimal Number of Clusters k in a Dataset Using Data Depth.” Data Sci. Eng., 4 (2): 132–140. Springer Berlin Heidelberg. https://doi.org/10.1007/s41019-019-0091-y.

Perica, S., S. Pavlovic, M. S. Laurent, C. Trypaluk, D. Unruh, and O. Wilhite. 2018. Precipitation-Frequency Atlas of the United States Volume 11 Version 2.0: Texas.

Priestley, M. J. N. 2000. “Performance based seismic design.” Bull. New Zeal. Soc. Earthq. Eng., 33 (3): 325–346. https://doi.org/10.5459/bnzsee.33.3.325-346.

Ragini, J. R., P. M. R. Anand, and V. Bhaskar. 2018. “Big data analytics for disaster response and recovery through sentiment analysis.” Int. J. Inf. Manage., 42 (May): 13–24. Elsevier. https://doi.org/10.1016/j.ijinfomgt.2018.05.004.

Rodrigues, M., and J. De la Riva. 2014. “An insight into machine-learning algorithms to model human-caused wildfire occurrence.” Environ. Model. Softw., 57: 192–201. Elsevier Ltd.

https://doi.org/10.1016/j.envsoft.2014.03.003.

Rözer, V., A. Peche, S. Berkhahn, Y. Feng, L. Fuchs, T. Graf, U. Haberlandt, H. Kreibich, R. Sämann, M. Sester, B. Shehu, J. Wahl, and I. Neuweiler. 2021. "Impact-Based Forecasting for Pluvial Floods." Earth's Futur., 9 (2). https://doi.org/10.1029/2020EF001851.

Salem, S., A. Siam, W. El-Dakhakhni, and M. Tait. 2020a. "Probabilistic Resilience-Guided Infrastructure Risk Management." J. Manag. Eng., 36 (6): 04020073. https://doi.org/10.1061/(asce)me.1943-5479.0000818.

Salem, S., A. Siam, W. El-Dakhakhni, and M. Tait. 2020b. "Probabilistic Resilience-Guided Infrastructure Risk Management." J. Manag. Eng., 36 (6): 04020073. https://doi.org/10.1061/(asce)me.1943-5479.0000818.

Seyed Shirkhorshidi, A., S. Aghabozorgi, and Y. Wah. 2015. "A Comparison Study on Similarity and Dissimilarity Measures in Clustering Continuous Data." https://doi.org/10.1371/journal.pone.0144059.

Shafizadeh-Moghadam, H., R. Valavi, H. Shahabi, K. Chapi, and A. Shirzadi. 2018. "Novel forecasting approaches using combination of machine learning and statistical models for flood susceptibility mapping." J. Environ. Manage., 217: 1–11. https://doi.org/10.1016/j.jenvman.2018.03.089.

da Silva, J., S. Kernaghan, and A. Luque. 2012. "A systems approach to meeting

the challenges of urban climate change." Int. J. Urban Sustain. Dev., 4 (2): 125–145. https://doi.org/10.1080/19463138.2012.718279.

Singh, H. 2018. "Understanding Gradient Boosting Machines | by Harshdeep Singh | Towards Data Science." Accessed May 12, 2021. https://towardsdatascience.com/understanding-gradient-boosting-machines-9be756fe76ab.

Stocker, T. F., Q. Dahe, G.-K. Plattner, M. M. B. Tignor, S. K. Allen, J. Boschung, A. Nauels, Y. Xia, V. Bex, and P. M. Vincent. 2013. Climate change 2013: The Physical Science Basis.

Swain, D. L., O. E. J. Wing, P. D. Bates, J. M. Done, K. A. Johnson, and D. R. Cameron. 2020. "Increased Flood Exposure Due to Climate Change and Population Growth in the United States." Earth's Futur., 8 (11). https://doi.org/10.1029/2020EF001778.

Sweet, W. V, G. Dusek, G. Carbin, J. Marra, D. Marcy, and S. Simon. 2020. "2019 State of U.S. High Tide Flooding and a 2020 Outlook." NOAA Tech. Rep., NOS CO-OPS (July): 1–12.

Trenberth, K. E., L. Cheng, P. Jacobs, Y. Zhang, and J. Fasullo. 2018. "Hurricane Harvey Links to Ocean Heat Content and Climate Change Adaptation." Earth's Futur., 6 (5): 730–744. https://doi.org/10.1029/2018EF000825.

Turkington, T., K. Breinl, J. Ettema, D. Alkema, and V. Jetten. 2016. “A new flood type classification method for use in climate change impact studies.” Weather Clim. Extrem., 14 (September): 1–16. Elsevier. https://doi.org/10.1016/j.wace.2016.10.001.

US Department of Commerce, NOAA, N. W. S. 2019. “Flooding in Oregon.” Accessed July 15, 2020. https://www.weather.gov/safety/flood-states-or.

Vrbik, I., and P. D. McNicholas. 2014. “Parsimonious skew mixture models for model-based clustering and classification.” Comput. Stat. Data Anal., 71: 196–210. Elsevier B.V. https://doi.org/10.1016/j.csda.2013.07.008.

Wagstaff, K., C. Cardie, S. Rogers, and S. Schrödl. 2001. “Constrained K-means Clustering with Background Knowledge.” Int. Conf. Mach. Learn. ICML, pages: 577–584.

Wilby, R. L., K. J. Beven, and N. S. Reynard. 2007. “Climate change and fluvial flood risk in the UK: more of the same?” Hydrol. Process., 2309 (December 2007): 2300–2309. https://doi.org/10.1002/hyp.

Witten, I. H., E. Frank, M. A. Hall, and C. J. Pal. 2017. Data Mining Practical Machine Learning Tools and Techniques Fourth Edition.

World Economic Forum. 2019a. The Global Risks Report.

World Economic Forum. 2019b. The Global Risks Report 2019 14th Edition.

Wu, T. F., C. J. Lin, and R. C. Weng. 2004. “Probability estimates for multi-class classification by pairwise coupling.” J. Mach. Learn. Res., 5: 975–1005.

Yagci, K., I. S. Dolinskaya, K. Smilowitz, and R. Bank. 2018. “Incomplete information imputation in limited data environments with application to disaster response.” Eur. J. Oper. Res., 269 (2): 466–485. Elsevier B.V. https://doi.org/10.1016/j.ejor.2018.02.016.

Zhang, H. 2004. The Optimality of Naive Bayes.

Zumel, N., and J. Mount. 2020. Practical Data Science with R.

Chapter 3

DATA-DRIVEN COMMUNITY FLOOD RESILIENCE PREDICTION

ABSTRACT

Climate change and the development of urban centers within flood prone areas have significantly increased in flood-related disasters worldwide. However, most flood risk categorization and prediction efforts have been focused on the hydrologic features of flood hazards, often not considering subsequent long-term losses and recovery trajectories (i.e., community's flood resilience). In this study, a two-stage Machine Learning (ML) based framework was proposed to accurately categorize and predict communities' flood resilience, and their response to future flood hazards. This framework is a step towards developing a comprehensive proactive flood disaster management plan to further ensure functioning urban centers and mitigate the risk of future catastrophic flood events. In this framework, resilience indices are developed considering resilience goals (i.e., Robustness and Rapidity) using unsupervised ML, coupled with climate indices to develop a supervised ML prediction algorithm. To showcase the utility of the framework, the data-driven approach was applied on historical flood disaster records collected by the US National Weather Services. These disaster records were subsequently used to develop the resilience indices, which were then coupled with associated historical climate data resulting in high accuracy predictions, and thus utility in flood resilience management studies. To further demonstrate the utilization of the framework, a spatial analysis was developed to quantify community's flood resilience and vulnerability across the selected spatial domain. The framework

presented in this study is employable in climate studies and Spatio-temporal vulnerability identification, Such a framework can empower decision makers to develop effective data-driven climate resilience strategies.

KEYWORDS: Community Resilience; Data-driven Methods; Machine Learning; Resilience; Flood Hazard.

The work in this chapter appears in the Manuscript published in the MDPI Water Journal. Minor modifications were made to improve the clarity of this work within the context of the thesis. The following is the citation of the published article:

Abdel-mooty, M. N., W. El-dakhakhni, and P. Coulibaly. 2022. "Data-Driven Community Flood Resilience Prediction." *Water (Switzerland)*, 14 (13): 2120. https://doi.org/10.3390/w14132120.

3.1. INTRODUCTION

The severity of climatological and hydrological hazards has been increasing over the past decades, with especially higher frequency of flood hazard over the past three decades, heavily impacting the livelihood of exposed communities (Dawod et al. 2014; Lian et al. 2017; Wilby et al. 2007). The changing climate has been significantly affecting the weather conditions and climatological factors (i.e., mean temperature, humidity, and precipitation) (Linkov et al. 2014; Stocker et al. 2013). Data records since 1996 show that in North America, and similarly around the world, the rate of extreme weather events and rainfall (i.e., more than 100 mm of rainfall in 24 hours) is alarmingly increasing, accompanied by an increased frequency of floods (Bertilsson et al. 2019). This is attributed to the higher rate of urbanization into flood-prone areas, where the urban environment now hosts over 50% of the world's population, with an expected increase to 70% by the year 2050, boosting the probability of flood related disasters through the vulnerable community's exposure (NOAA 2019; da Silva et al. 2012).

As a direct consequence of such increase in flood exposure and related losses, flood disaster management stakeholders have been moving to adopt a proactive risk-mitigation response, rather than a reactive post-disaster response approach(de Moel and Aerts 2011; World Economic Forum 2019). However, flood risk needs first to be quantified in order to efficiently develop better mitigation strategies and eventually enhance the resilience. In this respect, flood risk is identified as the

expected damage (i.e., consequence), resulting from a hazard's probability of occurrence, coupled with the at-risk-community's exposure and vulnerabilities, considering the levels of different uncertainties (Kron 2005; Nofal and van de Lindt 2020; Salem et al. 2020a).

With the increasing climatological disasters and flood risk, community resilience research is steadily gaining more traction worldwide. While a community is defined as "Place designated by geographical boundaries that function under the jurisdiction of a governance structure (e.g., town, city, or county)" (National Institute of Standards and Technology 2020), community resilience is the ability of a community to adapt to, predict, and rapidly recover from future disruptions back to a predefined target state (National Institute of Standards and Technology 2020). Flood risk is a result from the simultaneous realization of three aspects; i) flood hazard: the potential, or probability, of a flood event of certain characteristics occurring at a given location, ii) flood vulnerability: a measure of the susceptibility, and the adaptability, of the exposed community to the flood hazard, and finally iii) flood exposure: the assets, humans and otherwise (i.e., infrastructure systems), that are located in a flood-prone area (Jabareen 2012; Kron 2005; Nofal and van de Lindt 2020). This indicates that a severe flood hazard does not necessarily yield a high-risk flood, as it can occur in an area with a low number of exposed elements, but flood risk can be quantified only when the exposed and vulnerable community prone to said hazard are coupled with the hazard realization (Netherton and Stewart

2016; Salem et al. 2020a). As an extension, resilience analysis evaluates the extended functionality loss and recovery trajectory of communities prone to flood hazard, taking into account the direct and indirect losses, as well as restoration costs (Linkov et al. 2014; Salem et al. 2020a).

Previously, resilience has been defined differently across different fields, however in the context of this study, resilience is defined as the ability to resist being affected by, and rapidly recover from some external disturbance (Cimellaro et al. 2009). Resilience is quantified through the four attributes including: two objectives (i.e., goals) of resilience: Robustness and Rapidity, enabled by two means: Resourcefulness and Redundancies (Bruneau et al. 2003; Murdock 2017). Robustness is the inherent ability of the system to retain its functionality level when exposed to stress or extreme demand; Rapidity is the time needed for the system to bounce back to a certain predefined target functionality level; Resourcefulness is the availability of adequate resources within the system to maintain its functionality under extreme demand levels, and finally; Redundancy is the availability of alternate components to maintain functionality during the external hazard (Bruneau et al. 2003; Minsker et al. 2015). It is worth noting that the rapidity measures the total time needed for the system to bounce back to its target functionality, including the downtime of the system (i.e., the duration of the hazard itself).

Over the years, numerous researchers have embarked on flood categorization and prediction studies (Australian Institute for Disaster Resilience 2017; FEMA

2012; Ragini et al. 2018; Turkington et al. 2016). However, most of such studies focused on the hazard's features, and to a lesser extent on the direct impact and losses due to the flood hazard, or long-term recovery cost and time (Ganguli et al. 2020; Ganguly et al. 2019; Hemmati et al. 2020; Murnane et al. 2017; Rözer et al. 2021; Swain et al. 2020). In this respect, this study aims at developing a prediction framework that classifies the long-term potential impacts, recovery, and resilience of the exposed community, a categorization that captures the resilience of the exposed communities rather than simply the hazard's characteristics. To achieve that, reliable data is imperative to accurately incorporate said damage and characteristics within an objective data-driven resilience prediction framework (Downton and Pielke 2005).The incorporation of the hazard, system vulnerability, and exposure employed in this framework would result in a comprehensive capture of the short-term potential impacts, direct and otherwise, of the flood event through robustness assessment (i.e., flood risk), as well as the long-term impact on the exposed community through rapidity evaluation (i.e., resilience assessment). The study presented herein is employable in vulnerability identification and flood prediction studies, providing an imperative decision support tool for stakeholders and policymakers to allocate resources and potentially save billions of dollars.

3.2. FLOOD RESILIENCE PREDICTION FRAMEWORK

3.2.1. FRAMEWORK DESIGN AND LAYOUT

The aim of this research is to develop a flood resilience prediction framework that captures the probable and resulting impacts of floods on respective exposed communities. Such framework would serve as a practical data-driven tool for quick and actionable early warning system. Such system will aid policy and decisionmakers in developing resilience-guided risk management strategies accounting for the four attributes of resilience. Classification and data driven models require a sufficient number of observations in a dataset to allow for meaningful classification and clustering (Turkington et al. 2016). While this necessitates the accessibility to a large volume of high-quality data, there are also alternative ways to account for missing data within an employable dataset.

As can be seen in Figure 3-1, the framework presented herein is comprised of two main parts: a) Resilience-based categorization, and b) Resilience-based prediction, and each part of the framework is comprised of different stages.

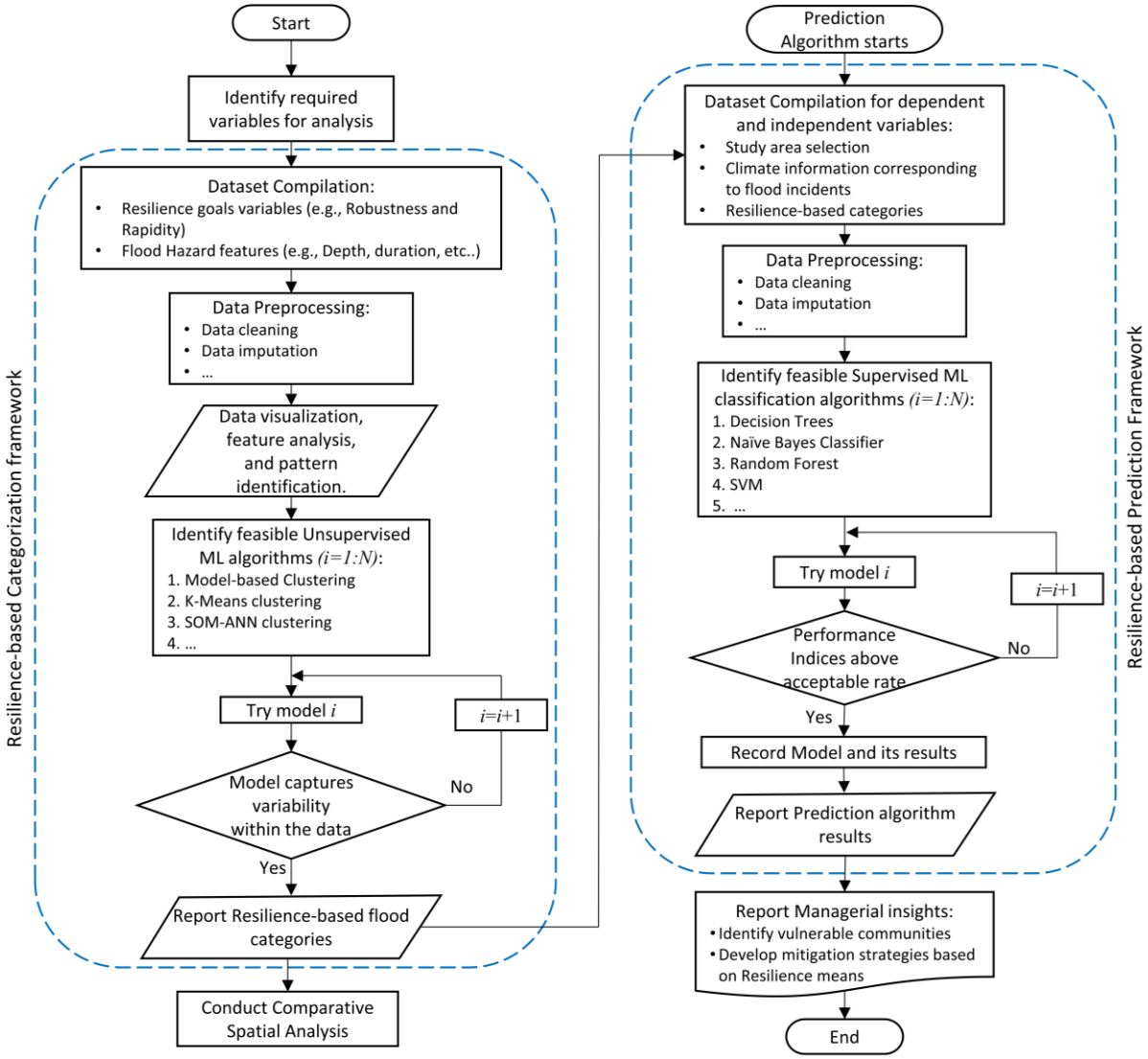

Figure 3-1: Multi-stage framework layout for resilience-based flood categorization and prediction

Part (a): Resilience-based categorization framework: this part is divided into three main stages: Stage i) Data Compilation, Cleaning and Visualization: The first step is to compile a comprehensive dataset, with enough variables to capture the resilience attributes, as well as the features of the flood events (e.g., flood depth and

duration). Following data gathering, data preprocessing starts to ensure its suitability for a reliable analysis, and data imputation for missing values. Datasets are investigated for the identification of any biases or skewness within the dataset, as well as the accommodation for missing data. Missing data can induce disruptions in the ML algorithm, rendering it essential to replace or remove observation with missing variables. Accounting for missing variables can be done through multiple approaches, 1] by removing observations with missing variables altogether, 2] averaging the readings from other nearby observations with similar conditions to the observation with missing variables, or 3] using unsupervised learning to cluster the dataset and take the average of the cluster variables as the reading for the missing variables. In this study, a combination between approach 1 and 2 were employed (Haggag et al. 2021b; Patil et al. 2010; Yagci et al. 2018).

Finally, data visualization is conducted to identify inherent characteristics and interdependencies within the dataset, which is pivotal in choosing an appropriate model for the following stage.

Stage ii) Selection of Machine Learning (ML) Model: ML models are designed to analyze high-dimensional data. It has been utilized across different fields such as engineering, biology and medicine, and in different applications such as banking, targeted advertisement, social networks, and image and pattern recognition (Bose and Mahapatra 2001; Goos et al. 2006; King et al. 1992; Mckinney et al. 2006). ML models are used to identify pattens and discover behaviors in large datasets, while

continuously adapting to new data features to enhance model performance. ML are expected to handle large datasets with complex interdependent features, and identify hidden patterns (Hastie et al. 2009). ML models are divided into supervised and unsupervised algorithms (also named classification and clustering algorithms, respectively), and will be discussed in more detail in the following section. In the proposed framework, the categorization in part (a) employs unsupervised (clustering) techniques, while part (b) employs supervised (classification) algorithms (Gentleman et al. 2008; Hastie et al. 2009).

Stage iii) Features and Clusters Analysis: The results of stage ii in part (a) are used in developing the features of each category (cluster). By conducting a feature analysis, the developed clusters can be used in developing a spatial analysis to identify vulnerable communities based on the considered resilience metrics. The deployment of the clustering algorithm results ensures the development of unbiased managerial insights, facilitating the decision-making process for utilizing the resilience means (i.e., Redundancies, and Resourcefulness) to better enhance the resilience of the more vulnerable communities. The developed clusters in Part (a) are vital in the development of the predictive analysis in Part (b), where this categorization framework can aid decision makers in translating predicted flood hazards and risks into actionable plans, increasing the robustness by reducing the loss of functionality, and ensuring a quick recovery to the target state.

Part (b): Resilience-based Prediction Framework: Similar to Part (a), Part (b) is also comprised of different stages, while these stages are similar in concept with their counterparts in Part (a), the details and the nature of the algorithms differ greatly.

Stage (i) Data Compilation: The first step is compiling the dependent and independent variables of the dataset. In this stage, the study area is identified for the development of the predictive model where the features, characteristics, and exposure are fairly similar. The dependent variables selected for this framework are climate information corresponding to recorded flood events (e.g., maximum temperature, minimum temperature, precipitation, wind speed, air pressure, humidity, etc. …) whereas the independent variable would be the resilience-based categories developed in part (a) of the proposed framework. Similar to most ML algorithms, the dataset should be comprehensive and of good quality and diversity to produce actionable results. Data imputation and cleaning are conducted to ensure the reliability of the data and avoid skewness and imbalances in the dataset.

Stage (ii) Data preprocessing and analysis: For this stage, the gathered dataset is studied to identify the interrelationship between the different variables, and thoroughly examine which variables to be included in the analysis to reduce the noise in the data while ensuring that all the resilience metrics and the hazard features are comprehensively represented. This feature selection can be achieved through exploratory and sensitivity data analysis, feature selection, or correlation

analysis between different variables of the available data. Following that step, data cleaning and preprocessing commences. The performance of data-driven models are strictly tied to the quality and quantity of the dataset involved in the development of the model, as finding a readily available dataset that matches all the required criteria for analysis is typically very challenging. Therefore, numerous methods have been developed to deal with missing data, unbalanced data, and skewed data (e.g., Data imputation, removing datapoints with missing variables, take average readings from nearby sources, etc. …) (Patil et al. 2010; Patil and Baidari 2019; Yagci et al. 2018).

Stage (iii) Development and testing of Machine Learning Models: In this stage, a supervised ML model is developed to predict flood resilience categories based on climate data corresponding to the recorded flood events. Supervised ML models can be used in predicting discreet, continuous, or categorical data. The classification required for the analysis herein falls under the multi-class classification category, where the dependent variables are used to predict a categorical independent variable, of more than 2 classes (Wu et al., 2004). For this classification, different algorithms were validated and tested to determine the most suitable algorithm for the current dataset (e.g., Naïve Bayes Classifier, Support Vector Machine, Decision Trees, Artificial Neural Networks, Ensemble techniques, etc. …), where they were assessed based on a common performance criteria, to be explored further in the

Methodology section (Haggag et al. 2021b; Mojaddadi et al. 2017; Mosavi et al. 2018; Shafizadeh-Moghadam et al. 2018).

3.2.2. METHODOLOGY

Machine Learning is an artificial intelligence tool designed to learn autonomously from a training dataset, mimicking the behavior of the human brain through the learning process. By deploying ML models on appropriate datasets, the model extract the dataset's inherent features, and adjust itself to better enhance its performance(Rodrigues and De la Riva 2014). As mentioned, ML models are broadly divided into two types, supervised and unsupervised learning models, where they use labelled and unlabeled data, respectively, for training and validation. In the field of natural hazard and community resilience, ML and data-driven models have been recently employed in achieving the overarching goal of increasing community resilience in face of natural and anthropic hazards (Ganguly et al. 2019; Haggag et al. 2021a; Hanewinkel et al. 2004; Rodrigues and De la Riva 2014; Shafizadeh-Moghadam et al. 2018). For the framework developed herein, both ML model types are utilized, where the unsupervised learning is utilized in the development of the community resilience categories, and supervised ML techniques are employed to predict the community resilience metrics under future flood hazards.

UNSUPERVISED LEARNING: CLUSTERING

Unsupervised ML models use partitioning algorithms to cluster observations based on a predefined similarity measure, such that observations with common features are placed in the same cluster (Otterbach et al. 2017). This is an unguided process that does not require a predefined objective, ensuring that the clustering is based on inherent features of the dataset. This similarity measure is assessed by measuring the distance between different observations, where two, or more, observations are considered similar when the distance between them is minimal. Henceforth, observations within a cluster should be closer to one another than that of other clusters.

Choosing the similarity measure depends heavily on the type of data, and objective of the study, such measures include: Euclidean, Cosine similarity, Manhattan, and Gower distances (Jain et al. 2000). For this study, multiple similarity measures were explored to determine their applicability with the available mixed-type dataset (i.e., dataset containing both categorical and numerical data). For Gower distance within Partitioning Around Medoids algorithm, the developed dissimilarity matrix from the dataset was skewed, which results in a biased algorithm favoring seasonal clustering instead of resilience-based clustering. Eventually, weighted Euclidean distance was adopted in this study as it measures the weighted proximity of the observations within a three-dimensional space (Jain

et al. 2000; Seyed Shirkhorshidi et al. 2015). It is important to note that other approaches could also be employed in the current study.

For the framework presented herein, two clustering algorithms were employed to develop the resilience-based flood categories. Namely: K-means clustering, and Self Organizing Maps. K-means clustering technique, and its variations, are the most heavily used partitioning (clustering) algorithm (MacQueen 1967), where observations are divided into a predefined number of clusters (*K)*. Prior to the partitioning algorithm, multiple values are assumed for *K,* and the optimal value is that with the minimum intra-cluster variation (i.e., the total within-cluster sum of squares (WSS)). For the current study, the WSS utilized the squared Euclidean distance between the observations and their respective cluster's centroid (Alsabti et al. 1997; Hartigan and Wong 1979; Wagstaff et al. 2001).

SOM is a type of Artificial Neural Networks (ANN) algorithm that is trained to cluster data into groups in an unsupervised approach. The input space is organized according to a predefined topology of neurons, where each neuron is assigned a number of observations. ANN is an artificial intelligence techniques by which complex relationships, and interrelationships, within a dataset are uncovered automatically based on inherent patterns in the dataset (Mitra et al. 2016; Park 2000), by mimicking the behavior of the human brain when transmitting signals through neurons, albeit through artificial neurons. There have been numerous ANN techniques developed to date, each of which may befit a specific application (e.g.,

self-organizing maps, recurrent neural networks, and feed-forward back-propagation neural networks). However, ANN is more commonly employed in predictive algorithms (Khajwal and Noshadravan 2020; Kwayu et al. 2020; Mitra et al. 2016) and pattern recognition applications (Gnanaprakkasam and Ganapathy 2019; King et al. 1992; Park 2000; Turkington et al. 2016). For the study presented herein, SOM was utilized using the Deep Learning Toolbox in MATLAB, where the Kohonen rule was adopted (Abdel-Mooty et al. 2021; Park 2000).

SUPERVISED LEARNING: CLASSIFICATION

Classification is a supervised ML technique that learns and utilizes features of a dataset to derive patterns and classify new input data. Supervised ML models learn from a training dataset, which is comprised of dependent (i.e., predictor variables) and independent variables (i.e., predictand variable), and applies the identified patterns on a testing dataset, while applying optimization techniques to increase the model's performance (Khalaf et al. 2018; Mosavi et al. 2018; Zumel and Mount 2020). Numerous classification techniques have been developed to date (e.g., continuous, discreet, numerical, or categorical). In the present study, the independent variable is class-based, therefore multiclass classification techniques will be employed in the current study (e.g., Naïve Bayes classifier, Classification Trees, Support Vector Machine, ANN, etc.). To improve the performance of said

models, classification models employ ensemble techniques— bagging, random forest, boosting (Boehmke and Greenwell 2019; Nagpal 2017; Singh 2018).

Naïve Bayes Classification

Naïve Bayes Classifier algorithm employs Bayes' theorem with the assumption that the variables are conditionally independent given the value of the class variable (i.e., Naïve). The algorithm employs joint conditional probabilities of the dependent variable of the training dataset given their respective independent variable (Gondia et al. 2020; Gong et al. 2011; Wu et al. 2004). The output of said model is the conditional probabilities of the class labels assigned based on the highest class-label's joint probability for each observation in the dataset. The theorem employed in this algorithm calculates the conditional probability for class variable *y* using equation (3-1), where (x_1, …, x_n) are the *n* dependent variables.

$$P(y|x_1, \dots, x_n) = \frac{P(y)P(x_1, \dots, x_n|y)}{P(x_1, \dots, x_n)} \tag{3-1}$$

By applying the naïve assumption for all *i*, and substituting with $P(x_1, \dots, x_n)$ as a constant, the resulting conditional probabilities can be expressed as equation (3-2):

$$P(y|x_1, \dots, x_n) \propto P(y)\Pi_{i=1}^{n} P(x_i\,|y) \tag{3-2}$$

Where i=1, …, n. This theorem can be interpreted such that a data record belongs to a certain class (M) when the conditional probability $P(M_i|x_1, \dots, x_n)$ returns the highest value of all classes. The reader is referred to the studies by Mccallum & Nigam (1998) and Zhang (2004) for further details on Naïve bayes classification.

Decision Trees

Within the Classification and Regression Trees (CART) algorithm, classification trees are utilized to predict categorical (discriminate) data, unlike regression trees which deal with predicting continuous independent variables (Mosavi et al. 2018).

Decision Trees (DT) utilize a binary recursive partitioning algorithm, since each split (i.e., rule or partitioning step) depends on the prior splitting step. The data is partitioned into homogenous subgroups (i.e., nodes) using binary Yes-or-No questions about each feature of the sub-group, where this process is repeated until a suitable stoppage criterion is reached (e.g., maximum number of splits). For each split, the objective is to identify the optimum feature upon which the data can be split, where the overall error between the actual response and the predicted response is minimal. The analysis presented herein is concerned with classification trees, where the partitioning is set to maximize the cross-entropy or the Gini index (Breiman et al. 1984; Hastie et al. 2009). The Gini index is a measure of purity (or impurity) in the classification model, where a small value indicates that a subgroup

(i.e., node) contains predominantly observations from a similar class. High values of mean decrease in Gini index correspond to a more important variable (i.e., feature) within the classification model (Hastie et al. 2009). The Gini index is relied upon given the type of data utilized in the demonstration application presented later in this study.

For model accuracy and performance enhancement, there exist numerous employable ensemble techniques (e.g., bagging, boosting, and random forest) (Boehmke and Greenwell 2019; Nagpal 2017). Bagging is a bootstrap aggregating technique used for fitting multiple versions of the model drawn from the training dataset. Bootstrapping is a random sampling technique of the data, taken by replacement, such that a datapoint can still be available for selection in subsequent models, while using all the predictors for the sampling technique (Efron and Tibshirani 1986). Each model is then used to generate training for the Decision Tree model, and the averaging of all the predictions is subsequently used, resulting in a more robust model than a single tree (Breiman 1996; Breiman et al. 1984; Nagpal 2017).

Random forest further improves over bagging techniques to enhance model performance, where the selection of the predictors is also randomized at each split at the node within the tree rather than using all the predictors. The size of the tree is maximized by repeating the aforementioned process iteratively, and the prediction is based on the aggregation of the prediction from the total number of

trees (Brownlee 2016; Feofilovs and Romagnoli 2017; Fielding 2006; Liaw and Wiener 2002; Nagpal 2017).

Prediction Model Performance

For classification models, the overall model accuracy and misclassification errors are widely used. However, this criterion is not always suitable for asymmetric or skewed datasets where the majority of the data falls within a single category. To introduce a more accurate measure of the predictive performance, the Precision, Recall, and F1-score for each category in the testing and training datasets were calculated. In this respect, Precision is the number of correct predictions per class within multiclass classification, which is a measure of how accurate each class prediction is. Recall (i.e., sensitivity) on the other hand is the number of correct class predictions out of all correct examples in the dataset, it captures the ratio between the correct classifications and the actual classification for the dataset. Finally, the F1-score is considered an integration between the Precision and Recall of the model, where it balances the concerns of both performance measures (Brownlee 2020). Precision, Recall, and the F1-score are evaluated according to equations (3-3), (3-4), and (3-5) respectively, where the information can be extracted from the confusion matrix of each model.

$$Precision = \frac{TP}{TP + FP} \tag{3-3}$$

$$Recall = \frac{TP}{TP + FN} \tag{3-4}$$

$$F1\text{–}score = 2 * \frac{Precision * Recall}{Precision + Recall} \tag{3-5}$$

In the equations above, TP refers to **T**rue **P**ositive, which is the number of correctly predicted observations, and FP refers to **F**alse **P**ositive which is the number of predictions incorrectly assigned to a class, whereas FN refers to **F**alse **N**egative which is the number of observations incorrectly assigned to a wrong class (Khalaf et al. 2018).

3.3. FRAMEWORK APPLICATION DEMONSTRATION

To showcase the employability of the developed framework, the data from the National Weather Service (NWS) was adopted for the derivation of the resilience-based categories. Subsequently these categories were then coupled with climate data extracted from the National Oceanic and Atmospheric Administration's (NOAA) National Centers for Environmental Information. The framework was thus applied to: *i*) identify the features of the exposed communities along with their vulnerability using descriptive data analysis, *ii*) identify interdependence between different features of the adopted dataset to appropriately choose a suitable ML model, *iii*) categorize the communities' flood resilience by combining flood features with resilience metrics within the dataset (i.e., Robustness and Rapidity),

iv) test the model performance in terms of accurately predicting the communities' resilience when exposed to flood hazard, using climate data as predictand.

The earlier work presented in the study by Abdel-Mooty et al. (2021) serves as a foundation for the categorization stage of the prediction framework developed herein. In their study, Abdel-Mooty et al. (2021) developed a flood resilience categorization, resulting in 5 community flood resilience categories. These categories are thus employed through the second stage of the framework developed in the current study. In the following section, a brief summary of their findings is presented, followed by a description of the flood prediction demonstration.

3.3.1. PART (A): RESILIENCE-BASED CATEGORIZATION

In the first stage, the dataset compiled by the NWS was employed. This dataset is one of the longest-run annual flood damage recorded in the United States (Murphy 2018). The data are gathered through third party organizations, and directly reported to the NWS database according to the predefined guidelines. As such, the quantity and quality of the gathered data is governed by the available resources (e.g., time and funding availability) of said agencies (Murphy 2018). The dataset contains records of flood events occurring across the United States between 1996 and 2019. The related damages, time, geographical center, month, and year for each recorded flood event are compiled within this database (Downton et al. 2005; Murphy 2018). Within the dataset, the recorded damage was divided into property and crop damages, which were subsequently combined into a single

variable within the analysis named *Monetary Damages*. It is worth noting that the damages recorded in this dataset pertains to only the direct damage resulting from the flooding water on the exposed assets and does not considering the indirect (cascade) damages (e.g., opportunity loss). Within the present dataset the term "flood event" refers to only the flooding aspect of any natural disaster. Despite the aforementioned limitations, this dataset is still considered one of the best resources for flood damage records in the United States (Downton et al. 2005; Downton and Pielke 2005). Figure 3-2(a) shows a temporal analysis, while Figure 3-2(b) shows a spatial analysis of the flood events occurring within the same period, where the numbers on each state are the number of recorded floods, and the colors are used to indicate the relative total monetary damage of each state. This analysis shows that the largest number of records and the largest monetary damage are within the state of Texas. This is attributed to the increased heat content over the western Gulf of Mexico, as it produces higher humidity and temperature. This heat content is directly proportional to the precipitation resulting from different storms (Trenberth et al. 2018), and can also be attributed to the tropical weather region that Texas falls within, given that this region is susceptible to a large number of devastating hurricanes and extreme rainfall, coupled with the increased exposure caused by the increased urbanization rate (FEMA 2012).

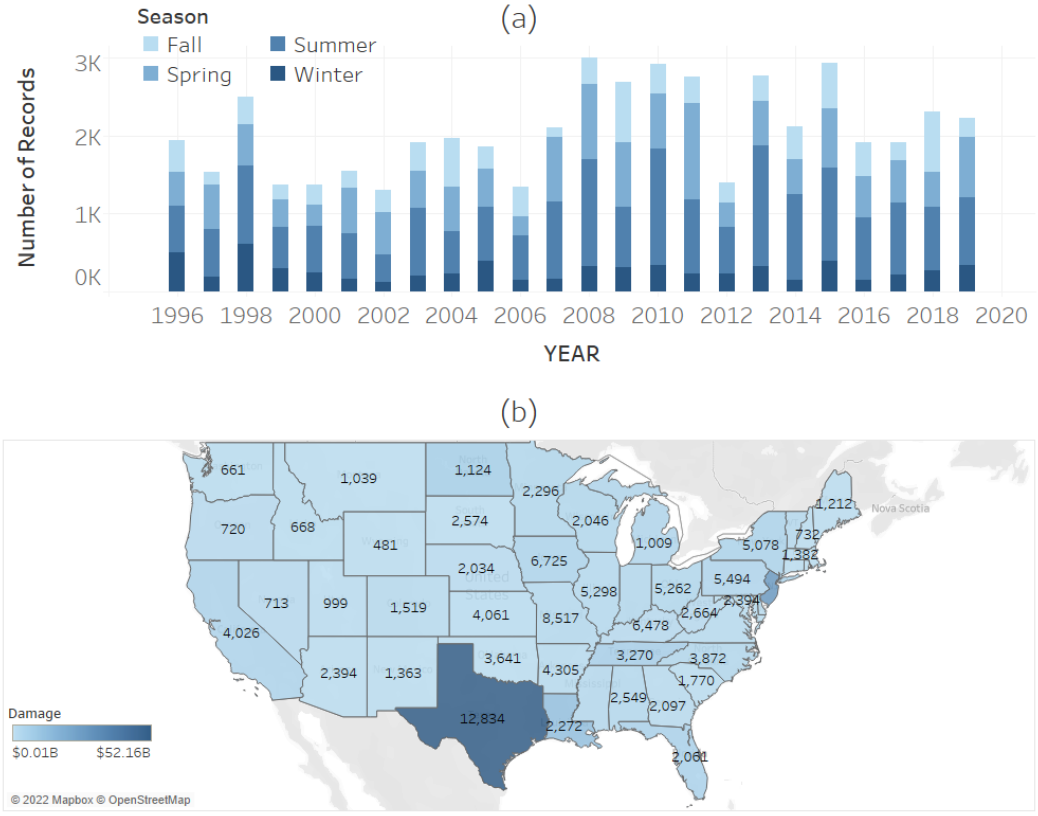

Figure 3-2: Descriptive Spatio-temporal Analysis of the employed dataset where (a) the annual number of floods between 1996 and 2019 indicated by season, and (b) a multilayer spatial analysis of the dataset with the total number of records and the total damage in US$ per state indicated by color.

Considering the objective of the current study, incorporating resilience metrics is key in identifying resilience-based categories. As such: *i*) the flood records that did not cause any monetary damage, injuries, or fatalities were excluded from the dataset, as they will not produce any resilience metrics to measure, and will induce bias within the categorization model, *ii*) the property and crop damage were summed up into a total monetary damage, and as mentioned earlier was adjusted to

accommodate the inflation rate over the years using the Customer Price Index from the Bureau of Labor Statistics (FRED 2020). This monetary damage, along with the injured people and fatalities represent the Robustness of the exposed community, while the duration of the flood event represents downtime of the exposed community, which is a component of the Rapidity metric.

The analysis showed that: i) flood events that occurred during the spring were split into two categories based on their impacts, ii) flood events causing longer disruptions were separated in a separate cluster, identifying a correlation between event duration and the impact of the flood event on the exposed community (i.e., relating robustness with rapidity and overall resilience), iii) flood events that resulted in loss of human lives were clustered together. Events falling in Categories 1,2, and 4 are more common than categories 3 and 5 in terms of annual number of events. Given the multidimensional nature of resilience, more emphasis in the analysis was places on the value of human injuries and fatalities than monetary loss. As such, although events in Category 3 follow those of Category 5 in terms of average damage per event, events falling in Category 4 follow that of category 5 in terms of average affected people per event, hence it was assigned a higher Category than Category 3. It should be recalled that the event duration mentioned herein is the hazard's duration, which represents the down time of the community before the initiation of recovery efforts, representing a part of the total Rapidity of the community. It is also worth noting that longer flood duration corresponds to a less

robust infrastructure system (e.g., drainage networks) to accommodate the hazard's capacity effectively, resulting in a lower overall resilience of the exposed community. The results were analyzed for the inherent features of each cluster, and each category was assigned a Flood Resilience Index (FRI) that increases gradually as the robustness decreases (i.e., functionality loss increases). As such, communities that are exposed to flood disasters with impacts falling in Category Ɱ are more resilient than those of Category Ɱ+1, with Ɱ having values between 1 and 4. A detailed description of the categories can be found in Table 3-1. It is worth noting that a community can be placed in a different category each time it is exposed to a flood disaster, however, by averaging all the resilience indices subsequent to the corresponding recorded flood disasters, an average index can be assigned to that community, comprehensively representing its overall resilience while accounting for all the previous disasters. The reader is referred to the study by Abdel-Mooty et al. (2021) for more details on the resilience-based categories employed herein.

Table 3-1: The Community Flood Resilience-Based Categories

Community Flood Resilience Category	Category Description
1	Communities exposed to events that occur in the summer, causing disturbance less than 264 hours (11 days) and/or causes up to 250 injuries, and damage less than $2.5B without fatalities
2	Communities exposed to events that occur in the spring, causing any disturbance duration, causes up to 20 injuries, and damage up to $1.5B without fatalities
3	Communities exposed to events occurring in any season, causing disturbance more than 264 hours (11 days), and causing up to 250 injuries with any damage value, and without fatalities
4	Communities exposed to events that occur in winter or fall, causing disturbance less than 264 hours (11 days) causes up to 250 injuries and damage up to $2.5B without fatalities
5	Communities exposed to events occurring in any season, causing any disturbance duration that results in more than 250 injuries, causing damage more than $2.5B, with fatalities. And Communities exposed to events occurring in the spring that are not under class 2.

3.3.1. PART (B): RESILIENCE-BASED PREDICTION

For this stage of the framework, a smaller geographical location needed to be identified such that the meteorological features of the dataset would be comparable, comprehensively representing the seasons and their respective hazard for said communities. This was also needed such that the built environment would match its respective hazard, given that different seasons (and subsequently the characteristics of the natural hazard) differ drastically across the United States (e.g.,

the winter in Michigan is drastically different than that of Florida and Texas). However, the framework is applicable on any test location within the United States mainland as long as it is included in the development of the indices in Part (a) of the framework. By inspecting Figure 3-2, as mentioned earlier, the state of Texas had the most recorded number of flood disasters between 1996 and 2019, and the most recorded damage as well. The high number of records is suitable for the development of the prediction model, as the model will need a large dataset for development, training, and testing. As such, the state of Texas was selected for the development of the prediction stage of the framework. The disaster database recorded between 1996 and 2019 in the state of Texas was paired with the developed categories in Table 3-1 on a county level, where each event was assigned an index across the different counties, and the average index is calculated and assigned for each county. Figure 3-3 shows the spatial distribution of the total number of recorded disasters and average FRI across the counties. The spatial analysis shows a low correlation between the number of events and the FRI of a community, given that the more common flood events are those of low severity (Kron 2005). It is also worth mentioning that the spatial analysis shows a concentration of high FRI across the coastal area around the Gulf of Mexico. This can be attributed to High-Tide flooding, which is becoming increasingly common in the past years as a result of relative increase in sea level (Sweet et al. 2020). According to NOAA, coastal communities are witnessing an increase in high-tide

flooding, with some areas reporting a rapidly increasing rate (NOAA 2020; Sweet et al. 2020). This can also be attributed to nature of the natural hazards affecting the area, where a damage of $6B was recorded in 2018, and the devastating Hurricane Harvey which affected the entire state, in 2017 causing an extreme rainfall event resulting in a widespread devastation across different counties. The total damage from hurricane Harvey reached $128.8B, leading to one of the most expensive natural disasters in modern history (NOAA 2020; NOAA Office for Coastal Management 2021; Sweet et al. 2020). The spatial Analysis presented in Figure 3 is also in line with the Cartographic Maps of Precipitation Frequency Estimates published by NOAA in Atlas 14 Volume 11 of Texas in 2018, showing an increased precipitation frequency and magnitude over the coastal area with the gulf of Mexico (Perica et al. 2018).

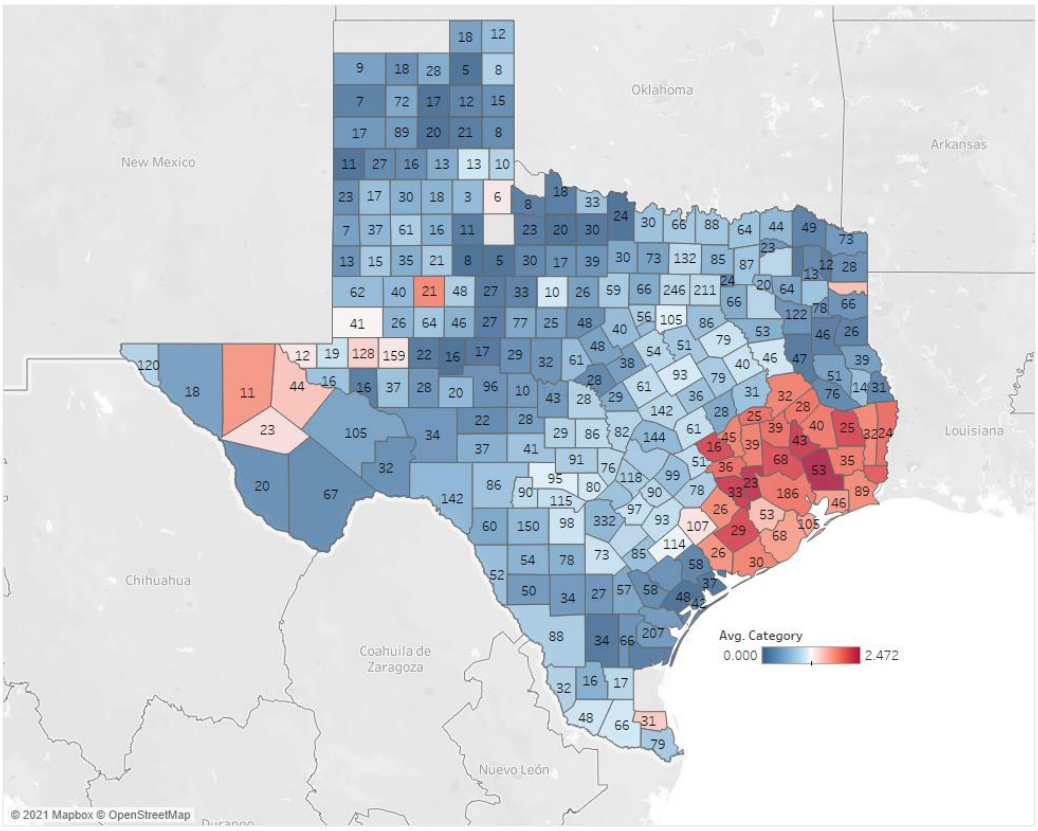

Figure 3-3: Spatial distribution of the number of records and the average FRI over different counties in the state of Texas

3.3.2. MANAGERIAL INSIGHTS AND RESULTS

To complete the dataset for the prediction framework, climate information corresponding to each recorded flood event in each county was then extracted from the Global Historical Climatology Network (GHCN-Daily) under the National Center for Environmental Information (Menne et al. 2012, 2021). To draw reliable insights from the proposed methodology, a comprehensive dataset must be present that includes all the pertinent variables with enough observations over the years to

avoid biases. However, the present dataset implicitly presents this information through the spatio-temporal characteristics of the flood events when exposed to their relative communities.

The extracted climate data, as available, contained four variables for each recorded flood event: Maximum Daily Temperature, Minimum Daily Temperature, Average Daily Temperature, and Maximum Recorded Precipitation. These variables were then employed as predictors (dependent variables) for the FRI resulting from the recorded flood events (Independent variable) to be used in the development of the prediction model. The dataset is subsequently divided into two subsets— Training and Testing (70% and 30% respectively). The training subset was used in the development and training of the ML model, where the FRI implicitly contains information about the resilience (i.e., robustness and rapidity) of the exposed communities, and the climate variables contain information on the climatological features of the location, weather extremes, and different attributes, and causes, of the flood hazard. This comprehensive dataset is then inspected using exploratory data analysis and correlation plots as shown in Figure 3-4. This figure presents a 5 × 5 matrix, in which the variables are labelled on the columns and rows. The matrix contains 4 information groups: *i*) Frequency scatter plots located at the lower triangle of the matrix, excluding the last column; *ii*) Smoothed frequency curves located at the diagonal of the matrix, where the last cell at the bottom right is a histogram for the categorical variable; *iii*) The correlation coefficients located

at the upper triangle of the matrix, excluding the last column; and finally *iv*) The box plots located at the last column of the matrix. It is worth noting that this figure also presents statistical data analyses, as it shows the statistical distribution of the dataset within its variable space, as well as the correlation between different variables. The box plots in Figure 3-4 show that the maximum, minimum, and average temperature variables are overlapping, evenly distributed and with a low range of outliers. This indicates that these variables are interdependent, which shows a consistency in the climatological features of the selected geographical study area. This is also supported by the correlation coefficients as the correlation between these variables is high across all the FRI categories. However, the precipitation variables contain heavy-tailed distribution with a larger range for the outliers, indicating an exceptionally large surge in the value of precipitation, which leads to the recorded flood events. This is supported by the correlation coefficient values between precipitation and other indices, especially at FRI-1, where the severity of the flood event is low, yet the frequency of occurrence is high (Abdel-Mooty et al. 2021). This analysis supports the need of using ML models over traditional statistical learning models, as ML models are better equipped to deal with complex interdependent data for numerous applications (Abdel-Mooty et al. 2021; Witten et al. 2017).

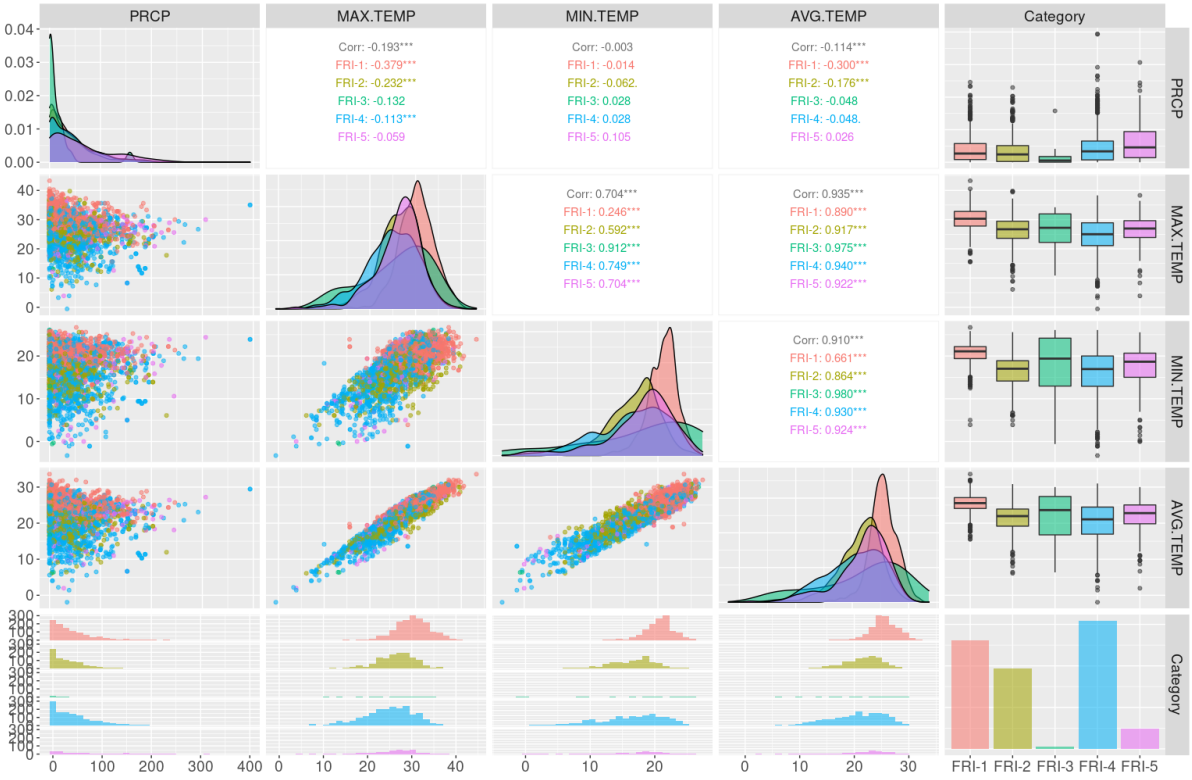

Figure 3-4: Exploratory and sensitivity data analysis of the climate information, and the FRI variables used in the prediction framework.

3.3.3. Model Performance and Discussion

For this analysis, multiple ML classification models were tested; namely, Bagged Decision Trees (DT), and Random Forest (RF)Techniques as ensemble-type models. The dataset was split as mentioned earlier to training and testing dataset, where the split was done randomly to ensure a homogenous distribution of the data in both subsets since the dataset is not evenly distributed along all FRI categories. In this analysis, (*i*) Bagging with 1000 bootstrap replications was used in as an ensemble method, with a minimum split of four, (*ii*) Random Forest (RF)

models with a wide range of trees up to 6000 was tested, while all of them had similar performances, two models were highlighted in this study— RF with 300 trees, and RF with 1000 trees, both with four variables randomly sampled at each split, and a shrinkage parameter of 0.01 (referred to herein as RF 300 and RF 1000, respectively), and finally (*iii*) Naïve Bayes Classification as discussed earlier with a 70-30% split between training and testing data subsets. Each of the aforementioned models have their own assessment measures for model performance (e.g., Gini Impurity, Entropy measure for DT, Mean Square Error, etc.). As such, other performance evaluation indices were utilized in this analysis to objectively compare the predictive performance in replicating the testing data subset of the employed algorithms. To that end, the Precision, Recall, and F10-score have been employed per [Eq(3-3), Eq(3-4), and Eq(3-5), respectively]. The performance indices can be seen in Figure 3-5, the accuracy and misclassification for all the models are compared where it can be seen that the models perform adequately (for training subset: 53.8%, 97.8%, 98.2%, and 98.2% for NB, RF 300, RF 1000, and Bagged DT respectively, and for the testing subset: 50.9%, 57.9. 57.8%, and 57.3% for the NB, RF 300, RF 1000, and Bagged DT respectively). It can be concluded that the DT ensemble models are over-trained in the training dataset but perform better than the NB classifier in the testing dataset even if the results are comparable. This proves the need for a better performance measure for class in each model, the Precision, Recall, F1-score for the training and testing

subsets across all the classes. Figure 3-5, shows an enhanced visual inspection of the performance indices of the four models, where it can be concluded that the performance of the NB classification model is inferior to the ensemble techniques in terms of correctly classifying the data, this can be attributed to the fact that NB models perform better with smaller datasets, as they follow the laws of independent probabilities, indicating it does not perform well with correlated data (Ashari 2013). In the training subset, the Precision, Recall, and F1-score for the ensemble models (i.e., Bagged DT, RF 300, and RF 1000) do not fall below 85% for all classes, which indicates a very good fit for the employed dataset. However, in the testing subset, the results vary for each category. While the results are overall satisfactory for all the ensemble models, the Bagged DT model had better performance when it comes to category 5 (RF models resembled 23% of the precision of the Bagged DT) where the data point falling in this category are scarce compared to the other categories. However, the RF models outperformed the Bagged DT in the precision of Category 3 (65% for the RF models compared to 20% for the Bagged DT model), indicating that random sampling for the variables in addition to the observations in the training algorithm yielded favorable results than the Bagged DT. The results displayed in Figure 3-5 show that even though the models are comparable, given the importance of correctly classifying flood events falling in Category 5 due to its severity and impact, the Bagged DT is thus preferred over the RF models.

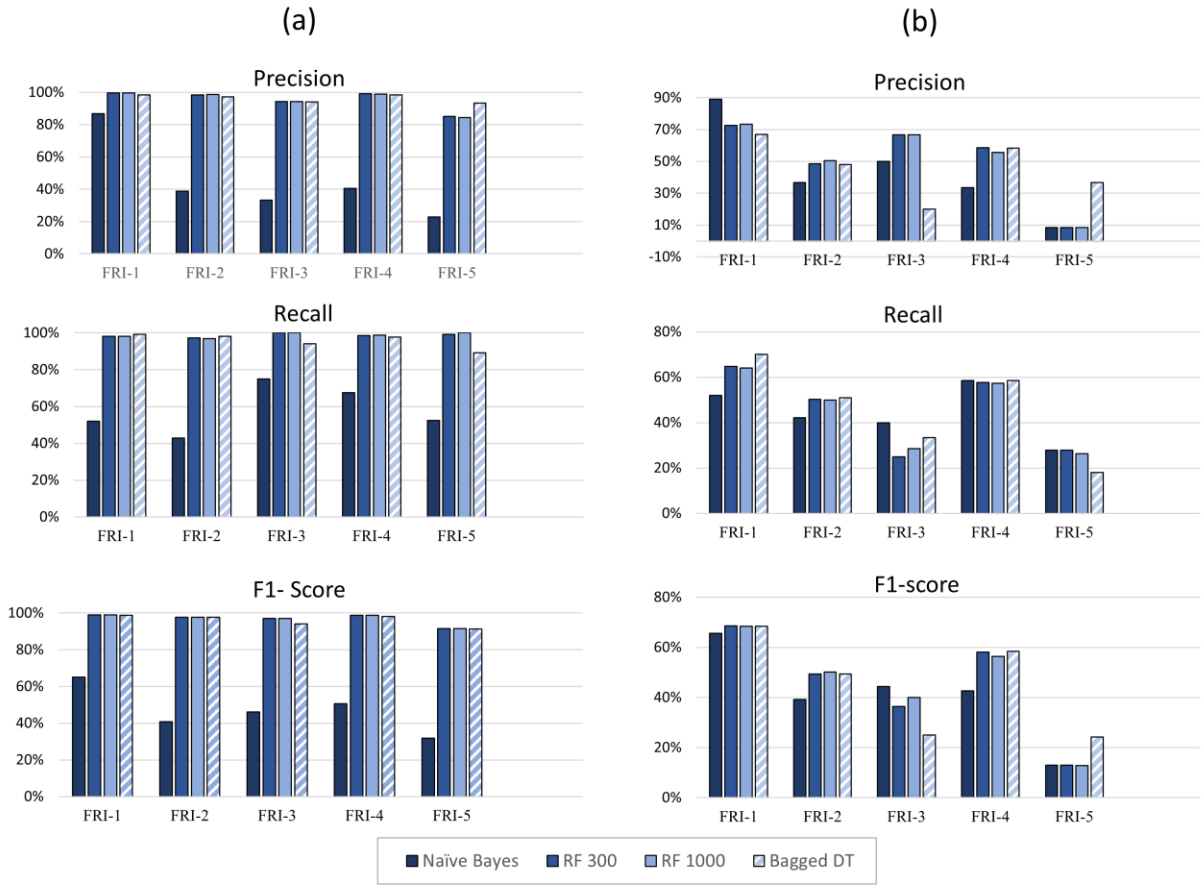

Figure 3-5: Prediction performance indices for the four utilized models where: (a) is the training subset performance, and (b) is the testing subset performance.

Further investigation of the RF and Bagged DT models shows that the variables used as predictors in the current study influence the behavior of the predictive analysis at each class. This indicates the need for a more comprehensive, and climatological representative variables to be used as predictors. In data-driven studies, model performance depends heavily on the available dataset, as such, the authors were constrained by the available data to use in the validation of the developed methodology. A comprehensive dataset would include as much

observations as possible over a wider time span, with numerous variables (e.g., atmospheric pressure, wind speed, wind direction, humidity, topology exposure, etc.). To assess the importance of the individual variables in the analysis, the Mean Decrease Gini (MDG) is employed in the Random Forest ensemble models. Figure 3-6 shows the MDG and the Mean decrease accuracy for the RF with 300 and 1000 tree models, the MDG indicates that the average temperature is the most important variable in both models, followed by the precipitation in the RF 1000 models, and the minimum temperature in the RF 300 model, albeit with a very small difference with the precipitation in the RF 300 model. This supports that the Average temperature (correlated with the minimum temperature) and the precipitation are key variables when predicting the community-flood resilience in exposed communities.

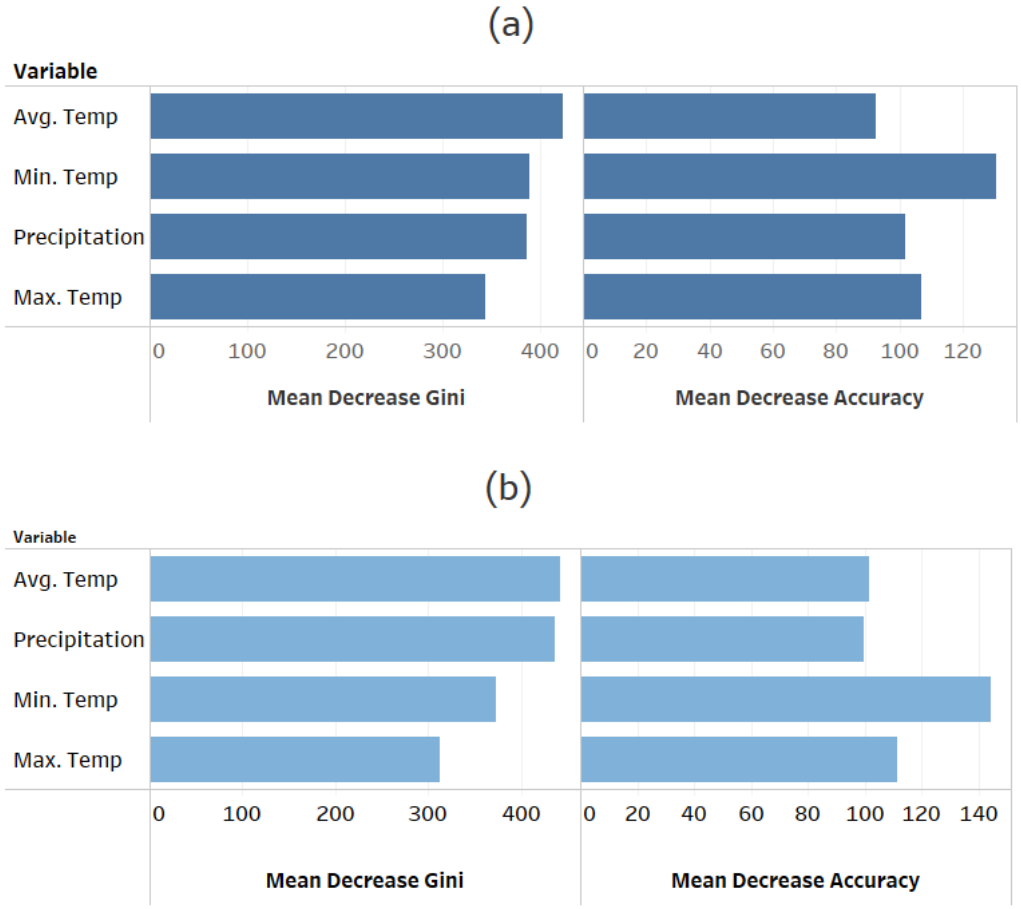

Figure 3-6: Mean Decrease Gini and Mean Decrease Accuracy in (a) Random Forest Model with 300 trees, and (b) Random Forest Model with 1000 trees.

The results of the analysis displayed in the current study show that the framework and methodology presented herein are applicable in resilience-focused flood prediction studies. This framework informs decision-making process through developing an early warning system that can be continuously updated by including new, and more accurate, climate data. The framework presented herein can also be coupled with global climate models to study the temporal changes in flood

resilience, and the climate impact on infrastructure resilience. This coupling would enable informed decisions and policies for a better utilization of resilience means (i.e., resourcefulness and redundancy) to enhance the community's climate resilience. It's worth noting that these predictions and projections will be subject to the uncertainty associated with the climate models, as such, a reliable ensemble from multiple models needs to be used in order to reduce the effect of this uncertainty and reduce the variability between these different models.

The framework presented herein can also be applicable in different data-driven studies, where the purpose is to investigate the spatio-temporal vulnerability of a system facing an external disruption (e.g., vulnerability-based evacuations).

3.4. DISCUSSION AND CONCLUSION

As the IPCC 2021 report stated, extreme rainfall events are expected to increase in frequency and intensity over the next decade, with an increase of over 2.0 m in the average sea level by the end of the current century. Numerous studies were developed to assess community resilience, mostly considering the feature of the hazard rather than the features of the exposed system at risk. The current work aims to: 1) identify specific variables to represent Resilience means across a specific time-span to develop an comprehensive dataset for data-driven models, 2) develop resilience indices using unbiased data-driven methods under different weather conditions across a specific region, 3) develop a comparative spatial

analysis to identify at-risk communities and assess their vulnerabilities to further enhance their resilience (Abdel-Mooty et al. 2021) 4) couple the indices with climate information to develop a well synchronized dataset to be used with future climate models for accurate resilience prediction, and finally 5) test the framework using the NWS disaster records to develop flood resilience indices. The output of said categorization is then coupled with the historic climate information from NOAA corresponding to the disaster records from 1996 to 2019. The resulting dataset is used to develop, train, and test the prediction ML model.

The demonstration application of the framework was developed using Unsupervised ML techniques in part (a), and Supervised ML in part (b). In part (a), the model was applied to the NWS's historical disaster database, collected across the United States from 1996 to 2019. This dataset included variables with information regarding the damage, duration, indirect/direct injuries and fatalities, these variables were used to extract resilience information correspondence to each recorded disaster (i.e., Robustness and Rapidity), so that the developed categorization would capture the resilience of the exposed community, resulting in five categories (i.e., indices). For the second part of the framework, the State of Texas was chosen as a test location, given the uniformity of the meteorological conditions over the state, and the uniformity of the built environment (with few acceptable exceptions). A county-based spatial analysis within the state of Texas was conducted using the developed indices in part (a), highlighting the more

vulnerable counties within the state. This spatial analysis concluded that the coastal areas around the Gulf of Mexico are subjected to flood events that result in a higher index than other counties, resulting in a larger impact on the robustness of said communities. This highlights the need for a methodology to accurately predict future impact on said communities, to be able to develop proactive flood risk management strategies and enhance their overall resilience.

The second part of the application utilized numerous ensemble prediction techniques (i.e., Random Forest with 300 and 1000 trees, bagged Decision Trees, and Naïve Bayes classification). The output of this stage demonstrated the applicability of the developed framework, with comparable results across the different models. While the bagged DT outperformed the RF models in categories where the data is scarce, they performed similarly in other categories. To objectively assess the performance of all the models, Precision, Recall, and F-1 Score were employed across different categories, in training and testing datasets, resulting in a comprehensive conclusion that the prediction framework is employable in resilience-guided studies. However, to objectively develop a data-driven method, a comprehensive enough dataset with variable across different regions and across the years, with enough variables should be employed. In the current study, the authors were limited by the available data, however, the prediction performance of the framework can be improved given more climate information (i.e., wind speed, humidity, and air pressure, etc.). These variables

would increase the correlation with the developed resilience indices, resulting in a more robust dataset for the training and testing of the prediction model. A limitation of the work presented herein is that future climate projections is not considered in the demonstration application. Provided the availability of said projections, the trajectory of the resilience of the exposed community can be determined, and the vulnerability and resilience can be evaluated ahead of projected extreme events, giving policy makers the opportunity to develop mitigation and resilience enhancement plans to avoid future disasters. The framework can be adapted to account for the uncertainty induced by the climate projections' nature, and the probabilistic nature of the hazard as well as the response of the community and the resulting resilience (Hasan et al. 2002; Nofal et al. 2020; Priestley 2000; Salem et al. 2020b). This can be carried out through accumulating probabilities resulting from Monte Carlo simulations on to determine the response to the hazard itself and including it in the prediction framework.

To that end, further research can be implemented to advance this framework through 1) Incorporating more variables within the utilized datasets. 2) Combining the results of the different ensemble ML models used in this study to further enhance the prediction performance, and 3) Applying the framework on future climate projections to predict the expected change in the resilience of the exposed communities

3.5. DATA AVAILABILITY STATEMENT

The datasets used in this article are publicly available. The meteorological disaster database used to generate the resilience-based categories is provided by the NWS a sub-agency under the National Oceanic and Atmospheric Administration (NOAA), available at (https://www.ncei.noaa.gov/pub/data/swdi/stormevents/csvfiles/). The historical climate data used as dependent variables in the ML model is provided by Global Historical Climatology Network, a sub-agency under NOAA, and is available at (https://www.ncdc.noaa.gov/cdo-web/search?datasetid=GHCND).

3.6. ACKNOWLEDGMENTS

The work presented herein is supported by the Vanier Canada Graduate Scholarship (Vanier-CGS) awarded to the corresponding author, and the Natural Science and Engineering Research Council (NSERC) through the CaNRisk— Collaborative Research and Training Experience (CREATE) program. Additional support through the INViSiONLab and the INTERFACE Institute at McMaster University is also acknowledged.

3.7. CONFLICT OF INTEREST

The authors declare that they have no known competing financial interests or personal relationships that could have appeared to influence the work reported in this paper.

3.8. REFERENCES

Abdel-Mooty, M. N., A. Yosri, W. El-Dakhakhni, and P. Coulibaly. 2021. "Community Flood Resilience Categorization Framework." Int. J. Disaster Risk Reduct., 61 (November 2020): 102349. Elsevier Ltd. https://doi.org/10.1016/j.ijdrr.2021.102349.

Alsabti, K., S. Ranka, and V. Singh. 1997. An efficient k-means clustering algorithm. Syracuse, Italy.

Ashari, A. 2013. "Performance Comparison between Naïve Bayes, Decision Tree and k-Nearest Neighbor in Searching Alternative Design in an Energy Simulation Tool." Int. J. Adv. Comput. Sci. Appl., 4 (11): 33–39.

Australian Institute for Disaster Resilience. 2017. Flood Emergency Response: Classification of the Floodplain. Guideline 7-2.

Bertilsson, L., K. Wiklund, I. de Moura Tebaldi, O. M. Rezende, A. P. Veról, and M. G. Miguez. 2019. "Urban flood resilience – A multi-criteria index to integrate flood resilience into urban planning." J. Hydrol., 573 (February 2016): 970–982. Elsevier. https://doi.org/10.1016/j.jhydrol.2018.06.052.

Boehmke, B., and B. M. Greenwell. 2019. Hands-On Machine Learning with R. Taylor & Francis.

Bose, I., and R. K. Mahapatra. 2001. "Business data mining - a machine learning

perspective.” Inf. Manag.

Breiman, L. 1996. Bagging Predictors.

Breiman, L., J. H. Friedman, R. A. Olshen, and C. J. Stone. 1984. Classification And Regression Trees. Routledge.

Brownlee, J. 2016. “Bagging and Random Forest Ensemble Algorithms for Machine Learning.” Accessed May 12, 2021. https://machinelearningmastery.com/bagging-and-random-forest-ensemble-algorithms-for-machine-learning/.

Brownlee, J. 2020. “How to Calculate Precision, Recall, and F-Measure for Imbalanced Classification.” Accessed June 16, 2021. https://machinelearningmastery.com/precision-recall-and-f-measure-for-imbalanced-classification/.

Bruneau, M., S. E. Chang, R. T. Eguchi, G. C. Lee, T. D. O’Rourke, A. M. Reinhorn, M. Shinozuka, K. Tierney, W. A. Wallace, and D. Von Winterfeldt. 2003. “A Framework to Quantitatively Assess and Enhance the Seismic Resilience of Communities.” Earthq. Spectra, 19 (4): 733–752. https://doi.org/10.1193/1.1623497.

Cimellaro, G. P., C. Fumo, A. M. Reinhorn, and M. Bruneau. 2009. Quantification of Disaster Resilience of Health Care Facilities. Mceer-09-0009.

Dawod, G. M., M. N. Mirza, K. A. Al-Ghamdi, and R. A. Elzahrany. 2014. "Projected impacts of land use and road network changes on increasing flood hazards using a 4D GIS: A case study in Makkah metropolitan area, Saudi Arabia." Arab. J. Geosci., 7 (3): 1139–1156. https://doi.org/10.1007/s12517-013-0876-7.

Downton, M. W., J. Z. B. Miller, and R. A. Pielke. 2005. "Reanalysis of U.S. National Weather Service flood loss database." Nat. Hazards Rev., 6 (1): 13–22. https://doi.org/10.1061/(ASCE)1527-6988(2005)6:1(13).

Downton, M. W., and R. A. Pielke. 2005. "How accurate are disaster loss data? The case of U.S. flood damage." Nat. Hazards, 35 (2): 211–228. https://doi.org/10.1007/s11069-004-4808-4.

Efron, B., and R. Tibshirani. 1986. "Bootstrap Methods for Standard Errors, Confidence Intervals, and Other Measures of Statistical Accuracy." Stat. Sci., 1 (1): 54–75.

FEMA. 2012. "Definitions of FEMA Flood Zone Designations." 1–2.

Feofilovs, M., and F. Romagnoli. 2017. "Resilience of critical infrastructures: Probabilistic case study of a district heating pipeline network in municipality of Latvia." Energy Procedia, 128: 17–23. Elsevier B.V. https://doi.org/10.1016/j.egypro.2017.09.007.

Fielding, A. H. 2006. “Introduction to classification.” Clust. Classif. Tech. Biosci., 78–96. Cambridge: Cambridge University Press.

FRED, F. R. B. of S. L. 2020. “U.S. Bureau of Labor Statistics, Consumer Price Index for All Urban Consumers: All Items in U.S. City Average [CPIAUCSL].” Accessed May 5, 2020. https://fred.stlouisfed.org/series/CPIAUCSL.

Ganguli, P., D. Paprotny, M. Hasan, A. Güntner, and B. Merz. 2020. “Projected Changes in Compound Flood Hazard From Riverine and Coastal Floods in Northwestern Europe.” Earth’s Futur., 8 (11). https://doi.org/10.1029/2020EF001752.

Ganguly, K. K., N. Nahar, and B. M. Hossain. 2019. “A machine learning-based prediction and analysis of flood affected households: A case study of floods in Bangladesh.” Int. J. Disaster Risk Reduct., 34 (March 2018): 283–294. Elsevier Ltd. https://doi.org/10.1016/j.ijdrr.2018.12.002.

Gentleman, R., K. Hornik, and G. Parmigiani. 2008. Bicondutor Case Studies.

Gnanaprakkasam, S., and G. P. Ganapathy. 2019. “Evaluation of regional flood quantiles at ungauged sites by employing nonlinearity-based clustering approaches.” Environ. Sci. Pollut. Res., 22856–22877. Environmental Science and Pollution Research. https://doi.org/10.1007/s11356-019-05473-8.

Gondia, A., A. Siam, W. El-Dakhakhni, and A. H. Nassar. 2020. "Machine Learning Algorithms for Construction Projects Delay Risk Prediction." J. Constr. Eng. Manag., 146 (1): 1–16. https://doi.org/10.1061/(ASCE)CO.1943-7862.0001736.

Gong, J., C. H. Caldas, and C. Gordon. 2011. "Learning and classifying actions of construction workers and equipment using Bag-of-Video-Feature-Words and Bayesian network models." Adv. Eng. Informatics, 25 (4): 771–782. Elsevier Ltd. https://doi.org/10.1016/j.aei.2011.06.002.

Goos, G., J. Hartmanis, J. Van, L. E. Board, D. Hutchison, T. Kanade, J. Kittler, J. M. Kleinberg, F. Mattern, E. Zurich, J. C. Mitchell, M. Naor, O. Nierstrasz, B. Steffen, M. Sudan, D. Terzopoulos, D. Tygar, M. Y. Vardi, and G. Weikum. 2006. Computer Vision.

Haggag, M., A. S. Siam, W. El-Dakhakhni, P. Coulibaly, and E. Hassini. 2021a. "A deep learning model for predicting climate-induced disasters." Nat. Hazards, (0123456789). Springer Netherlands. https://doi.org/10.1007/s11069-021-04620-0.

Haggag, M., A. Yorsi, W. El-dakhakhni, and E. Hassini. 2021b. "Infrastructure performance prediction under Climate-Induced Disasters using data analytics." Int. J. Disaster Risk Reduct., 56 (February): 102121. Elsevier Ltd. https://doi.org/10.1016/j.ijdrr.2021.102121.

Hanewinkel, M., W. Zhou, and C. Schill. 2004. “A neural network approach to identify forest stands susceptible to wind damage.” For. Ecol. Manage., 196 (2–3): 227–243. https://doi.org/10.1016/j.foreco.2004.02.056.

Hartigan, J. A., and M. A. Wong. 1979. “A K-means Clustering Algorithm.” J. R. Stat. Soc. Ser. C (Applied Stat., 28 (1): 100–108.

Hasan, R., L. Xu, and D. E. Grierson. 2002. “Push-over analysis for performance-based seismic design.” Comput. Struct., 80 (31): 2483–2493. https://doi.org/10.1016/S0045-7949(02)00212-2.

Hastie, T., R. Tibshirani, and J. Friedman. 2009. The Elements of Statistical Learning: Data Mining, Inference, and Prediction. Springer Ser. Stat. Springer US.

Hemmati, M., B. R. Ellingwood, and H. N. Mahmoud. 2020. “The Role of Urban Growth in Resilience of Communities Under Flood Risk.” Earth’s Futur., 8 (3). https://doi.org/10.1029/2019EF001382.

Jabareen, Y. 2012. “Planning the resilient city: Concepts and strategies for coping with climate change and environmental risk.” Int. J. Urban Policy Plan., (31): 220–229.

Jain, A. K., M. N. Murty, and P. J. Flynn. 2000. Data Clustering: A Review.

Khajwal, A. B., and A. Noshadravan. 2020. “Probabilistic Hurricane Wind-Induced

Loss Model for Risk Assessment on a Regional Scale." ASCE-ASME J. Risk Uncertain. Eng. Syst. Part A Civ. Eng., 6 (2): 1–9. https://doi.org/10.1061/AJRUA6.0001062.

Khalaf, M., A. J. Hussain, D. Al-Jumeily, T. Baker, R. Keight, P. Lisboa, P. Fergus, and A. S. Al Kafri. 2018. "A Data Science Methodology Based on Machine Learning Algorithms for Flood Severity Prediction." 2018 IEEE Congr. Evol. Comput. CEC 2018 - Proc., 1–8. IEEE. https://doi.org/10.1109/CEC.2018.8477904.

King, R. D., S. Muggletont, R. A. Lewiso, and M. J. E. Sternberg. 1992. Drug design by machine learning: The use of inductive logic programming to model the structure-activity relationships of trimethoprim analogues binding to dihydrofolate reductase (arfcl integence/ee acv/prote l/active sites). Biophysics (Oxf).

Kron, W. 2005. "Flood risk = hazard • values • vulnerability." Water Int., 30 (1): 58–68. https://doi.org/10.1080/02508060508691837.

Kwayu, K. M., V. Kwigizile, J. Zhang, and J. S. Oh. 2020. "Semantic N-Gram Feature Analysis and Machine Learning-Based Classification of Drivers' Hazardous Actions at Signal-Controlled Intersections." J. Comput. Civ. Eng., 34 (4). https://doi.org/10.1061/(ASCE)CP.1943-5487.0000895.

Lian, J., H. Xu, K. Xu, and C. Ma. 2017. "Optimal management of the flooding risk

caused by the joint occurrence of extreme rainfall and high tide level in a coastal city." Nat. Hazards, 89 (1): 183–200. Springer Netherlands. https://doi.org/10.1007/s11069-017-2958-4.

Liaw, A., and M. Wiener. 2002. Classification and Regression by RandomForest.

Linkov, I., T. Bridges, F. Creutzig, J. Decker, C. Fox-Lent, W. Kröger, J. H. Lambert, A. Levermann, B. Montreuil, J. Nathwani, R. Nyer, O. Renn, B. Scharte, A. Scheffler, M. Schreurs, and T. Thiel-Clemen. 2014. "Changing the resilience paradigm." Nat. Clim. Chang., 4 (6): 407–409. Nature Publishing Group. https://doi.org/10.1038/nclimate2227.

MacQueen, J. 1967. "Some Methods for Classification and Analysis of Multivariate Observations." Proc. 5th Berkeley Symp. Math. Stat. Probab., 281–297.

Mccallum, A., and K. Nigam. 1998. A Comparison of Event Models for Naive Bayes Text Classification.

Mckinney, B. A., D. M. Reif, M. D. Ritchie, and J. H. Moore. 2006. BIOMEDICAL GENOMICS AND PROTEOMICS Machine Learning for Detecting Gene-Gene Interactions A Review. Appl Bioinforma.

Menne, M. J., I. Durre, R. S. Vose, B. E. Gleason, and T. G. Houston. 2012. "An overview of the global historical climatology network-daily database." J. Atmos. Ocean. Technol., 29 (7): 897–910. https://doi.org/10.1175/JTECH-D-

11-00103.1.

Menne, M. J., I. Durre, R. S. Vose, B. E. Gleason, and T. G. Houston. 2021. “Global Historical Climatology Network - Daily (GHCN-Daily), Version 3.” NOAA Natl. Clim. Data Cent. Accessed June 10, 2021. https://www.ncei.noaa.gov/access/metadata/landing-page/bin/iso?id=gov.noaa.ncdc:C00861.

Minsker, B., L. Baldwin, J. Crittenden, K. Kabbes, M. Karamouz, K. Lansey, P. Malinowski, E. Nzewi, A. Pandit, J. Parker, S. Rivera, C. Surbeck, W. A. Wallace, and J. Williams. 2015. “Progress and recommendations for advancing performance-based sustainable and resilient infrastructure design.” J. Water Resour. Plan. Manag., 141 (12). https://doi.org/10.1061/(ASCE)WR.1943-5452.0000521.

Mitra, P., R. Ray, R. Chatterjee, R. Basu, P. Saha, S. Raha, R. Barman, S. Patra, S. S. Biswas, and S. Saha. 2016. “Flood forecasting using Internet of things and artificial neural networks.” 7th IEEE Annu. Inf. Technol. Electron. Mob. Commun. Conf. IEEE IEMCON 2016, 1–5. IEEE.

de Moel, H., and J. C. J. H. Aerts. 2011. “Effect of uncertainty in land use, damage models and inundation depth on flood damage estimates.” Nat. Hazards, 58 (1): 407–425. https://doi.org/10.1007/s11069-010-9675-6.

Mojaddadi, H., B. Pradhan, H. Nampak, N. Ahmad, and A. H. bin Ghazali. 2017.

"Ensemble machine-learning-based geospatial approach for flood risk assessment using multi-sensor remote-sensing data and GIS." Geomatics, Nat. Hazards Risk, 8 (2): 1080–1102. Taylor & Francis. https://doi.org/10.1080/19475705.2017.1294113.

Mosavi, A., P. Ozturk, and K. W. Chau. 2018. "Flood prediction using machine learning models: Literature review." Water (Switzerland), 10 (11): 1–40. https://doi.org/10.3390/w10111536.

Murdock, H. J. 2017. "Resilience of Critical Infrastructure to Flooding: Quantifying the resilience of critical infrastructure to flooding in Toronto, Canada."

Murnane, R. J., J. E. Daniell, A. M. Schäfer, P. J. Ward, H. C. Winsemius, A. Simpson, A. Tijssen, and J. Toro. 2017. "Future scenarios for earthquake and flood risk in Eastern Europe and Central Asia." Earth's Futur., 5 (7): 693–714. https://doi.org/10.1002/2016EF000481.

Murphy, J. D. 2018. NWSI 10-1605, Storm Data Preparation.

Nagpal, A. 2017. "Decision Tree Ensembles- Bagging and Boosting | by Anuja Nagpal | Towards Data Science." Accessed May 12, 2021. https://towardsdatascience.com/decision-tree-ensembles-bagging-and-boosting-266a8ba60fd9.

National Institute of Standards and Technology. 2020. COMMUNITY

RESILIENCE PLANNING GUIDE FOR BUILDINGS AND INFRASTRUCTURE SYSTEMS: A Playbook. Gaithersburg, MD.

Netherton, M. D., and M. G. Stewart. 2016. "Risk-based blast-load modelling: Techniques, models and benefits." Int. J. Prot. Struct., 7 (3): 430–451. https://doi.org/10.1177/2041419616666455.

NOAA. 2019. "National Climate Report - Annual 2018 | State of the Climate | National Centers for Environmental Information (NCEI)." Accessed May 5, 2020. https://www.ncdc.noaa.gov/sotc/national/201813#over.

NOAA. 2020. "U.S. high-tide flooding continues to increase | National Oceanic and Atmospheric Administration." Accessed June 10, 2021. https://www.noaa.gov/media-release/us-high-tide-flooding-continues-to-increase.

NOAA Office for Coastal Management. 2021. "Texas." Accessed June 10, 2021. https://coast.noaa.gov/states/texas.html.

Nofal, O. M., and J. W. van de Lindt. 2020. "Understanding flood risk in the context of community resilience modeling for the built environment: research needs and trends." Sustain. Resilient Infrastruct., 00 (00): 1–17. Taylor & Francis. https://doi.org/10.1080/23789689.2020.1722546.

Nofal, O. M., J. W. van de Lindt, and T. Q. Do. 2020. "Multi-variate and single-

variable flood fragility and loss approaches for buildings." Reliab. Eng. Syst. Saf., 202 (March): 106971. Elsevier Ltd. https://doi.org/10.1016/j.ress.2020.106971.

Otterbach, J. S., R. Manenti, N. Alidoust, A. Bestwick, M. Block, B. Bloom, S. Caldwell, N. Didier, E. S. Fried, S. Hong, P. Karalekas, C. B. Osborn, A. Papageorge, E. C. Peterson, G. Prawiroatmodjo, N. Rubin, C. A. Ryan, D. Scarabelli, M. Scheer, E. A. Sete, P. Sivarajah, R. S. Smith, A. Staley, N. Tezak, W. J. Zeng, A. Hudson, B. R. Johnson, M. Reagor, M. P. Da Silva, and C. Rigetti. 2017. Unsupervised Machine Learning on a Hybrid Quantum Computer.

Park, D. C. 2000. "Centroid neural network for unsupervised competitive learning." IEEE Trans. Neural Networks, 11 (2): 520–528. https://doi.org/10.1109/72.839021.

Patil, B. M., R. C. Joshi, and D. Toshniwal. 2010. "Missing Value Imputation Based on K-Mean Clustering with Weighted Distance." 600–609.

Patil, C., and I. Baidari. 2019. "Estimating the Optimal Number of Clusters k in a Dataset Using Data Depth." Data Sci. Eng., 4 (2): 132–140. Springer Berlin Heidelberg. https://doi.org/10.1007/s41019-019-0091-y.

Perica, S., S. Pavlovic, M. S. Laurent, C. Trypaluk, D. Unruh, and O. Wilhite. 2018. Precipitation-Frequency Atlas of the United States Volume 11 Version 2.0:

Texas.

Priestley, M. J. N. 2000. “Performance based seismic design.” Bull. New Zeal. Soc. Earthq. Eng., 33 (3): 325–346. https://doi.org/10.5459/bnzsee.33.3.325-346.

Ragini, J. R., P. M. R. Anand, and V. Bhaskar. 2018. “Big data analytics for disaster response and recovery through sentiment analysis.” Int. J. Inf. Manage., 42 (May): 13–24. Elsevier. https://doi.org/10.1016/j.ijinfomgt.2018.05.004.

Rodrigues, M., and J. De la Riva. 2014. “An insight into machine-learning algorithms to model human-caused wildfire occurrence.” Environ. Model. Softw., 57: 192–201. Elsevier Ltd. https://doi.org/10.1016/j.envsoft.2014.03.003.

Rözer, V., A. Peche, S. Berkhahn, Y. Feng, L. Fuchs, T. Graf, U. Haberlandt, H. Kreibich, R. Sämann, M. Sester, B. Shehu, J. Wahl, and I. Neuweiler. 2021. “Impact-Based Forecasting for Pluvial Floods.” Earth’s Futur., 9 (2). https://doi.org/10.1029/2020EF001851.

Salem, S., A. Siam, W. El-Dakhakhni, and M. Tait. 2020a. “Probabilistic Resilience-Guided Infrastructure Risk Management.” J. Manag. Eng., 36 (6): 04020073. https://doi.org/10.1061/(asce)me.1943-5479.0000818.

Salem, S., A. Siam, W. El-Dakhakhni, and M. Tait. 2020b. “Probabilistic Resilience-Guided Infrastructure Risk Management.” J. Manag. Eng., 36 (6):

04020073. https://doi.org/10.1061/(asce)me.1943-5479.0000818.

Seyed Shirkhorshidi, A., S. Aghabozorgi, and Y. Wah. 2015. "A Comparison Study on Similarity and Dissimilarity Measures in Clustering Continuous Data." https://doi.org/10.1371/journal.pone.0144059.

Shafizadeh-Moghadam, H., R. Valavi, H. Shahabi, K. Chapi, and A. Shirzadi. 2018. "Novel forecasting approaches using combination of machine learning and statistical models for flood susceptibility mapping." J. Environ. Manage., 217: 1–11. https://doi.org/10.1016/j.jenvman.2018.03.089.

da Silva, J., S. Kernaghan, and A. Luque. 2012. "A systems approach to meeting the challenges of urban climate change." Int. J. Urban Sustain. Dev., 4 (2): 125–145. https://doi.org/10.1080/19463138.2012.718279.

Singh, H. 2018. "Understanding Gradient Boosting Machines | by Harshdeep Singh | Towards Data Science." Accessed May 12, 2021. https://towardsdatascience.com/understanding-gradient-boosting-machines-9be756fe76ab.

Stocker, T. F., Q. Dahe, G.-K. Plattner, M. M. B. Tignor, S. K. Allen, J. Boschung, A. Nauels, Y. Xia, V. Bex, and P. M. Vincent. 2013. Climate change 2013: The Physical Science Basis.

Swain, D. L., O. E. J. Wing, P. D. Bates, J. M. Done, K. A. Johnson, and D. R.

Cameron. 2020. “Increased Flood Exposure Due to Climate Change and Population Growth in the United States.” Earth’s Futur., 8 (11). https://doi.org/10.1029/2020EF001778.

Sweet, W. V, G. Dusek, G. Carbin, J. Marra, D. Marcy, and S. Simon. 2020. “2019 State of U.S. High Tide Flooding and a 2020 Outlook.” NOAA Tech. Rep., NOS CO-OPS (July): 1–12.

Trenberth, K. E., L. Cheng, P. Jacobs, Y. Zhang, and J. Fasullo. 2018. “Hurricane Harvey Links to Ocean Heat Content and Climate Change Adaptation.” Earth’s Futur., 6 (5): 730–744. https://doi.org/10.1029/2018EF000825.

Turkington, T., K. Breinl, J. Ettema, D. Alkema, and V. Jetten. 2016. “A new flood type classification method for use in climate change impact studies.” Weather Clim. Extrem., 14 (September): 1–16. Elsevier. https://doi.org/10.1016/j.wace.2016.10.001.

Wagstaff, K., C. Cardie, S. Rogers, and S. Schrödl. 2001. “Constrained K-means Clustering with Background Knowledge.” Int. Conf. Mach. Learn. ICML, pages: 577–584.

Wilby, R. L., K. J. Beven, and N. S. Reynard. 2007. “Climate change and fluvial flood risk in the UK: more of the same?” Hydrol. Process., 2309 (December 2007): 2300–2309. https://doi.org/10.1002/hyp.

Witten, I. H., E. Frank, M. A. Hall, and C. J. Pal. 2017. Data Mining Practical Machine Learning Tools and Techniques Fourth Edition.

World Economic Forum. 2019. The Global Risks Report 2019 14th Edition.

Wu, T. F., C. J. Lin, and R. C. Weng. 2004. "Probability estimates for multi-class classification by pairwise coupling." J. Mach. Learn. Res., 5: 975–1005.

Yagci, K., I. S. Dolinskaya, K. Smilowitz, and R. Bank. 2018. "Incomplete information imputation in limited data environments with application to disaster response." Eur. J. Oper. Res., 269 (2): 466–485. Elsevier B.V. https://doi.org/10.1016/j.ejor.2018.02.016.

Zhang, H. 2004. The Optimality of Naive Bayes.

Zumel, N., and J. Mount. 2020. Practical Data Science with R.

Chapter 4

INTERPRETABLE SPATIOTEMPORAL CLIMATE CHANGE IMPACT ON FLOOD RESILIENCE

ABSTRACT

Current flood risk mapping studies have been heavily relying on historical events, implicitly assuming they are a reliable source of information for future flood projections. Subsequently, such studies may not explicitly account for different climate change trajectories and their impact on flood risk, and by extension, climate change impact on the affected communities' resilience. While there have been numerous efforts to study the impact of flood hazard on urban communities, only very few have considered specific aspects of the resilience of the exposed community. However, none have been comprehensive enough to capture the resilience features of the community, as well as the features of hazard and climate change. By incorporating the recent Bias Corrected Spatial Disaggregation Coupled Model Intercomparison Project 5 (BCSD CMIP 5) global climate simulations, the impact of climate change on community flood resilience under multiple emission scenarios is investigated. Specifically, this study develops accurate data-driven prediction model to strategize climate resilience planning. The modelling herein identifies a 15.5% and 28% increase in the resilience index for RCP 6.0 and RCP 8.5, accounting for a disproportionate increase in damage and monetary losses of $900M and $1.8B per decade until 2050 for the selected locations, respectively, with the potential to be applicable on a global scale. The study also identifies an equivalent increase in disruption to livelihood, whether through evacuations, displacement, or injuries throughout the projected flood events. This modeling

approach identifies the most influential climatological information and their influence on community resilience projection, reaffirming the need for immediate global intervention to steer the climate trajectory away from extreme scenarios, and the development of resilience-informed mitigation strategies to halt the evolving climate risks.

KEYWORDS: Interpretability; Climate Impact; Flood Hazard; Flood Risk; Machine Learning; Resilience; Risk Classification; Robustness.

The work in this chapter is featured in a Manuscript currently submitted in the "Nature Communications" Journal. No Copy right is yet assigned, and the final version is different than the version presented herein. However, the work and analysis are the same. The manuscript is currently in second round of peer review, submission number: NCOMMS-22-35434

Abdel-mooty, M. N., W. El-dakhakhni, and P. Coulibaly. "Interpretable Spatio-temporal Climate Change Impact on Flood Resilience." *Nature Communications.*

4.1. INTRODUCTION

4.1.1. FLOOD RISK AND RESILIENCE

Over the past three decades, the magnitude and frequency of climate-induced (e.g., climatological and hydrological) disasters have been increasing at an alarming rate, jeopardizing the livelihood of millions living in at-risk communities (Dawod et al. 2014; Lian et al. 2017; Wilby et al. 2007). However, most current methodologies adopted for flood risk management assume that historical data serves as a good predictor for future projections in its current trajectory(Wing et al. 2022).The weather conditions have been heavily impacted by the changing climatological conditions (i.e., air humidity, precipitation, and temperature). The data recorded by the National Weather Service (NWS) shows that north America is suffering from an increased rate of extreme rainfall events (i.e., rainfall of at least 100 mm in 24 hours), coupled with an increased rate of urban flooding events (Bertilsson et al. 2019; Stocker et al. 2013; Thomas et al. 2014). This is also exasperated by the increased urbanization and population growth into flood prone areas, where it is expected that by the year 2050, 70% of the world population will be inhabiting urban environments, in contrast to the 2020 figure of 50%(NOAA 2019; da Silva et al. 2012). This increased flood risk, exposure, and losses call for the adoption of more aggressive *proactive* resilience-guided risk-mitigation

response and planning, rather than a *reactive* response to disasters (de Moel and Aerts 2011; World Economic Forum 2019).

To that end, *community resilience* is gaining traction in the research community worldwide, and has been defined as the ability of a community, regardless of the size of said community, to predict, withstand, adapt to, and rapidly recover from external disruptive events befalling it, back to its pre-hazard state, or at a higher functionality levels (Abdel-Mooty et al. 2023; National Institute of Standards and Technology 2020). Flood resilience evaluation is the necessary and natural extension of traditional flood risk studies. While flood risk considers the coupling of community exposure, its elements at-risk, flood hazard, and vulnerability, flood resilience deals with the extended loss in functionality, and recoverability trajectory of the exposed communities, considering both the direct and indirect impacts of said disasters (Abdel-Mooty et al. 2021; Salem et al. 2020). Although there have been numerous definitions of resilience to date, and across many fields (i.e., physics, medical sciences, socio-economic fields, etc.), in this manuscript, resilience is defined as the ability of a community to resist the effects of a realized flood risk, and rapidly recover from the former to its pre-event, or other target, functionality(Bruneau et al. 2003). Resilience is thus identified by its two goals: *Robustness*, the inherent capacity of the system to withstand the effect of an external disruptive event without a loss in functionality, and, *Rapidity*, the ability of a system to recover back to its pre-event levels in a timely manner. These

goals are enabled by the resilience means: *Resourcefulness*, the available resources at the system's disposal to allocate for a rapid recovery, and *Redundancie*s, the inherent system's replacements (i.e., alternative resources) for adaptive behavior for functionality retention during a disruptive event(Bruneau et al. 2003).

4.1.2. METHODOLOGY LAYOUT

While there has been an extensive work in the field of flood risk management (Auerbach et al. 2015; Nofal and van de Lindt 2020a; Rufat et al. 2015; Sen et al. 2020), most of these efforts have been to mitigate the effects of flood hazards on the exposed community and built environment, developing strategies without accounting for the trajectory of climate change, and its effect on the flooding scenarios, frequency, or magnitude (Nofal et al. 2020; Nofal and van de Lindt 2020b; de Paor et al. 2019). Progress has been made to employ physics-based (hydrological-hydraulic) models to map flood plains and generate future projections for damage quantification (Hosseiny et al. 2020; Li et al. 2022; Mosavi et al. 2018; Wing et al. 2022). However, such efforts proved to be extremely computationally expensive, resulting in high degree of complexity hindering accurate modelling (Hosseiny et al. 2020; Mosavi et al. 2018; Shafizadeh-Moghadam et al. 2018). Notwithstanding its complexity, said work however fails in capturing the effect of different climate change emission scenarios in the development of such standards and regulations. The work presented herein employs

multiple Machine Learning (ML) algorithms to capture the effect of climate change projections on future community resilience. Specifically, this work employs a framework that seeks to broaden the understanding of resilience-guided flood risk management, integrating the effect of climate change into community resilience studies by: (1) bypassing the complexity and uncertainty of physics-based modelling through employing direct data-driven techniques; (2) projecting the effect of climate-impacts on community resilience considering multiple climate change emission scenarios; (3) Incorporating, explicitly and implicitly, the different attributes of resilience (i.e., Robustness and Rapidity) and information about the vulnerability of the exposed community, as well as the nature of the induced hazard under investigation. These steps would ensure the inclusion of multiple interdependent subcomponents of the community, enabling drawing a clear picture of future climate projection impacts on resilience trajectory.

The adopted methodology layout presented in Figure 4-1 summarizes a three-step data-centric procedure for achieving the objective of this study. This methodology acts as a tool for enabling informed decision-making processes for vulnerability identification and resource allocation by stakeholders, essentially an early warning system. This tool will also enable governing bodies and decision makers to develop climate resilience-guided management plans that account for climate-change impact as well as the different attributes of resilience, and the nature of the exposed environment, whether in terms of the physical infrastructure or the

socioeconomic attributes of the community. The methodology is divided into 3 steps: Step (a) Development of Resilience-based Community Classification: this part employs unsupervised ML algorithms (i.e., clustering techniques) to develop the resilience-guided indices (i.e., categories) that would be built on in later stages of the methodology. This step is adopted from the study conducted by Abdel-Mooty et. al (2021)(Abdel-Mooty et al. 2021) through preprocessing and compiling a comprehensive enough dataset, with enough variability, observations and attributes, and different variables to capture the state of the community and its resilience features, and the features of the flood hazard most common and bound to that area (i.e., flood duration, down time following the flood, flood depth, and frequency). Post data gathering and preprocessing, different unsupervised ML models were employed to categorize the available dataset, and the model with the most explained variability, and least within cluster variation is employed.

Prior to commencing Step (b) of the framework, the resulting Classes are employed to develop a spatial analysis, identifying the most-vulnerable and exposed communities (aggregated to a regional-level analysis), which provides insights for climate informed resilience-guided strategies, and aids in the selection of a suitable testbed for Step (b) of the methodology applied herein.

Step (b) of the methodology integrates and couples the categories developed in Step (a) with climate information; this integration contains information on the resilience of the community under investigation, where the categories contain

information on the vulnerability and exposure, as well as resilience attributes, and the climate data provides information on the climatological condition of the area under investigation. This step allows for the integration of multiple Global Climate Models (GCMs), exploring the impact of climate change on the resilience of the study area and its future trajectory. It also allows for the incorporation of different climate emission scenarios to assess the impact of the employed strategies on the future of the global resilience, and the effect of global intervention measures.

Step (c) is the analysis of the output of the Supervised ML models by employing interpretability techniques, identifying the important features and their influence over the predicted categories, and accurately capture the spatio-temporal change for future resilience under multiple emission scenarios. This step would then allow for an employable spatio-temporal analysis at any desired scale, for decision makers and community leaders to rely on for the development of climate and resilience strategies. Details on each step and the used algorithms are provided in the upcoming sections.

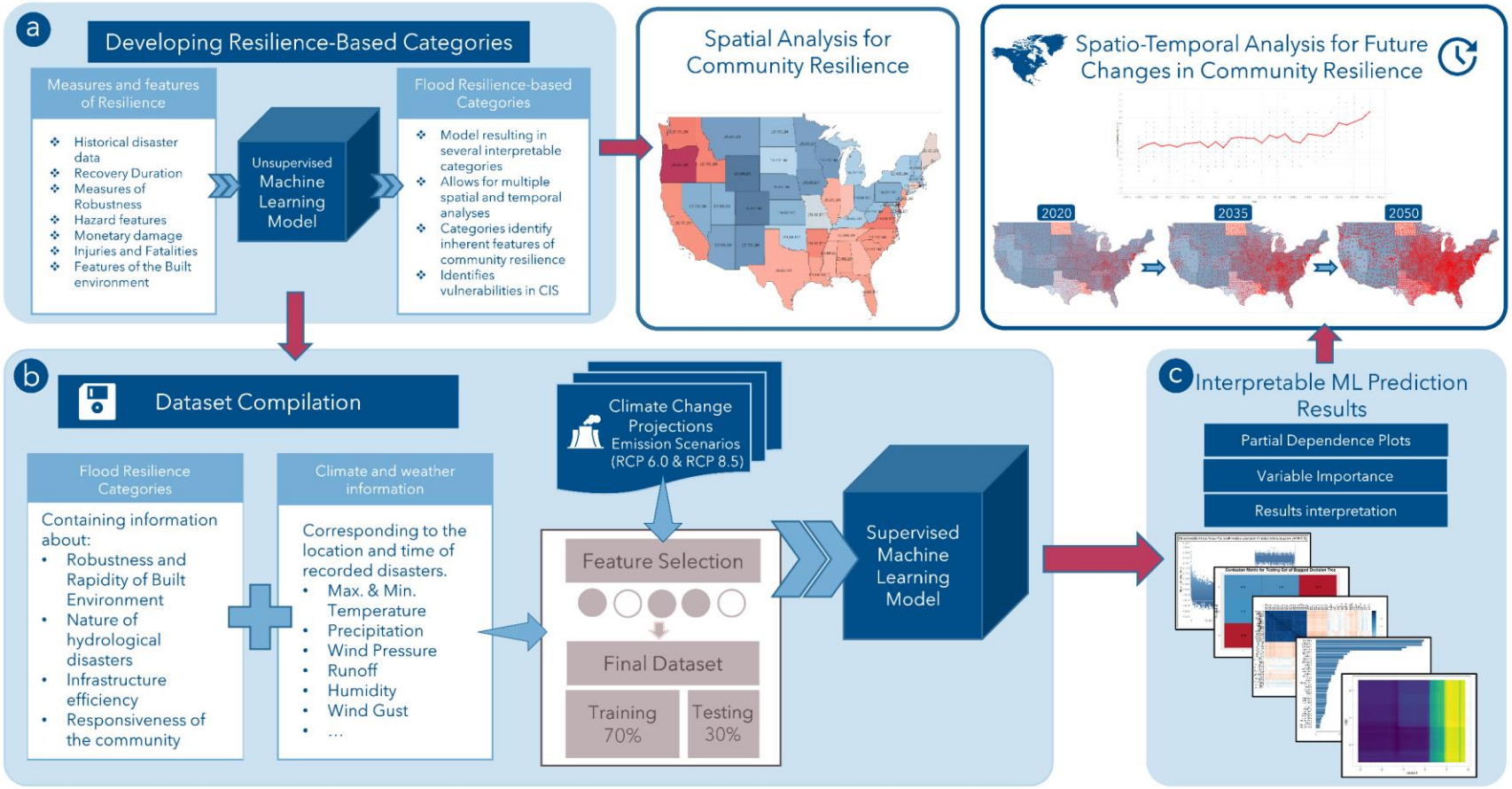

Figure 4-1: Framework for developing the Machine Learning-based prediction of community resilience under climate change

In this study, the developed categories for step (a) adopted from Abdel-Mooty et. al. (2021)(Abdel-Mooty et al. 2021) were applied on the data provided for the United States mainland states, and using the disaster database records for at a county level (aggregated to a state level in the spatial analysis). These categories were then coupled with climate data provided by the National Oceanic and Atmospheric Administration (NOAA), coupling it with numerous GCMs for future projection of climate change under different emission scenarios. For this step, the State of Texas was chosen as a case study location, and future trajectories were developed until the year 2050.

4.2. DATA AND METHODS

4.2.1. DATASETS

Developing the Resilience based Categories: For part (a) adopted in this study, the historical disaster data records from the National Weather service (NWS) were adopted. This dataset is used for the derivation of the resilience-based categories employed in this study. The NWS is considered one of the longest-run organizations concerned with recording annual flood damage in the United States(Downton et al. 2005). The dataset employed here while compiled into the database of the NWS, was nonetheless gathered by third-party organizations and data-collection agencies. Although these agencies followed the standards and guidelines provided by the NWS, the diversity, quality and quantity of the collected

data are highly dependent on the resources of these organizations, and their constraints, financial and otherwise(Murphy 2018). This dataset of historical disasters contains a total of 49,775 records between 1996 and 2020 for the United States mainland. For each data record, there are multiple variables – start time, end time, geographical location, year, month, duration, and related damages. The recorded damages in this dataset include the direct and indirect injuries and fatalities, crop damages and property damages. The start and end data of the flood event were used to calculate the total event duration, representing a portion of the down time (i.e., Rapidity), and the month was used to represent the seasonality of the flood event. The damages recorded in the flood database were summed up to represent the total impact of the flood event, and was adjusted using the Customer Price Index from the Bureau of Labor Statistics to account for the corresponding inflation over the years (Downton and Pielke 2005; FRED 2020; Jaagus and Ahas 2000; Murphy 2018). For reliable resilience-guided insights to be drawn from this analysis, the features of the flood hazard need to be considered, this information is implicitly stated through the typical spatial and temporal attributes of the hazards in the dataset, where each community is defined by its inherent characteristics. It is essential to identify that the damages (monetary and otherwise) recorded in this dataset are all direct damages, resulting from the direct contact of the flooding water with the structures or the components of the community, not accounting for the opportunity loss or the indirect damages of resulting from this event. To that end,

the term “Flood Event” mentioned in this dataset refers to the flooding component of any multi-hazard event; such that if a flood is a result of a cyclone or a tornado, the recorded damages in this dataset only relate to the flooding component of this multi-hazard environment (Downton et al. 2005; Downton and Pielke 2005; Morss et al. 2005).

Climate information corresponding to historical Disaster records: The previous dataset provided by the NWS was used to develop resilience-based categories. These categories were then coupled with climate information corresponding to the date and location of these flood events. This data was extracted from the Global Historical Climatology Network (GHCN-Daily) of the National Center for Environmental Information (Menne et al. 2021). For a comprehensive analysis with reliable information and insights, a diverse and comprehensive dataset that includes all the relative variables with enough observations over the years to avoid bias needs to be utilized. To that end, the purpose of this study is to develop a methodology that can employ global climate models to predict future changes in the inherent resi

lience of the built environment. Using historical data, as proposed in the study by Abdel-Mooty et. al. (2022)(Abdel-mooty et al. 2022) although beneficial and critical to the accurate synchronization of the dataset, will not aid in the development of an accurate prediction algorithm. As such, the Bias Correction with Spatial Disaggregation (BCSD) Downscaled Coupled Model Intercomparison

Project – Phase 5 (CMIP5) is employed in this study as the most complete and tested GCMs (Reclamation 2013, 2014). This dataset employs a large ensemble of GCMs based on multiple Green House Gas (GHG) emission scenarios. Upon comparing the GCM simulation results with historical observations it was evident that the models required bias-correction, accounting for seasonal and location variability. The gridding of the dataset is accordingly adjusted to a course 1^{o} resolution, with a downscaled spatial resolution of $1/8^{o}$. The bias identification was based on the overlapping period in the historical observations and the modeled GCMs from the years 1950-1999 and was carried on a temporal and spatial basis (i.e., for common months and basins) with the location provided at a grid-cell resolution. The correction of the bias was made by looking at the associated rank probability (p) at a certain timestep from the GCMs historical quantile map and comparing it to that of the historical dataset. This results in all the bias corrected GCM results being associated with monthly Cumulative Distribution Functions (CDF). The results are then linked and used in correcting the bias of the future projections from those GCMs in the CIMP5 dataset(Reclamation 2013, 2014; Vano et al. 2020). However, this assumes that the GCM bias structure is the same during both the 20^{th} and the 21^{st} century. For hydrological projection, the Variable Infiltration Capacity (VIC) hydrologic model is adopted for the GCMs, this method is based on the study by Wood et al. (2004)(Wood et al. 2004), where the grid-based hydrological model parameterized the dominant hydrometeorological

process at the interface between land surface and the atmosphere. The climate input for those VIC models are daily precipitation, temperature (maximum and minimum) and average wind speed for each of the $(1/8)^{o}$ resolution grid cell(Heidbach et al. 2007; Vano et al. 2020; Wood et al. 2004).

The Intergovernmental Panel on Climate Change (IPCC) identified multiple benchmark GHG emission scenarios as the Representative Concentration Pathway (RCPs) where each RCP represents a scenario of a total radiative forcing until the year 2100 relative to the year 1750 (with a unit of W m^{-2})(IPCC 2014). These "benchmark" scenarios are: RCP 2.6, RC P4.5, RCP 6.0, and RCP 8.5 (equivalent to greenhouse gas concentration of 450, 650, 850, and 1370 ppm CO_2 eq), such that the number represents the ratio of total radiative forcing (i.e., 2.6 W m^{-2} for RCP 2.6, and 4.5 W m^{-2} for RCP 4.5, etc.) (IPCC 2014). These scenarios were developed to cover a wide range of key factors of the human development that influence the GHG emissions and the mitigation of climate change in different policies. The RCP 2.6 scenario assumes that the peak CO_2 is to be reached in 2020 followed by a decrease in emissions, while RCP 4.5 is an intermediate scenario where it assumes that the emissions will peak at the year 2040 before declining, RCP 6.0 assumes the peak is at 2080, and RCP 8.5 assumes the GHG emissions to increase beyond 2100 before the start of the decline (IPCC 2014; Reclamation 2014). The research community has now reached a consensus that the trajectory of GHG emissions is past the threshold for scenarios RCP 2.6 and on the verge of passing RCP 4.5(Lyon

et al. 2022). To that end, the more realistic scenario for investigation is RCP 6.0, and assuming no intervention or improvement in climate change mitigation, RCP 8.5 should also be considered (IPCC 2014; Lyon et al. 2022). The extracted climate data, as available, contained five hydrologic variables for each recorded flood event: maximum surface air temperature (^{o}C), minimum surface air temperature (^{o}C), mean wind speed (m/s), and total runoff (sum of surface runoff and baseflow, mm), and precipitation (mm). In this study, the employed BCSD CMIP5 modelling has 16 GCMs for RCP 6.0 and 36 GCMs for RCP 8.5. However, only 16 models were adopted in each of the emission scenarios, as shown in Table 4-1 for RCP 6.0, and Table 4-2 for RCP 8.5.

Table 4-1: The 16 Global Climate Models for RCP 6.0

	Model Name	Institution	Modeling Center
1	BCC-CSM 1.1	Beijing Climate Center, China Meteorological Administration	BCC
2	CCSM 4	National Center for Atmospheric Research	NCAR
3	CESM1 (CAM5)	National Science Foundation, Department of Energy, National Center for Atmospheric Research	NSF-DOE-NCAR
4	CSIRO-MK3.6.0	Commonwealth Scientific and Industrial Research Organization in collaboration with the Queensland Climate Change Centre of Excellence	CSIRO-QCCCE
5	FIO-ESM	The First Institute of Oceanography, SOA, China	FIO
6 7 8	GFDL-CM3 GFDL-ESM2G GFDL-ESM2M	Geophysical Fluid Dynamics Laboratory	NOAA-GFDL
9	GISS-E2-R	NASA Goddard Institute for Space Studies	NASA GISS
10	HadGEM2-AO	National Institute of Meteorological Research/Korea Meteorological Administration	NIMR/KMA
11	HadGEM2-ES	Met Office Hadley Centre (additional HadGEM2-ES realizations contributed by Instituto Nacional de Pesquisas Espaciais)	MOHC (additional realizations by INPE)
12	IPSL-CM5A-MR	Institute Pierre-Simon Laplace	IPSL
13 14 15	MIROC-ESM MIROC-ESM-CHEM MIROC5	Japan Agency for Marine-Earth Science and Technology, Atmosphere and Ocean Research Institute (The University of Tokyo), and National Institute for Environmental Studies	MIROC
16	NorESM1-M	Norwegian Climate Centre	NCC

Table 4-2: The lobal Climate Models for RCP 8.5

	Model Name	Institution	Modeling Center
1	ACCESS1.0	CSIRO (Commonwealth Scientific and Industrial Research Organization, Australia), and BOM (Bureau of Meteorology, Australia)	CSIRO-BOM
2	BCC-CSM1.1	Beijing Climate Center, China Meteorological Administration	BCC
3	BCC-CSM1.1(m)		
4	CanESM2	Canadian Centre for Climate Modelling and Analysis	CCCma
5	CCSM 4	National Center for Atmospheric Research	NCAR
6	CESM1(BGC)	National Science Foundation, Department of Energy, National Center for Atmospheric Research	NSF-DOE-NCAR
7	CESM1(CAM5)		
8	CMCC-CM	Centro Euro-Mediterraneo per I Cambiamenti Climatici	CMCC
9	CNRM-CM5	Centre National de Recherches Meteorologiques / Centre Europeen de Recherche et Formation Avancees en Calcul Scientifique	CNRM-CERFACS
10	CSIRO-MK3.6.0	Commonwealth Scientific and Industrial Research Organization in collaboration with the Queensland Climate Change Centre of Excellence	CSIRO-QCCCE
11	FGOALS-g2	LASG, Institute of Atmospheric Physics, Chinese Academy of Sciences; and CESS, Tsinghua University	LASG-CESS
12	FIO-ESM	The First Institute of Oceanography, SOA, China	FIO
13	GFDL-CM3	Geophysical Fluid Dynamics Laboratory	NOAA-GFDL
14	GFDL-ESM2G		
15	GFDL-ESM2M		
16	GISS-E2-R	NASA Goddard Institute for Space Studies	NASA GISS

For this stage in the methodology, the historical data from the GCMs were compared to the recorded data, and the models with the least bias were selected to create an ensemble for the ML prediction algorithm.

4.2.2. MACHINE LEARNING MODEL ARCHITECTURE

ML Model selection and interpretation: Machine Learning (ML) algorithms are an extension to advanced statistical learning, where the former compliments the latter by autonomously learning through different exposure techniques to the training datasets. ML models mimic the sentient behavior of human brains by learning from new experiences and datasets. By exposing the ML models to appropriate datasets, it extracts inherent features from the dataset and self-adjust to enhance its performance for the intended purpose, as defined by the user (Brownlee 2020; Rodrigues and De la Riva 2014). ML models have been gaining increased traction in the field of community resilience and anthropic and natural hazards(Abdel-mooty et al. 2022; Ganguly et al. 2019; Haggag et al. 2021; Hanewinkel et al. 2004; Rodrigues and De la Riva 2014; Shafizadeh-Moghadam et al. 2018). For the study presented herein, supervised ML models were employed to predict the future trajectory of community flood resilience categories using the hydrological information resulting from the employed GCMs. This multiclass classification heavily depends on the variables included in the development of the algorithm(Wu et al. 2004). As such, different techniques were deployed on this

dataset to develop the most accurate interpretable results for the development of reliable managerial insights for decision makers and policy developers.

ML models are typically referred to as “Black Box” models, while this definition is accurate in most cases. However, some ML algorithms are termed “Glass Box” algorithm (e.g., Decision Trees (DT), Random Forest (RF)) by introducing means of interpretability techniques and rules that can be set to enhance the interrelation between the model output and input variables, allowing the users to draw the required insights (Davoudi Kakhki et al. 2019; Li et al. 2012; Liu et al. 2018). Random Forests is an ensemble technique, adopting multiple DTs by aggregating their results and likelihood predictions, which improves the performance metrics of the model, but imposes a challenge for interpretability(Chi et al. 2012). This study adopts these ML algorithms to develop an empirical framework for resilience prediction (Figure 4-1) for identification of vulnerabilities in the trajectory of the current built environment. However, as all data-driven techniques, the quality of the work is tied directly to the quality and diversity of available data, highlighting the need for a comprehensive dataset with enough variables and time range spanning multiple years(Abdel-Mooty et al. 2021). This necessitates the need for data preprocessing, identifying the interdependencies within a dataset, and addressing missing results through data cleaning and imputation, ensuring the reliability of the data and eliminating the skewness and any induced biases(Patil and Baidari 2019; Yagci et al. 2018). In the study herein,

the independent variable is class-based, as such, multiclass classification techniques will be adopted. Additionally, for performance enhancement, ensemble techniques will be employed to complement the adopted algorithm (i.e., bagging, random forest, boosting) (Boehmke and Greenwell 2019; Nagpal 2017; Singh 2018).

Within the supervised ML techniques, there are the Classification and Regression Trees (CART) algorithms, where the classification trees are most suitable for the prediction of categorical (discriminate) independent variables, as opposed to regression trees that are more suitable to continuous variables (Mosavi et al. 2018). DT are based on a binary recursive partitioning algorithm with a set of rules (i.e., partitioning steps) that depend on their preceding steps. The partitioning is carried out such that the data is partitioned homogenously into nodes (i.e., subgroups) using binary questions with Yes-or-No answers about the features of each subgroup, repeating this process until a suitable stoppage criterion is achieved (e.g., maximum splitting). If all the subsets of the training dataset is correctly classified then a leaf node is created, and this process is recursively repeated until either all the training dataset is correctly classified, or the features are entirely exhausted (Hastie et al. 2009; Mosavi et al. 2018). In the classification tree algorithm, this feature selection process is based on information gain (i.e., decrease in entropy) or Gini index (Breiman et al. 1984; Hastie et al. 2009). Where Entropy (E) is the measure of purity of the sample, the Information gain (g) is the decrease

in Entropy (*E*) after a split based on a feature or attribute (*A*) in the training dataset (*T*), and is expressed in [Eq. (4-1)] through [Eq. (4-3)] (Ashari 2013):

$$g(T, A) = E(T) - E(T|A) \qquad (4\text{-}1)$$

Such that:

$$E(T) = -\sum_{k=1}^{k} \frac{|C_k|}{|T|} \log_2 \frac{|C_k|}{|T|} \qquad (4\text{-}2)$$

$$E(T|A) = \sum_{j=1}^{|A|} \frac{|T_j|}{|T|} \sum_{k=1}^{K} \frac{|T_{jk}|}{|T_j|} \log_2 \frac{|T_{jk}|}{|T_j|} = \sum_{j=1}^{|A|} \frac{|T_j|}{|T|} E(T_j|A) \qquad (4\text{-}3)$$

Where *k* is the number of class (with a total of *K* classes); C_k is the sample assigned to class *k*, T_j is the sample in the *T* dataset corresponding to j^{th} value of attribute *A*; T_{jk} is the j^{th} sample in attribute *A* that is assigned to class *K*; and |*A*| is the number of values of attribute *A*. Higher values of the Gini Index and higher information gain (*g*) denotes to a more important feature within the CART classification algorithm(Hastie et al. 2009). However, to enhance the performance of the model, numerous ensemble techniques were adopted in this study, including bagging, boosting, and random forest (Boehmke and Greenwell 2019; Nagpal 2017).

Bagging is a form of bootstrapping technique, which is a random sampling process of the data, taken by replacement, where each datapoint can be available for selection in multiple subsequent models, while still using all the predictors in the sampling process (Efron and Tibshirani 1986). In bagging however, the

aggregating technique is used for fitting multiple versions of the model within the training dataset, where each model is then used in the training of the DT model, followed by averaging all the predictions, providing a more reliable and robust model than a single DT (Breiman 1996; Breiman et al. 1984; Nagpal 2017). On the other hand, *Random Forest* (RF) models are considered a step further and an extension to Bagging techniques for model performance enhancement. In RF, the predictors are also randomized at each node at a split within the DT rather than doing so iteratively. Subsequently, the results are the aggregation of the prediction from the entire set of trees(Brownlee 2016; Feofilovs and Romagnoli 2017; Fielding 2006; Liaw and Wiener 2002; Nagpal 2017).

Model Performance Measures: The models employed for the analysis herein are: *i*) Decision trees with 100-fold cross validation, *ii)* Bagged decision trees, tested with up to 15,000 bootstrap replications as an ensemble method, with a minimum split of 4, *iii*) RF models with the Out-of-Bag Error tested for up to 3000 trees, showing a uniform plateau after 500 trees, indicating the unnecessity of increasing the number of trees in the forest more than 500, with four randomly sampled variables at each split, and a shrinkage parameter of 0.01(Brownlee 2016). With such models, finding universal performance measure can be challenging to compare the results of the models, as such, other performance indices were adopted for this study. The overall model misclassification error was utilized to identify the highest performing models [Eq. (4-4)]. However, with the skewness of the data, the

multiclass nature of the independent variable, and for further interpretability for the models, more in-depth measures needed to be utilized. As such, the Precision, Sensitivity (i.e., Recall), and F1-score for each category were utilized in both datasets, namely training and testing. *Precision* is the measure of accuracy of each class in the prediction algorithm, denoted by the number of accurately predicted datapoints in that class as shown in [Eq. (4-5)]. Recall on the other hand is the ratio between the accurate predictions to all correct examples in the dataset, it represents the correctness of the classification results of the ML model [Eq. (4-6)]. Finally, the F1-score, is the integration of both the Precision and Recall for the classification algorithm, where the concerns of both measures is balanced out [Eq. (4-7)](Brownlee 2016, 2020).

$$Total\ Misclassification = \frac{\sum_{r=1}^{K}\sum_{c=1}^{K} N_{rc} - \sum_{i=1}^{K} TP_i}{\sum_{r=1}^{K}\sum_{c=1}^{K} N_{rc}} \quad (4\text{-}4)$$

$$Precision = \frac{TP}{TP+FP} \quad (4\text{-}5)$$

$$Recall = \frac{TP}{TP+FN} \quad (4\text{-}6)$$

$$F1\text{-}score = 2 * \frac{Precision * Recall}{Precision + Recall} \quad (4\text{-}7)$$

Where: K = number of Classes in the independent variable; N is the count number of observations allocated in each cell of the confusion matrix; TP= True Positive, which is the number of accurately predicted observations in a given class; FP= False Positive is the count number of predictions incorrectly assigned to a category; FN= False Negative is the count number of observations incorrectly

assigned to a wrong class(Khalaf et al. 2018). These values can be drawn from the Confusion Matrix, where the diagonal represents the accurately predicted observations, and the off diagonal depicts the incorrect predictions. In Figure 4-2, the example is based on a 3-class prediction model, where it shows the annotation of the TP, TN, FP, and FN of each category, such that (a) shows the annotated confusion matrix for Category 1, (b) for Category 2, and (c) for Category 3.

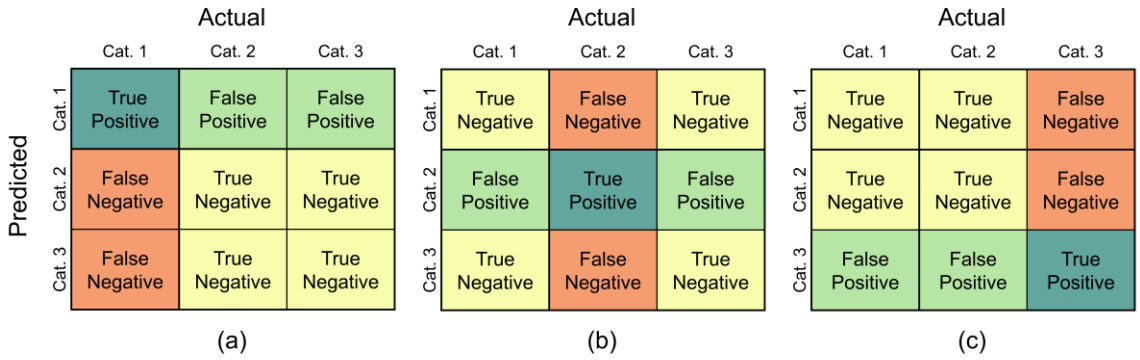

Figure 4-2: Confusion Matrix example showing the annotation for TP, TN, FP, and FN for each category, where (a) is for Category 1, (b) for Category 2, and (c) for Category 3

Model Interpretability Techniques. The ambiguity associated with these ML algorithms hindered the progressive utilization of such models in fields such as structural and civil engineering and community resilience planning(Doshi-Velez and Kim 2017; Murdoch et al. 2019). This phase of the methodology employs Partial Dependence Plots (PDP) as a tool for interpretability, where the input-output relationship between most variables is explored, and depicted into complex-linear relationships(Murdoch et al. 2019). The PDPs the impact of the input features—

whether single input or group of variables (e.g., Temperature or Temperature and Precipitation) is explored as the average prediction corresponding to the range of values for the other unused input features (Du et al. 2020; Feng et al. 2021). Other method for interpretability employed in this study is the Variable Importance (VI) algorithm. VI is used to infer the influence of a variable (e.g., Maximum Temperature of Model ACCESS1.0) on the prediction process, and the output of the model. Such method quantifies the extent upon which the model relies on each of the involved feature, identifying the most influential variables within the dataset for further investigation. This is done by evaluating the corresponding increase in model performance measure (e.g., information gain)(Doshi-Velez and Kim 2017; Du et al. 2020; Feng et al. 2021; Murdoch et al. 2019; Rözer et al. 2021).

4.3. MODEL DEPLOYMENT, RESULTS AND DISCUSSION

4.3.1. CATEGORIZATION AND SPATIAL ANALYSIS

For the categorization stage of this model, the categories present in the study by Abdel-Mooty et. al., (2021)(Abdel-Mooty et al. 2021) were employed. In that study, the historical disaster dataset by the NWS was employed, as mentioned in previous sections, this dataset is considered the longest run flood disaster damage recorded in the United States(Murphy 2018). The categorization process presented in that study resulted in a total of 5 categories. However, further investigation of the employable dataset in the current study with respect to the developed categories

revealed clear skewness in the categories, with just 20 observed events falling in category 3, and 102 falling in category 5, representing less than 2% of the dataset, making the inclusion of these categories in developing and training the ML algorithm next to impossible. As such, due to the proximity of the clusters in the unsupervised ML results displayed in Abdel-Mooty et. al. (2021), the Categories 3,4, and 5 were merged together, resulting in 3 Categories for deployment in the Current study. The resulting categories were used in the development of spatial and descriptive analyses of the disaster database, as shown in Figure 4-3, the state of Texas suffered the most damage resulting from flood disaster since the year 1996 and exposed to the highest number of recorded observations, making it appropriate as a testbed for the current study.

Table 4-3: The Employed Community Flood Resilience Cateories

Community Flood Resilience Category	**Class description**
1	Communities exposed to events that occur in the summer, causing disturbance less than 264 hours (11 days) and/or causes up to 250 injuries, and damage less than $2.5B without fatalities
2	Communities exposed to events that occur in the spring, causing any disturbance duration, causes up to 20 injuries, and damage up to $1.5B without fatalities
3	Communities exposed to events occurring in any season, causing any disturbance duration that results in more than 250 injuries, causing damage more than $2.5B, with fatalities, Communities exposed to events that occur in winter or fall, causing disturbance less than 264 hours (11 days) causes up to 250 injuries and damage up to $2.5B without fatalities, and Communities exposed to events occurring in the spring that are not under class 2.

Although Texas does not have the highest historical average Flood Resilience Index, it still suffered the highest damage at $46B, and a total of 12,834 recorded events. The clear difference between the state of Texas and other states in terms of vulnerability to flood hazard is attributed to the higher heat content associated with the western Gulf of Mexico, where it facilitates the increase of humidity and mean temperature over other places in the United States(Trenberth et al. 2018). This increased heat content is also proportional to the precipitation resulting from different storms, and causes the tropical weather region engulfing the state of Texas, resulting in an alarmingly increasing number of hurricanes and other extreme weather events(FEMA 2012). This phenomenon is only exacerbated by the increasing urbanization rate, increasing the vulnerable and exposed areas to such extreme weather events (FEMA 2012, 2018; Trenberth et al. 2018).

Figure 4-3a shows the spatial analysis conducted on the historical dataset, showing the monetary damage, and flood resilience category per state as identified in table 4-3; Figure 4-3b shows a spatial analysis of the state of Texas at a county level, showing a distribution of higher resilience categories along the eastern coast and the Gulf of Mexico. That is attributed to the high-tide flooding and increased sea level which is becoming increasingly common over the past decades (Sweet et al. 2020). The spatial distribution presented in Figure 4-3b aligns with the "Cartographic Maps of Precipitation Frequency Estimates" published by NOAA in the report Atlas 14 Volume 11 of Texas(Perica et al. 2018), showing an increase in

the severity of natural hazards befalling this area (e.g., Hurricane Harvey, with it's gigantic $128.8B tally on the coastal communities, identified as one of the most expensive natural disasters in recorded history)(NOAA 2020; NOAA Office for Coastal Management 2021; Sweet et al. 2020). Figure 4-3c, shows the identified locations where the GCM simulations were run, where 45 counties (listed in table 4-4) were selected for the collection of the CMIP5 simulation results, synchronizing them with the historical disaster dataset in these counties.

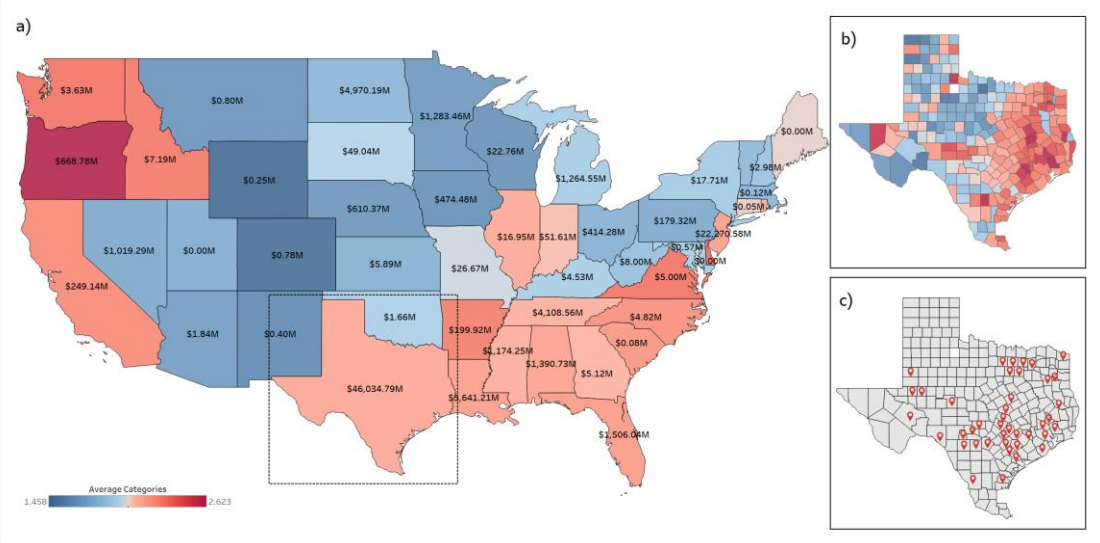

Figure 4-3: Spatial analysis of the United States showing Monetary Losses and the 3 Categories Flood resilience index, a) Country wide Spatial analysis at a state level; b) Spatial analysis for the state of Texas at a county level; c) location of collection stations for the climate projections and the employed GCMs.

Table 4-4: List of Counties for CMIP5 GCM Simulations

List of Counties were the CMIP5 GCMs Simulation results were extracted				
Bexar	Williamson	Lavaca	Johnson	Bastrop
Tarrant	Val Verde	Brazoria	Ellis	Medina
Travis	Bell	Liberty	Gaines	Tom Green
Dallas	Denton	Angelina	Pecos	Kerr
Nueces	Ector	Montgomery	Austin	McLennan
Midland	San Patricio	Smith	Waller	Gonzales
Uvalde	DeWitt	Gregg	San Jacinto	Gillespie
Bowie	Victoria	Real	Caldwell	Webb
Hunt	Collin	Fayette	Wise	

4.3.2. ML MODEL PERFORMANCE AND INTERPRETABILITY

The dataset employed in the development of the prediction algorithm is: Monthly Average Flood Resilience Category, collecting by calculating the average category of all recorded flood events occurring in the same geographical location (i.e., county), at the same month, from the year 1996 to the year 2020, this average monthly category is considered the independent variable in this analysis. The dependent variables were the hydrological data resulting from the CMIP5 simulated GCMs at each of the 45 selected locations. These variables are: Monthly average maximum surface air temperature (^{o}C), monthly average minimum surface air temperature (^{o}C), monthly mean wind speed (m/s), and average monthly runoff (mm), for each of the 16 selected GCM for each climate scenario (i.e., RCP 6.0, and RCP 8.5) as mentioned earlier, with a total of (4,324 observations) for model

development Dataset. This dataset was split into training and testing dataset at a ratio of 70% and 30% respectively (3,028 observations in training dataset, and 1,296 observations in testing dataset). With the results of all GCMs, the total number of variables is 80 (5 hydrological variables for each of the 16 models), proving it to be computationally expensive to develop interpretable results across the future projections. As such, the Brute-Force feature selection method was adopted in this study, instead of an ensemble of the GCMs to avoid any biases and include the benefits of all models.

The Brute-Force method relies on the computational capabilities to conduct an exhaustive search throughout all possible combinations of a certain set of variables(Jafarnezhad et al. 2016). As such, a list of all possible combinations of the 16 GCMs was developed into a binary variable, identifying at each step which GCM to include in the analysis. The total number of models resulted from all possible combinations for the 16 GCMs for testing were 65,535 models. The following step is to identify a performance measure to use for evaluation of the results of a ML model developed for each possible combination. In this step, a Bagged DT model was used for all combinations, and the total Misclassification error was selected as the appropriate performance measure per [Eq. (4-4)]. Figure 4-4 shows the results of all possible combinations for GHG emission scenario RCP 6.0, identifying the model number 32,517 as the one with least Misclassification error (3.05%) at only 8 GCMs included in the analysis (GCMs: 1, 6, 7, 9, 10, 11,

15, and 16, with their details in Table 4-1). Figure 4-5, shows the misclassification error for all possible combinations for GHG emission scenario RCP 8.5, identifying the model number 59,643 with 11 GCMs included in the analysis (3.1%) (GCMs: 1, 2, 3, 5, 6, 9, 11, 12, 14, 15, 16, with their details in Table 4-2).

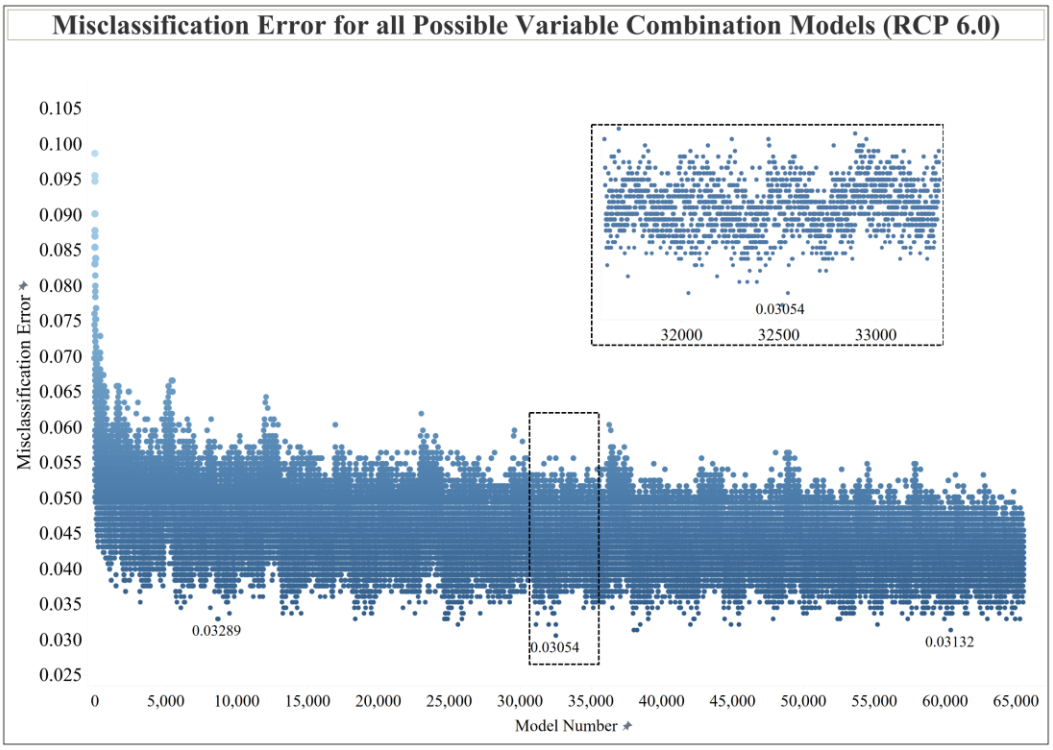

Figure 4-4: Total Misclassification error for all possible GCM combinations for RCP 6.0

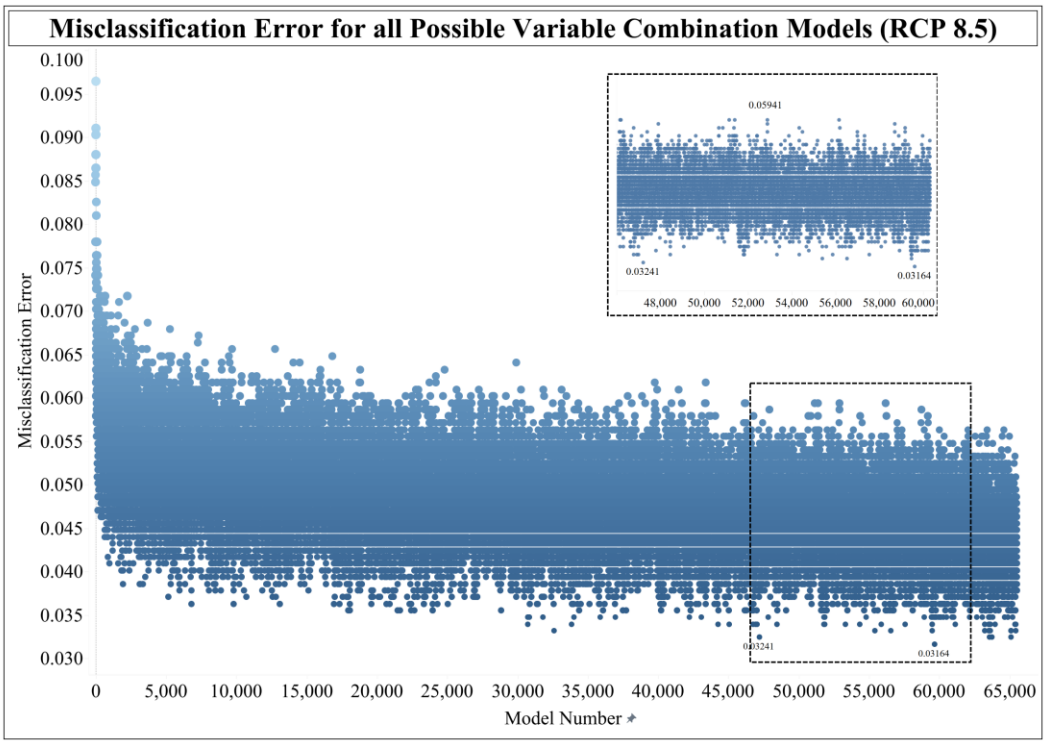

Figure 4-5: Total misclassification error for all possible GCM combinations for RCP 8.5

After model selection and variable identification, multiple ML models were developed for predicting the future projection of resilience category across the identified geographical locations within the state of Texas. The first model is a gradient boosted RF model, with a splitting of 70% to 30% of the data as mentioned earlier for training and testing, respectively. The model's performance was optimized with the average Out-of-Bag error (OOB) as shown in figure 4-5, where the number of trees is set between 1 and 3000 (only showing the first 1000 in Figure 4-5a), a step size of 1, and values of error calculated for each category separately to identify outlying behavior in the model's performance. The model shows no clear

improvement in performance beyond n_{tree} of 500 in RCP 6.0, and slight fluctuations in RCP 8.5 till n_{tree} = 1000. The optimal number of trees in both models was taken at 500 and 1000 for RCP 6.0 and RCP 8.5, respectively.

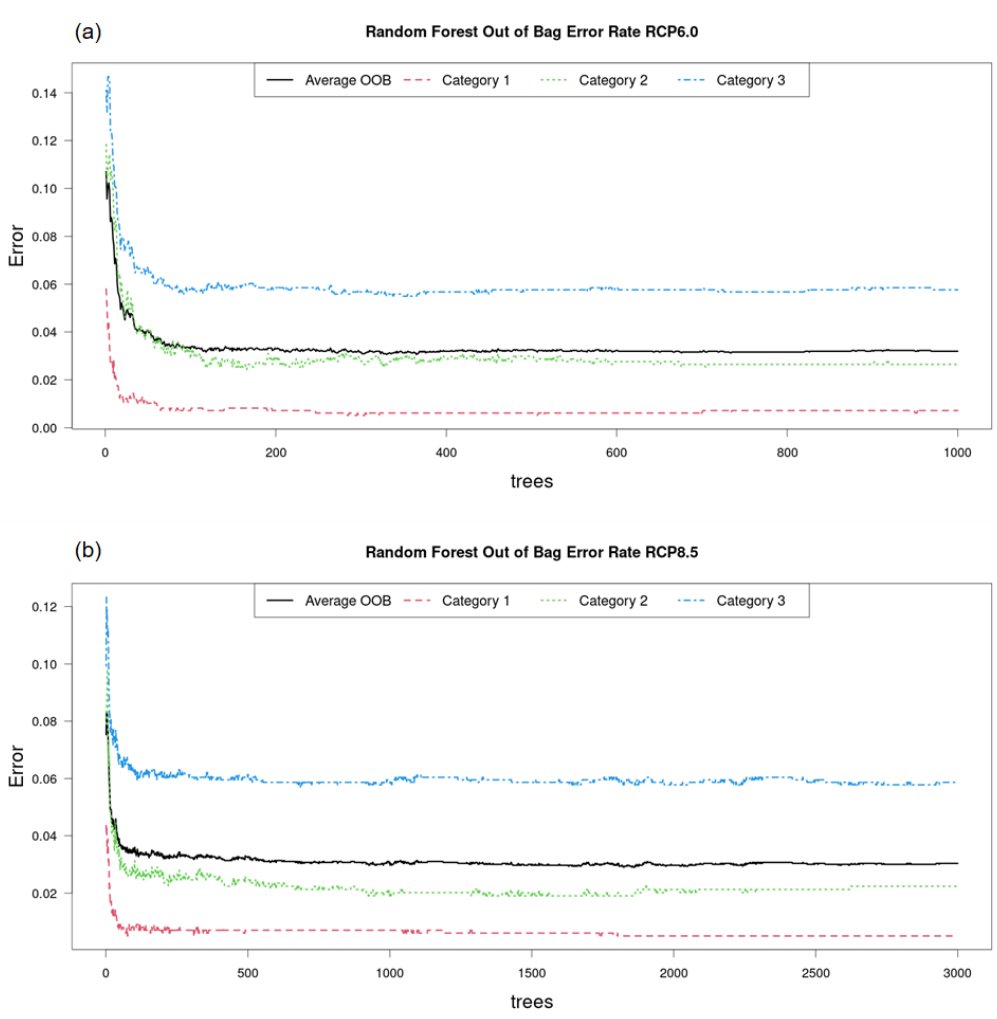

Figure 4-6: Out of Bag error for Random Forest prediction model where: a) for RCP 6.0, and b) for RCP 8.5

The second Model is DT with bagging performance enhancement, with 15,000 bootstrap replication, and 4 random splitting for variables at each split, and a shrinkage parameter of 0.01 for both emission scenarios. The model's results were further analyzed with model performance measures and interpretability techniques to choose the optimum model for future projections. Figures 4-7 and 4-8 show the visualization for the performance measures based on the performance indicators mentioned earlier; Namely F1-Score, Precision, and Recall (Sensitivity), with their calculations using [Eq. (4-5)] through [Eq. (4-7)]. This analysis shows us that although the prediction performance of the models are comparable in both, training and testing datasets, the Bagged Decision Tree model slightly outperforms the Random Forest model, however the performance of both models are achieving high efficacy with almost all measures above the 90% mark. Figure 4-7 shows the performance measures for the emission scenario RCP 6.0 for the training and testing datasets, where the Sensitivity, Precision, and F1-Score shown for all categories. Looking at the results of these performance measures, it is clear that the validation of the model performance and prediction objective are high, ensuring that the features included in the analysis yield favorable results in both training and testing datasets. By looking at the training dataset on its own, it can be assumed that the model is overtrained, however, the testing and cross-validation conducted on the dataset also yielded over 90% accuracy and efficacy, ensuring that the model does perform well for future projections. Figure 4-8, on the other hand, show that

the performance measures for the emission scenario RCP 8.5 where the Sensitivity, Precision, and F1-Score are shown for all categories. Similar to RCP 6.0, the RCP 8.5 model's performance measures are high with accuracy and efficacy above 90% in all categories, showing similar behavior in the testing category, showing that the prediction threshold is met in both models, albeit with a slight advantage to the performance of the Bagged DT model over the Boosted RF model in both emission scenarios. As such, moving forward, the bagged DT model is chosen for further analysis, interpretability, and future climate projections throughout this study.

Figure 4-7: Model performance indicators for RCP 6.0

Figure 4-8: Model performance for RCP 8.5

Figures 4-9 and 4-10 give deeper insight into the performance of the bagged DT model by showing the confusion matrices for the RCP 6.0 and RCP 8.5 respectively. Where (a) is for the training dataset and (b) is for the testing dataset in both figures. From Figure 4-9 we can see that the accuracy of the model is

(99.2%) for training dataset, and (95.2%) for testing dataset, showing a misclassification error of (4.7%) for the testing dataset based on [Eq. (4-4)]. While Figure 4-10 shows that the accuracy of the training dataset is (98.8%), and (96.3%) for the testing dataset, showing a misclassification error of just (3.6%) based on [Eq. (4-4)], proving to provide reliable projections for future resilience analysis and planning.

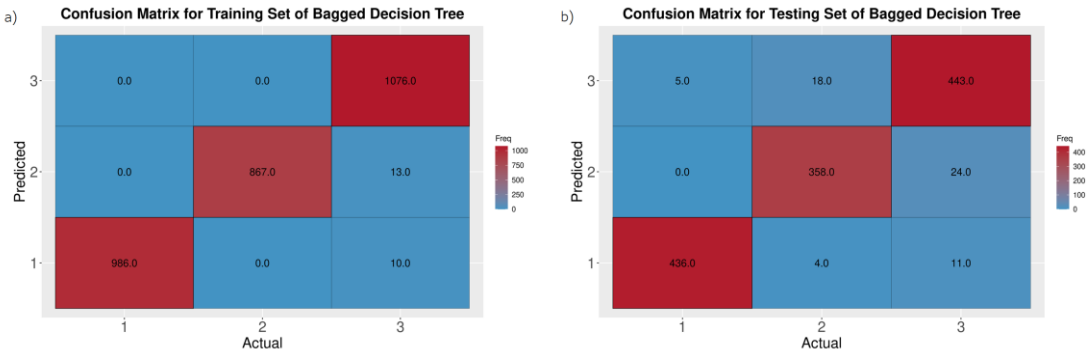

Figure 4-9: Confusion matrix for bagged DT model RCP 6.0 where (a) is training dataset, and(b) is the testing dataset

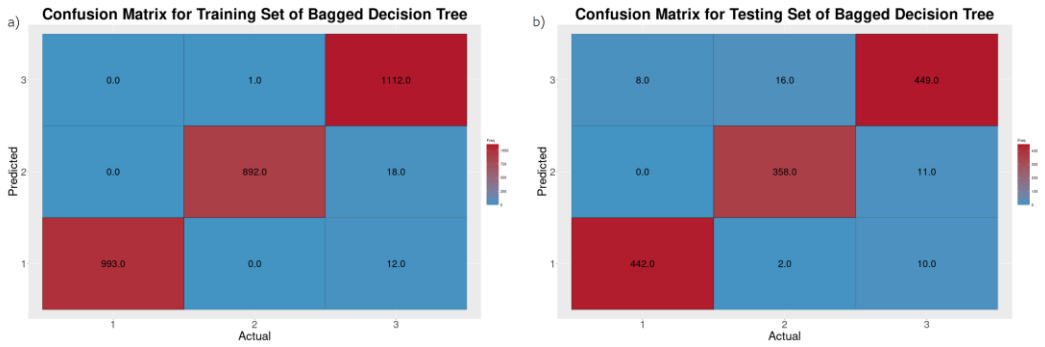

Figure 4-10: Confusion matrix for bagged DT model RCP 8.5 where (a) is training dataset, and (b) is the testing dataset

Interpretability: further inspection on all included variables in the bagged DT model for both emission scenarios was conducted. Figure 4-11 shows the correlation matrix for the bagged DT model for both emission scenarios where Fig.11 a) is correlation matrix for variables in bagged DT model for RCP 6.0, and b) is that for RCP 8.5. The correlation matrices include the correlation value between the input pairs considered in this study. It can be observed that the Temperature variables are highly correlated across different GCMs, however, it can also be observed that the temperature is inversely correlated to wind speed and runoff, but slightly correlated with precipitation. It can be concluded that the wind variables are not correlated with the precipitation and runoff, neither positively or inversely correlated, however, the precipitation and runoff variables are positively correlated for each GCM simulation, but not across different models, highlighting the need for an ensemble technique for including as many GCMs as possible to expand the range of variables in the analysis and their impact on the prediction models.

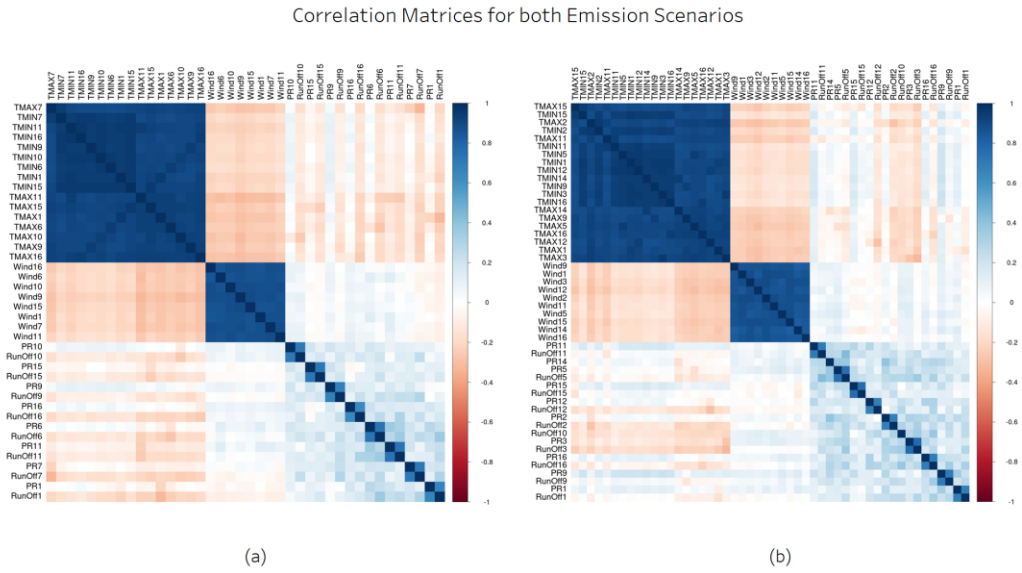

Figure 4-11: Correlation Matrix for included variables in bagged DT where; a) RCP 6.0, and b) RCP 8.5

The following analysis is the identifying the Variable Importance in the developed algorithm for both emission scenarios. Figure 4-12 shows the variable importance (VI) bar chart where Figure 4-12 a) for the RCP 6.0 scenario, and b) for the RCP 8.5 emission scenario. The VI included in this analysis is based on the Receiver Operating Characteristics (ROC) curve analysis conducted on each predictor. The ROC demonstrates the model's susceptibility to incorrectly classify the observations in the dataset, where a series of cutoff methods are applied to the predictors for the prediction to take place. The area of the ROC curve is then calculated for each class pair (i.e., Category 1 vs Category2, Category 2 vs Category 3, etc.) using the trapezoidal rule, then the maximum area under the curve across the relevant pair-wise curves is considered the VI in the model(Kuhn 2019). From

Figure 4-12 we can conclude that the temperature variables are most influential in the model's performance, having the first 11 variables based on their VI metric are maximum and minimum temperatures for the included ensemble of GCMs, which is confirmed by the high correlation of temperature variable with other variables in the dataset. For the RCP 8.5 scenario, the same pattern is identified, having the first 15 variables based on their VI as temperature outputs of the different GCMs. It is also clear that after a certain threshold, the VI drops significantly, indicating that some GCMs have a bigger influence on the probability of correctly classifying a class, however an ensemble of multiple GCMs is needed to increase the overall total performance and include as much variability and bias elimination in the prediction algorithm.

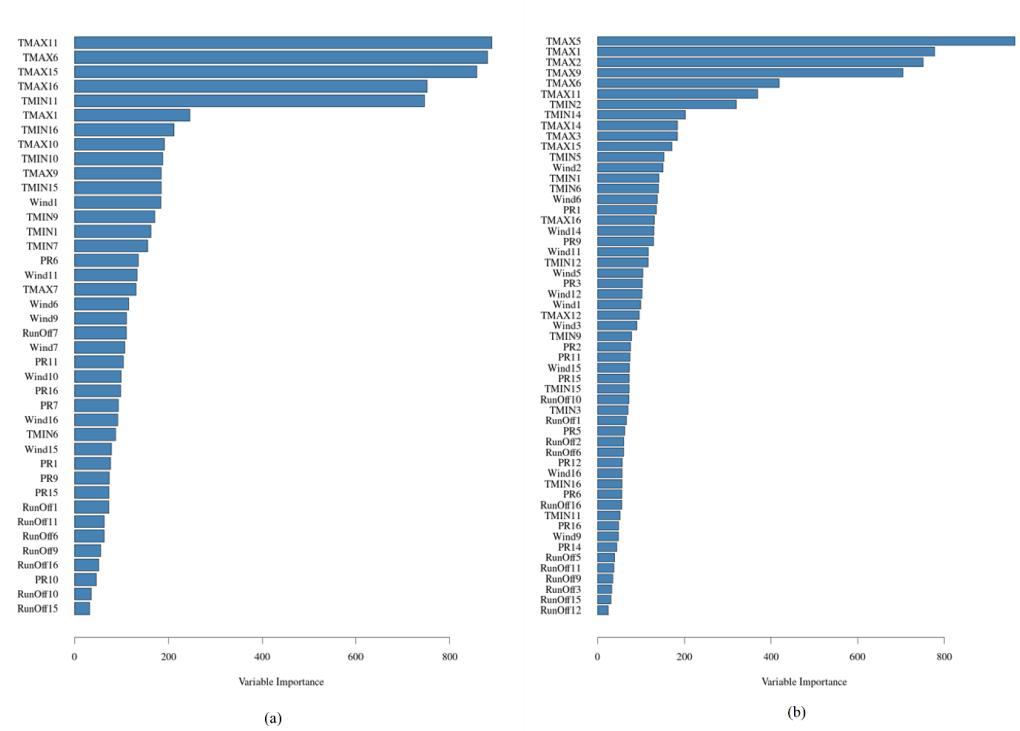

Figure 4-12: Variable Importance for included variable in bagged DT model where; a) RCP 6.0, and b) RCP 8.5

The last and essential interpretability technique included in this study is the Partial Dependence Plots (PDP) as shown in Figure 4-13 for RCP 6.0 and Figure 4-14 for RCP 8.5. PDPs help visualize the complex interrelationships between the predicted categories and the ML model inputs from the various GCMs, where the effect of change is represented in a single-variable plot. The PDP in Figures 4-13 and 4-14 shows the first four maximum temperature variables, the first two minimum temperatures, the first two precipitation variables, the first two wind speed variables, and the first two runoff variables based on their importance according to the VI plots as shown in Figures 4-12a and 4-12b. The values of the

variables in the model are normalized and scaled for an optimum homogeneity in the ML model, to avoid skewness in the model and account for the multiple different units of measurement for all variables, it was unscaled back to its original range for the development of the PDPs, to draw interpretability insights. While it is expected that the results will vary depending on the GCM model results being inspected within the input space of the ML model and the emission scenario under investigation, the overall behavior of these variables is expected to remain the same. For the RCP 6.0, the PDPs for the maximum temperatures all indicate a clear jump in the influence of the resilience category when the maximum temperatures are between 30 to 40 ^{o}C, showing that the risk of flooding disasters increase as the temperatures rise, the same applies for all GCMs included in the development of the predictive model. The minimum temperatures do not have an equivalent increase in predicted flood risk impact, but it shows a slight rise when monthly minimum temperature is between 15 to 30 ^{o}C. this can be attributed to the increased heat content over the gulf of Mexico, transforming the weather into a tropical atmosphere, positively correlated to increased rainfall and a suitable climate for the development of hurricanes (NOAA Office for Coastal Management 2021; Perica et al. 2018). The runoff doesn't have much impact on the predictive capability of the model beyond the 100 mm, however, the impact is slightly different from one GCM to another from 0 to 100 mm. The resilience category is higher at lower runoffs, then gradually fluctuates and falls until it reaches 100 mm. The precipitation

patterns heavily vary from one GCM to another, however at low values (below the 200 mm), their influence is similar to one another where it keeps fluctuating at lower values. The windspeed's influence over the resilience category is very high for values up to 6 (m/s), with a severe drop in influence over predicted resilience category increase once the speed goes beyond the 6 m/s threshold. For the RCP 8.5 PDPs, the behavior of maximum temperature, minimum temperature, and wind speed are almost the same as the RCP 6.0 simulations. However, the precipitation for RCP 8.0 shows a different behavior, where the influence partial dependence is much higher with a wider range at precipitations below 300 mm, and the runoff exhibits similar behavior, with a wide range of variability from different GCMs, however, they all show that their influence on the resilience category predictions stops right before the 100 mm total runoff.

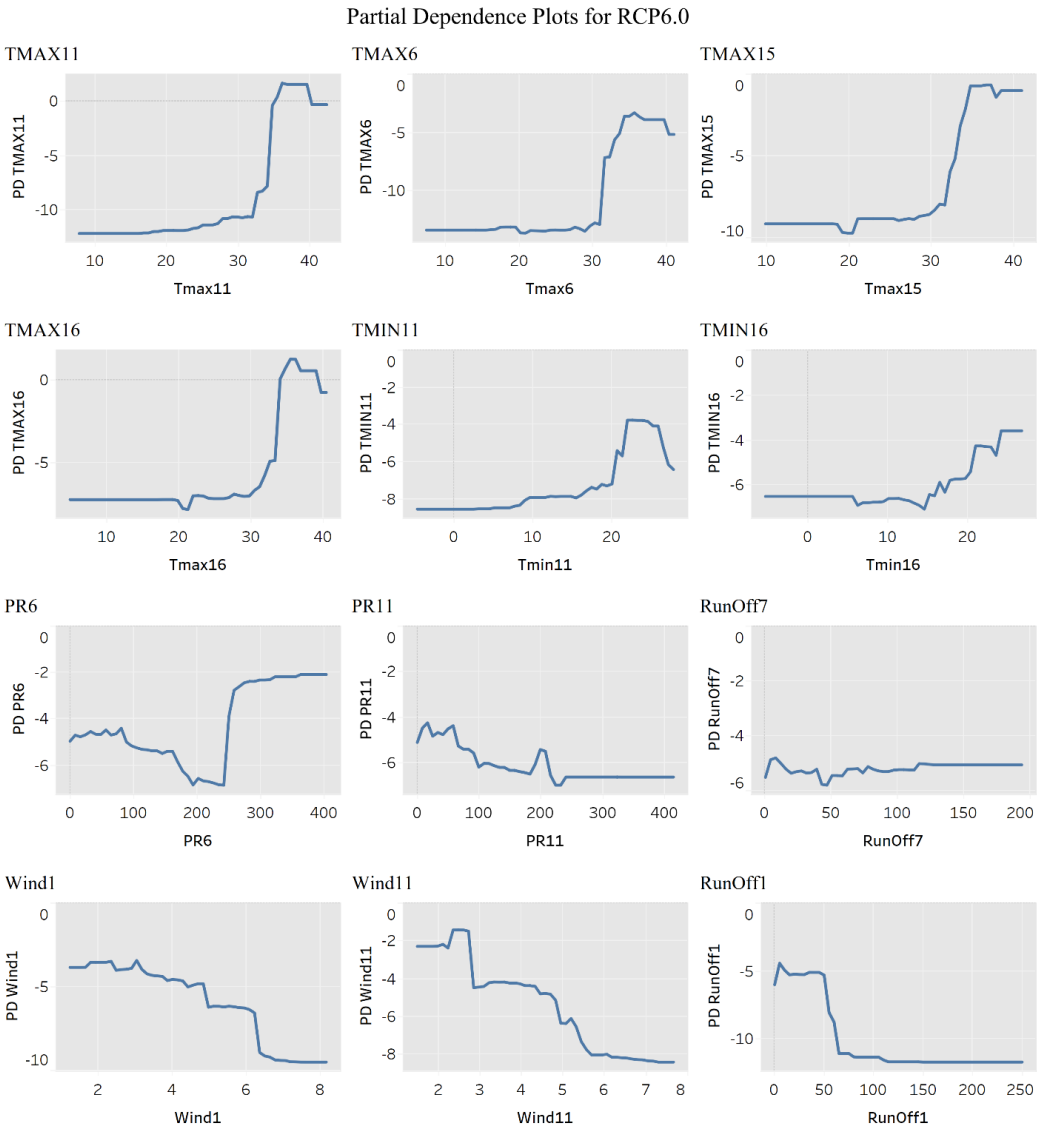

Figure 4-13: Partial Dependence Plots for RCP 6.0

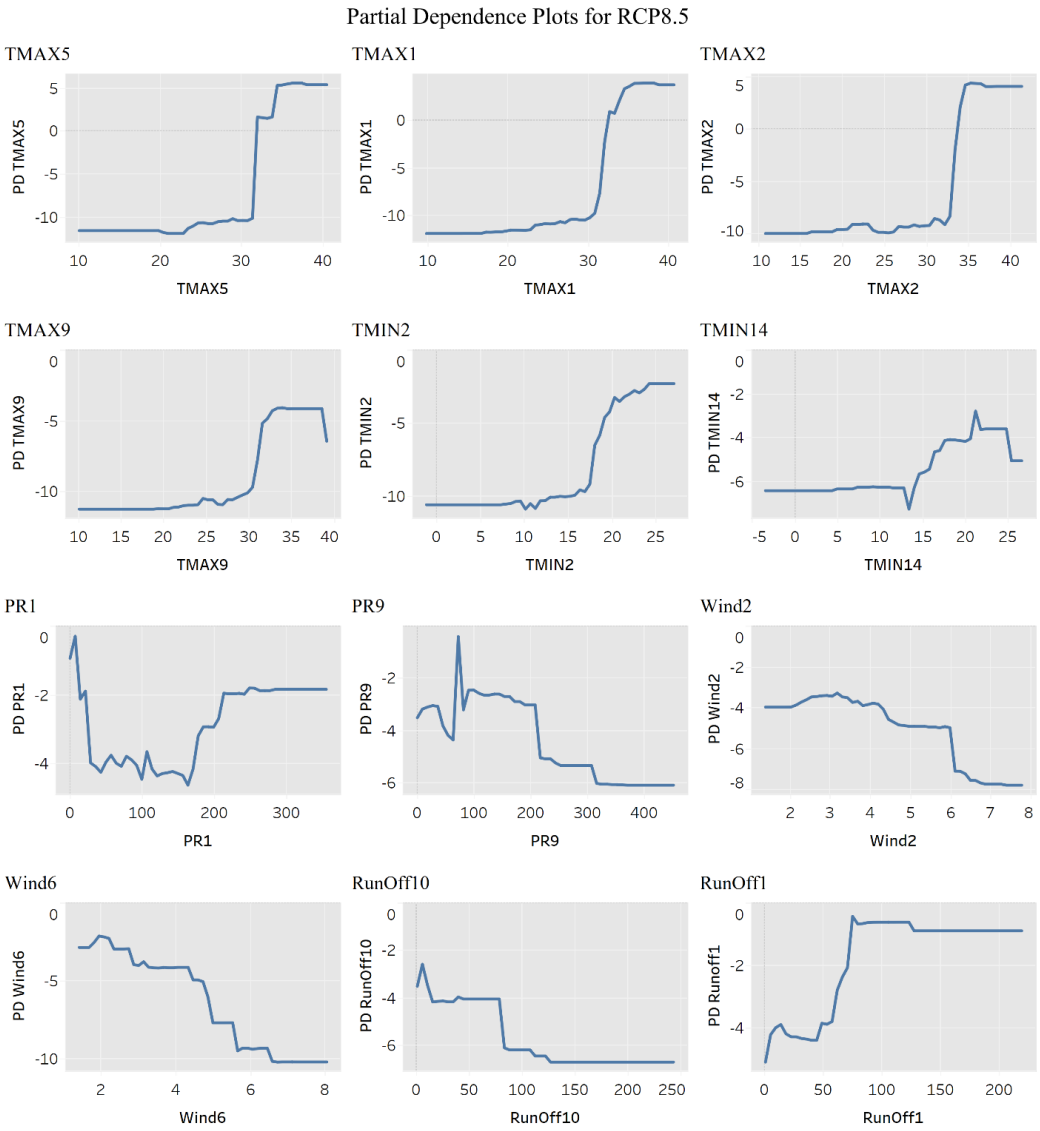

Figure 4-14: Partial Dependence Plot for RCP 8.5

Using such interpretability methods as shown in Figures 4-11 to 4-14 proves its employability in better understanding the behavior of the different variables within the ML algorithm, their influence on the prediction output, and the interrelationship and interdependencies between these variables. This

interpretability feature of ensures that the output of the ML prediction algorithm can be investigated more thoroughly, and the behavior of the input-output variables can be explained.

4.3.3. MODEL RESULTS AND DISCUSSION

By running the prediction algorithm on the GCMs projections till the year 2050, this study captures the change in resilience of the chosen 45 counties presented in table 4-4. A Spatio-temporal analysis was conducted to visualize the effect of climate change on the built environment and identify the vulnerabilities and climate change's impact on the flood exposure and resilience. Figure 4-15 a) is a temporal distribution of the yearly average resilience category per county per year between the years 2020 and 2050, b) is the spatial distribution of the counties involved in the analysis, *i*) is a multi-layer spatial distribution of the year 2020 where the location of each county is identified by a circle, the size and color of the circle represents the running cumulative average resilience category, *ii*) a multi-layer spatial distribution of the running cumulative average till the year 2030, *iii*) a multi-layer spatial distribution of the running cumulative average until the year 2040, iv) a multi-layer spatial distribution of the running cumulative average until the year 2050, also differentiated by size and color for visualization. This analysis shows that there is an increase in the yearly average flood resilience index for almost all counties involved in the analysis, amounting to an increase in the yearly

average across the years, albeit a small increase. The average category between the years 2020 and 2030 is 2.1, between the years 2030 and 2040 the average is 2.17, and 2.21 between the years 2040 and 2050. The historical recorded damage between the years 1996 and 2020 is $13,686M, amounting to an average of $5,702M per decade. Assuming the historical category is the same as that at the start of 2020, the projected damage based on the RCP 6.0 scenario between the years 2020 and 2030 is $6,260M, at an increase of 9.7% in monetary damage, between the years 2030 and 2040 the projected monetary loss is $6,498M at an increase of 13.9%, and between the years 2040 and 2050, the projected monetary loss is at $6,587M at an increase of 15.5%. Notwithstanding this monetary damage, the resilience category is also an indicator for other socio-economic components, like injuries, fatalities, evacuations, and the downtime of the community following the flood event. The indicator shows an increase of 15.5% per decade in these components leading up to the year 2050, showing the immediate need for intervention and mitigation measures and the development of a resilience-guided flood risk policies. These numbers, while alarming, they only amount for the counties and geographical locations included in the analysis presented herein, not the entirety of the state of Texas, which would amount to a much larger overall increase.

Figure 4-16 on the other hand shows, similar to figure 4-15, a) is a temporal distribution of the yearly average resilience category per county per year between the years 2020 and 2050, b) is the spatial distribution of the counties involved in

the analysis, *i*) is a multi-layer spatial distribution of the year 2020 where the location of each county is identified by a circle, the size and color of the circle represents the running cumulative average resilience category, *ii*) a multi-layer spatial distribution of the running cumulative average until the year 2030, *iii*) a multi-layer spatial distribution of the running cumulative average until the year 2040, iv) a multi-layer spatial distribution of the running cumulative average until the year 2050, also differentiated by size and color for visualization.

This analysis shows similar results to that of RCP 6.0, albeit at a more increase in average resilience index, and a more severe climate change scenario. The average category between the years 2020 and 2030 is 2.2, between the years 2030 and 2040 the average is 2.3, and 2.52 between the years 2040 and 2050. The historical recorded average damage per decade between the years 1996 and 2020 is $5,702M, with the same assumptions conducted for the RCP 6.0, the projected damage based on the RCP 8.5 scenario between the years 2020 and 2030 is $6,400M, at an increase of 12.2% in monetary damage, between the years 2030 and 2040 the projected monetary loss is $6,692M at an increase of 17.4%, and between the years 2040 and 2050, the projected monetary loss is at $7,331M at an increase of 28%. Similarly, the resilience category is also an indicator for other socio-economic components, like injuries, fatalities, evacuations, and the downtime of the community following the flood event. The indicator shows an increase of 28% per decade in these components leading up to the year 2050, an increase almost twice

as much damage as the RCP 6.0 scenario. This increase doesn't only show the need for intervention measures as mentioned earlier, but also the need for global effort to reduce carbon emissions and GHG into the atmosphere, in a desperate attempt to evade the RCP 8.5 scenario, since it is now almost inevitable to actualize the RCP 6.5 with the current global efforts. This global effort, coupled with multiple resilience-guided flood risk analysis could potentially save billions of dollars from tax-payers money.

The analysis conducted in this study can provide a large-scale data-driven study into climate change's impact over the United States at multiple spatial resolutions. Applying the methodology provided herein and adding more variables into the development of the ML model could potentially provide decision makers with a very powerful tool for resilience prediction and prevention, employing the spatial analyses provided herein for vulnerability identification and resource allocation. By increasing the resolution of the data, to a daily resolution instead of a monthly one, could be utilized as an early-warning-system to alert municipalities to increasing predicted flood disasters for preparedness measures to be employed. In addition, this framework could be integrated with the cloud system to develop a real life-engine for disaster prediction, expanding the types of dependent and independent variables to include more types of disasters and climate induced systemic risks.

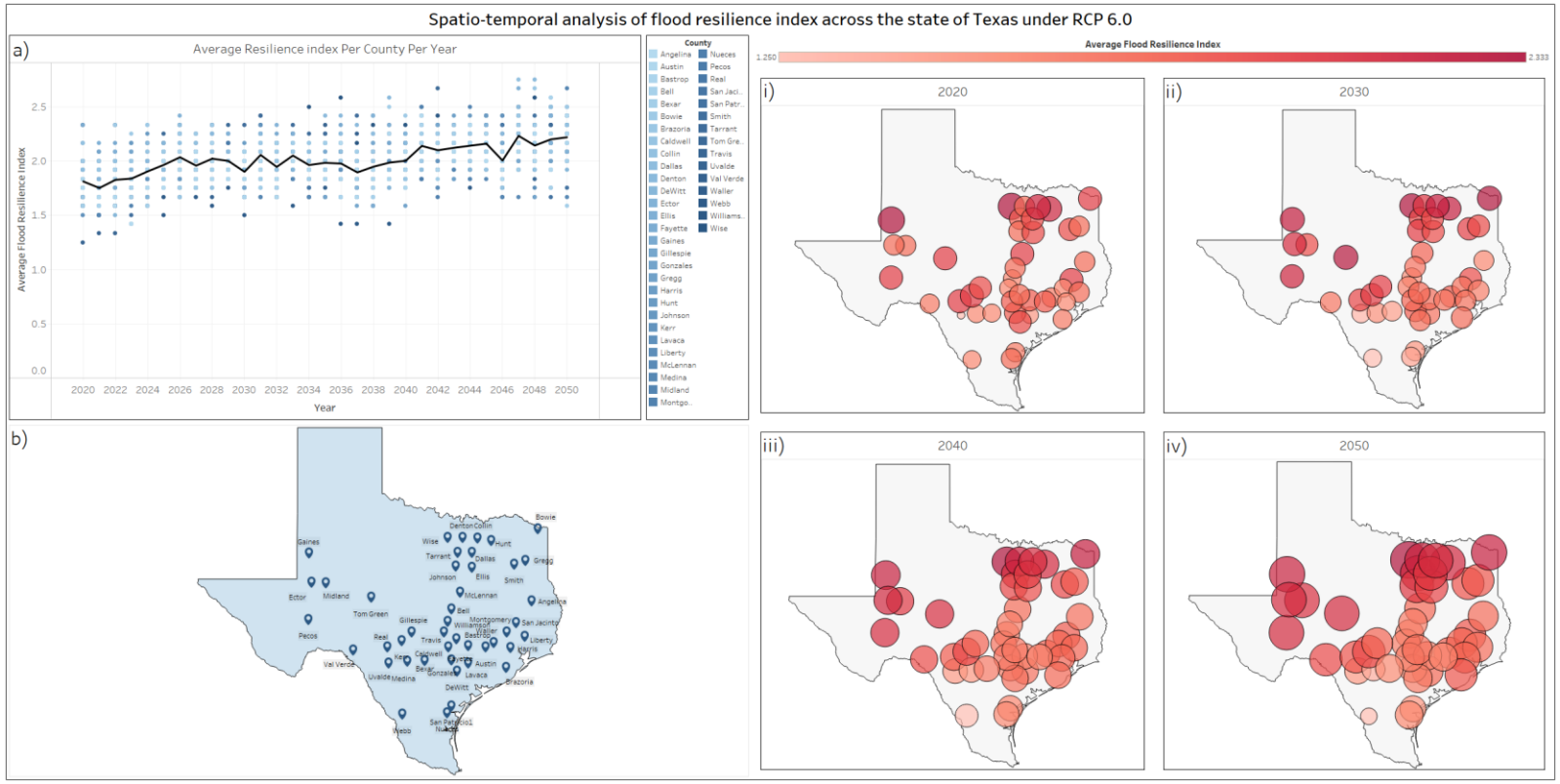

Figure 4-15: Spatio-temporal Model Output visualization for RCP 6.0, where; a) yearly average per county per year, with a running average for all included counties, b) spatial distribution of included counties and their GCM's stations, i) the spatial distribution of average Resilience index per county in the year 2020, ii) spatial distribution of average Resilience index per county till the year 2030, iii) spatial distribution of average Resilience index per county till the year 2040, iv) spatial distribution of average Resilience index per county till the year 2050

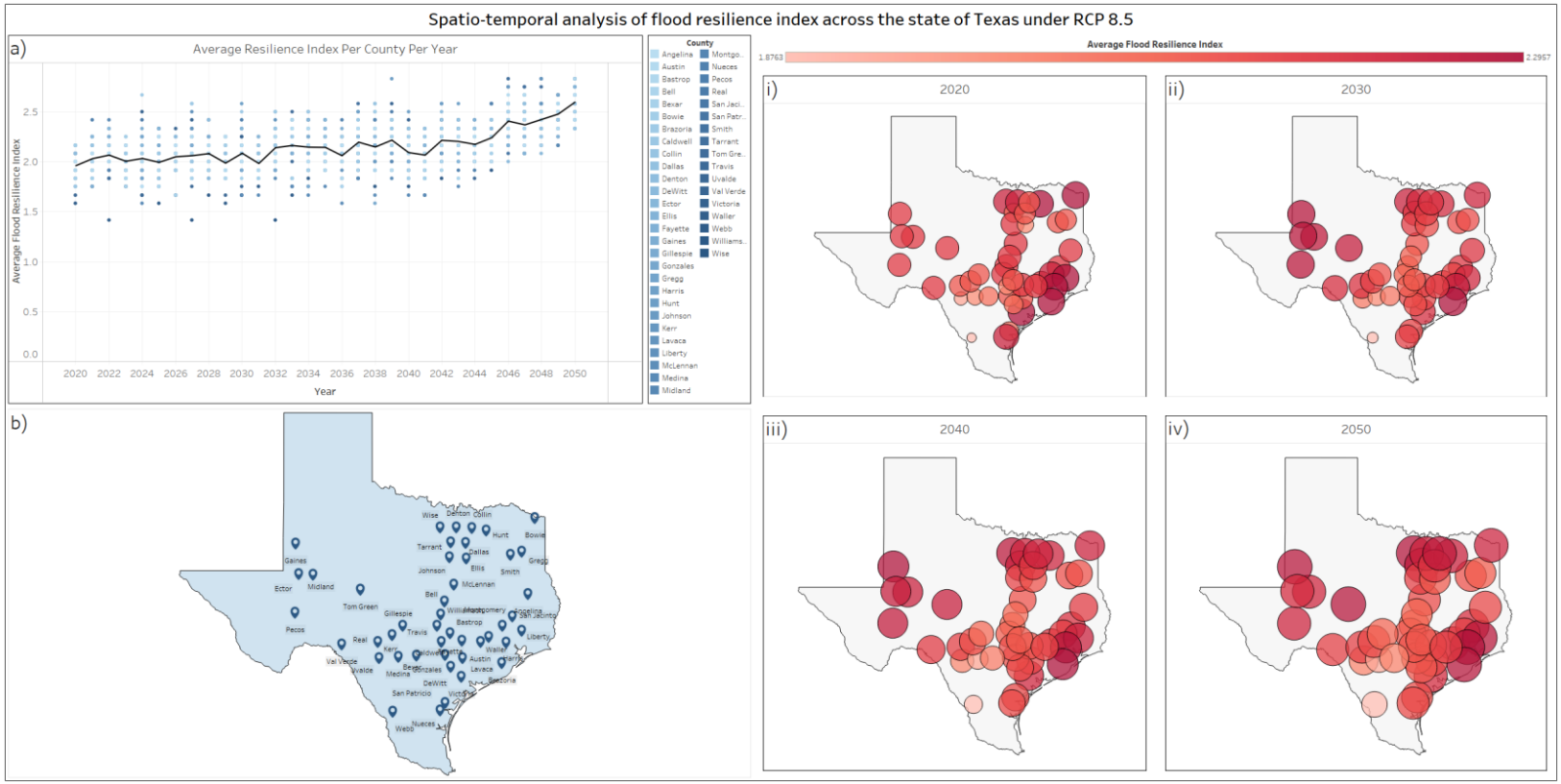

Figure 4-16: Spatio-temporal Model Output visualization for RCP 8.5, where; a) yearly average per county per year, with a running average for all included counties, b) spatial distribution of included counties and their GCM's stations, i) the spatial distribution of average Resilience index per county in the year 2020, ii) spatial distribution of average Resilience index per county till the year 2030, iii) spatial distribution of average Resilience index per county till the year 2040, iv) spatial distribution of average Resilience index per county till the year 2050.

4.4. CONCLUSION

Flood risk remains one of the costliest and most disruptive natural hazards worldwide. The IPCC 2021 report states that extreme rainfall events are increasing in severity and frequency over the next decade, with an expected rise of average sea water level by 2.0 m by the year 2100. This change is also governed by the global climate policies in place, and how the world abides by them on a global scale, dictating the direction upon which GHG emissions would determine which RCP scenario the climate would follow. These findings ascertain the need for a comprehensive flood-risk prediction methodology that is resilience-centric, employable in multiple scenarios and across a wide range of urban, geographical, and climatological conditions.

The work presented herein provides a comprehensive methodology for incorporating climate change impact with numerous community resilience features. This work aims at: *i*) identifying variables that comprehensively represent the resilience goals for incorporation within a data-driven multi-stage model, *ii*) employing the developed dataset to produce resilience indices appropriately representing the features of the community under investigation, ranging from the quality of the complex infrastructure system forming the functionality of the society, to the expected damages and the impact on the livelihood of the inhabitants,

iii) coupling the employed indices with climate change scenarios to develop a prediction model to investigate the impact of climate change on future resilience trajectory of the built environment, and *iv*) employing the developed models into developing a spatiotemporal analysis of the area under investigation, identifying future trends in community resilience, and the potential vulnerabilities in the built environment.

In this study, the BCSD CMIP5 models were employed for climate modeling under multiple emission scenarios (Namely RCP 6.0 and RCP 8.5), with 16 Global Climate Models employed for multiple scenarios. The Study also employs the disaster data records developed by the National Weather Service (NWS) from the years 1996 to 2020. Spatial analysis was conducted using the employed resilience categories, identifying the State of Texas as the one befalling the most monetary damage, and the most recorded flood disasters. Henceforth, 45 test locations (i.e., counties) were identified within the state of Texas for the CMIP5 GCMs simulations for the climate modelling, and the resulting models were coupled with the resilience index on each of the recorded disaster dataset observation.

Multiple Interpretability techniques were employed to interpret the results of the ML model to transform the model from its Black-box nature to a more readable model, enabling decision and policy makers to draw reliable managerial insights and information for the development of the much-needed mitigation plans. The

interpretability methods employed in this study identified the following insights: (1) the behavior and relative influence of the features across the multiple ensemble GCMs employed in the development of the algorithm is similar, identifying that some assumptions in the simulation of the different GCMs do not impact the behavior of the features, but rather varies in term of accuracy and prediction trajectory it provides, (2) the maximum and minimum temperatures are the most influential climate information in all models, correlating (whether directly or inversely) with most of the included features (i.e., precipitation, runoff, and windspeed), (3) the impact of the temperature on the community resilience increases exponentially between 30-40 ^{o}C for average maximum daily temperatures, and 15-30 ^{o}C for average minimum temperature in the region where the tests were conducted, (4) the influence of windspeed on the resilience categories is increasing up to 6 m/s, then starts slowing down significantly, and (5) the influence of the total precipitation comes to a halt beyond the 200 mm threshold, indicating a maximum damage reached in the case of extreme event, or that the infrastructure (i.e., drainage network) running at full capacity. Notwithstanding the interpretability of the ML model, the prediction results also provided key insights into the inherent resilience of the built environment. Showing an expected 15.5% increase in expected damage (monetary and otherwise) till the year 2050, amounting to a total of almost an extra $900M in damage per decade for RCP 6.0

scenario, and $1.8B in damage per decade for RCP 8.5 scenario. However, this damage is only in the 45 counties included in this study, with a much larger expected increase in flood damage for the entire state of Texas.

Future recommendation: The methodology adopted herein can be further developed into a global prediction algorithm, acting as an early warning system, and a corner stone for a comprehensive management system for the built environment. The analysis also calls for immediate global intervention to steer the global trajectory to a less severe emission scenario, since the expected impact on the built environment increases two-fold from one scenario to another in the next 30 years.

4.5. ACKNOWLEDGMENT

The work presented herein is supported by the Vanier Canada Graduate Scholarship (Vanier-CGS) awarded to the corresponding author, and the Natural Science and Engineering Research Council (NSERC) through the CaNRisk—Collaborative Research and Training Experience (CREATE) program. Additional support through the INViSiONLab and the INTERFACE Institute at McMaster University is also acknowledged. We acknowledge the World Climate Research Programme's Working Group on Coupled Modelling, which is responsible for CMIP, and we thank the climate modeling groups (listed in Tables 4-1 and 4-2 of

this paper) for producing and making available their model output. For CMIP the U.S. Department of Energy's Program for Climate Model Diagnosis and Intercomparison provides coordinating support and led development of software infrastructure in partnership with the Global Organization for Earth System Science Portals.

4.6. DATA AVAILABILITY

The datasets used in this article are publicly available. The meteorological disaster database used in the generation of the resilience categories is provided by the NWS, a sub-agency under the National Oceanic and Atmospheric Administration (NOAA), available at (https://www.ncei.noaa.gov/pub/data/swdi/stormevents/csvfiles/). The historical climate data used is provided by Global Historical Climatology Network, a sub-agency under NOAA, and is available at (https://www.ncdc.noaa.gov/cdo-web/search?datasetid=GHCND), and the BCSD CMIP5 projections and simulations can be conducted and accessed through (https://gdo-dcp.ucllnl.org/downscaled_cmip_projections/). All models, or codes, that support the findings of this study are available from the corresponding author upon request.

4.7. CONFLICT OF INTEREST

The authors declare that they have no known competing financial interests or personal relationships that could have appeared to influence the work reported in this paper.

4.8. REFERENCES

Abdel-mooty, M. N., W. El-dakhakhni, and P. Coulibaly. 2022. "Data-Driven Community Flood Resilience Prediction." Water (Switzerland), 14 (13): 2120. https://doi.org/10.3390/w14132120.

Abdel-Mooty, M. N., W. El-Dakhakhni, and P. Coulibaly. 2023. "Community Resilience Classification Under Climate Change Challenges." 227–237. Springer, Singapore. https://doi.org/10.1007/978-981-19-0507-0_21.

Abdel-Mooty, M. N., A. Yosri, W. El-Dakhakhni, and P. Coulibaly. 2021. "Community Flood Resilience Categorization Framework." Int. J. Disaster Risk Reduct., 61 (November 2020): 102349. Elsevier Ltd. https://doi.org/10.1016/j.ijdrr.2021.102349.

Ashari, A. 2013. "Performance Comparison between Naïve Bayes, Decision Tree and k-Nearest Neighbor in Searching Alternative Design in an Energy Simulation Tool." Int. J. Adv. Comput. Sci. Appl., 4 (11): 33–39.

Auerbach, L. W., S. L. Goodbred, D. R. Mondal, C. A. Wilson, K. R. Ahmed, K. Roy, M. S. Steckler, C. Small, J. M. Gilligan, and B. A. Ackerly. 2015. "Flood risk of natural and embanked landscapes on the Ganges-Brahmaputra tidal delta plain." Nat. Clim. Chang., 5 (2): 153–157. https://doi.org/10.1038/nclimate2472.

Bertilsson, L., K. Wiklund, I. de Moura Tebaldi, O. M. Rezende, A. P. Veról, and M. G. Miguez. 2019. "Urban flood resilience – A multi-criteria index to integrate flood resilience into urban planning." J. Hydrol., 573 (February 2016): 970–982. Elsevier. https://doi.org/10.1016/j.jhydrol.2018.06.052.

Boehmke, B., and B. M. Greenwell. 2019. Hands-On Machine Learning with R. Taylor & Francis.

Breiman, L. 1996. Bagging Predictors.

Breiman, L., J. H. Friedman, R. A. Olshen, and C. J. Stone. 1984. Classification And Regression Trees. Routledge.

Brownlee, J. 2016. "Bagging and Random Forest Ensemble Algorithms for Machine Learning." Accessed May 12, 2021. https://machinelearningmastery.com/bagging-and-random-forest-ensemble-algorithms-for-machine-learning/.

Brownlee, J. 2020. “How to Calculate Precision, Recall, and F-Measure for Imbalanced Classification.” Accessed June 16, 2021. https://machinelearningmastery.com/precision-recall-and-f-measure-for-imbalanced-classification/.

Bruneau, M., S. E. Chang, R. T. Eguchi, G. C. Lee, T. D. O’Rourke, A. M. Reinhorn, M. Shinozuka, K. Tierney, W. A. Wallace, and D. Von Winterfeldt. 2003. “A Framework to Quantitatively Assess and Enhance the Seismic Resilience of Communities.” Earthq. Spectra, 19 (4): 733–752. https://doi.org/10.1193/1.1623497.

Chi, S., S. J. Suk, Y. Kang, and S. P. Mulva. 2012. “Development of a data mining-based analysis framework for multi-attribute construction project information.” Adv. Eng. Informatics, 26 (3): 574–581. Elsevier Ltd. https://doi.org/10.1016/j.aei.2012.03.005.

Davoudi Kakhki, F., S. A. Freeman, and G. A. Mosher. 2019. “Evaluating machine learning performance in predicting injury severity in agribusiness industries.” Saf. Sci., 117 (April): 257–262. Elsevier. https://doi.org/10.1016/j.ssci.2019.04.026.

Dawod, G. M., M. N. Mirza, K. A. Al-Ghamdi, and R. A. Elzahrany. 2014. “Projected impacts of land use and road network changes on increasing flood

hazards using a 4D GIS: A case study in Makkah metropolitan area, Saudi Arabia." Arab. J. Geosci., 7 (3): 1139–1156. https://doi.org/10.1007/s12517-013-0876-7.

Doshi-Velez, F., and B. Kim. 2017. "Towards A Rigorous Science of Interpretable Machine Learning." (Ml): 1–13.

Downton, M. W., J. Z. B. Miller, and R. A. Pielke. 2005. "Reanalysis of U.S. National Weather Service flood loss database." Nat. Hazards Rev., 6 (1): 13–22. https://doi.org/10.1061/(ASCE)1527-6988(2005)6:1(13).

Downton, M. W., and R. A. Pielke. 2005. "How accurate are disaster loss data? The case of U.S. flood damage." Nat. Hazards, 35 (2): 211–228. https://doi.org/10.1007/s11069-004-4808-4.

Du, M., N. Liu, and X. Hu. 2020. "Techniques for interpretable machine learning." Commun. ACM, 63 (1): 68–77. https://doi.org/10.1145/3359786.

Efron, B., and R. Tibshirani. 1986. "Bootstrap Methods for Standard Errors, Confidence Intervals, and Other Measures of Statistical Accuracy." Stat. Sci., 1 (1): 54–75.

FEMA. 2012. "Definitions of FEMA Flood Zone Designations." 1–2.

FEMA. 2018. Spring Flooding: Risks and Protection.

Feng, D.-C., W.-J. Wang, S. Mangalathu, and E. Taciroglu. 2021. "Interpretable XGBoost-SHAP Machine-Learning Model for Shear Strength Prediction of Squat RC Walls." J. Struct. Eng., 147 (11): 04021173. https://doi.org/10.1061/(asce)st.1943-541x.0003115.

Feofilovs, M., and F. Romagnoli. 2017. "Resilience of critical infrastructures: Probabilistic case study of a district heating pipeline network in municipality of Latvia." Energy Procedia, 128: 17–23. Elsevier B.V. https://doi.org/10.1016/j.egypro.2017.09.007.

Fielding, A. H. 2006. "Introduction to classification." Clust. Classif. Tech. Biosci., 78–96. Cambridge: Cambridge University Press.

FRED, F. R. B. of S. L. 2020. "U. S. Bureau of Labor Statistics, Consumer Price Index for All Urban Consumers: All Items in U.S. City Average (CPIAUCSL)." Accessed May 5, 2020. https://fred.stlouisfed.org/series/CPIAUCSL.

Ganguly, K. K., N. Nahar, and B. M. Hossain. 2019. "A machine learning-based prediction and analysis of flood affected households: A case study of floods in Bangladesh." Int. J. Disaster Risk Reduct., 34 (March 2018): 283–294. Elsevier Ltd. https://doi.org/10.1016/j.ijdrr.2018.12.002.

Haggag, M., A. S. Siam, W. El-Dakhakhni, P. Coulibaly, and E. Hassini. 2021. "A

deep learning model for predicting climate-induced disasters." Nat. Hazards, (0123456789). Springer Netherlands. https://doi.org/10.1007/s11069-021-04620-0.

Hanewinkel, M., W. Zhou, and C. Schill. 2004. "A neural network approach to identify forest stands susceptible to wind damage." For. Ecol. Manage., 196 (2–3): 227–243. https://doi.org/10.1016/j.foreco.2004.02.056.

Hastie, T., R. Tibshirani, and J. Friedman. 2009. The Elements of Statistical Learning: Data Mining, Inference, and Prediction. Springer Ser. Stat. Springer US.

Heidbach, O., B. Müller, K. Fuchs, F. Wenzel, J. Reinecker, M. Tingay, B. Sperner, J.-P. Cadet, and P. Rossi. 2007. "World stress map published." Eos, Trans. Am. Geophys. Union, 88 (47): 504–504. https://doi.org/10.1029/2007eo470005.

Hosseiny, H., F. Nazari, V. Smith, and C. Nataraj. 2020. "A Framework for Modeling Flood Depth Using a Hybrid of Hydraulics and Machine Learning." Sci. Rep., 10 (1): 1–14. Springer US. https://doi.org/10.1038/s41598-020-65232-5.

IPCC. 2014. WG III Assessment Report 5. Zhurnal Eksp. i Teor. Fiz.

Jaagus, J., and R. Ahas. 2000. “Space-time variations of climatic seasons and their correlation with the phenological development of nature in Estonia.” Clim. Res., 15 (3): 207–219. https://doi.org/10.3354/cr015207.

Jafarnezhad, J., A. Salmanmahiny, and Y. Sakieh. 2016. “Subjectivity versus Objectivity: Comparative Study between Brute Force Method and Genetic Algorithm for Calibrating the SLEUTH Urban Growth Model.” J. Urban Plan. Dev., 142 (3): 05015015. https://doi.org/10.1061/(asce)up.1943-5444.0000307.

Khalaf, M., A. J. Hussain, D. Al-Jumeily, T. Baker, R. Keight, P. Lisboa, P. Fergus, and A. S. Al Kafri. 2018. “A Data Science Methodology Based on Machine Learning Algorithms for Flood Severity Prediction.” 2018 IEEE Congr. Evol. Comput. CEC 2018 - Proc., 1–8. IEEE. https://doi.org/10.1109/CEC.2018.8477904.

Kuhn, M. 2019. “The caret Package.” Accessed May 19, 2022. https://topepo.github.io/caret/index.html.

Li, C., J. Dash, M. Asamoah, J. Sheffield, M. Dzodzomenyo, S. H. Gebrechorkos, D. Anghileri, and J. Wright. 2022. “Increased flooded area and exposure in the White Volta river basin in Western Africa, identified from multi-source remote sensing data.” Sci. Rep., 12 (1): 1–13. Nature Publishing Group UK.

https://doi.org/10.1038/s41598-022-07720-4.

Li, Z., P. Liu, W. Wang, and C. Xu. 2012. “Using support vector machine models for crash injury severity analysis.” Accid. Anal. Prev., 45: 478–486. Elsevier Ltd. https://doi.org/10.1016/j.aap.2011.08.016.

Lian, J., H. Xu, K. Xu, and C. Ma. 2017. “Optimal management of the flooding risk caused by the joint occurrence of extreme rainfall and high tide level in a coastal city.” Nat. Hazards, 89 (1): 183–200. Springer Netherlands. https://doi.org/10.1007/s11069-017-2958-4.

Liaw, A., and M. Wiener. 2002. Classification and Regression by RandomForest.

Liu, X., Y. Song, W. Yi, X. Wang, and J. Zhu. 2018. “Comparing the Random Forest with the Generalized Additive Model to Evaluate the Impacts of Outdoor Ambient Environmental Factors on Scaffolding Construction Productivity.” J. Constr. Eng. Manag., 144 (6): 04018037. https://doi.org/10.1061/(asce)co.1943-7862.0001495.

Lyon, C., E. E. Saupe, C. J. Smith, D. J. Hill, A. P. Beckerman, L. C. Stringer, R. Marchant, J. McKay, A. Burke, P. O’Higgins, A. M. Dunhill, B. J. Allen, J. Riel-Salvatore, and T. Aze. 2022. “Climate change research and action must look beyond 2100.” Glob. Chang. Biol., 28 (2): 349–361. https://doi.org/10.1111/gcb.15871.

Menne, M. J., I. Durre, R. S. Vose, B. E. Gleason, and T. G. Houston. 2021. "Global Historical Climatology Network - Daily (GHCN-Daily), Version 3." NOAA Natl. Clim. Data Cent. Accessed June 10, 2021. https://www.ncei.noaa.gov/access/metadata/landing-page/bin/iso?id=gov.noaa.ncdc:C00861.

de Moel, H., and J. C. J. H. Aerts. 2011. "Effect of uncertainty in land use, damage models and inundation depth on flood damage estimates." Nat. Hazards, 58 (1): 407–425. https://doi.org/10.1007/s11069-010-9675-6.

Morss, R. E., O. V. Wilhelmi, M. W. Downton, and E. Gruntfest. 2005. "Flood risk, uncertainty, and scientific information for decision making: Lessons from an interdisciplinary project." Bull. Am. Meteorol. Soc., 86 (11): 1593–1601. https://doi.org/10.1175/BAMS-86-11-1593.

Mosavi, A., P. Ozturk, and K. W. Chau. 2018. "Flood prediction using machine learning models: Literature review." Water (Switzerland), 10 (11): 1–40. https://doi.org/10.3390/w10111536.

Murdoch, W. J., C. Singh, K. Kumbier, R. Abbasi-Asl, and B. Yu. 2019. "Definitions, methods, and applications in interpretable machine learning." Proc. Natl. Acad. Sci. U. S. A., 116 (44): 22071–22080. https://doi.org/10.1073/pnas.1900654116.

Murphy, J. D. 2018. NWSI 10-1605, Storm Data Preparation.

Nagpal, A. 2017. "Decision Tree Ensembles- Bagging and Boosting | by Anuja Nagpal | Towards Data Science." Accessed May 12, 2021. https://towardsdatascience.com/decision-tree-ensembles-bagging-and-boosting-266a8ba60fd9.

National Institute of Standards and Technology. 2020. COMMUNITY RESILIENCE PLANNING GUIDE FOR BUILDINGS AND INFRASTRUCTURE SYSTEMS: A Playbook. Gaithersburg, MD.

NOAA. 2019. "National Climate Report - Annual 2018 | State of the Climate | National Centers for Environmental Information (NCEI)." Accessed May 5, 2020. https://www.ncdc.noaa.gov/sotc/national/201813#over.

NOAA. 2020. "U.S. high-tide flooding continues to increase | National Oceanic and Atmospheric Administration." Accessed June 10, 2021. https://www.noaa.gov/media-release/us-high-tide-flooding-continues-to-increase.

NOAA Office for Coastal Management. 2021. "Texas." Accessed June 10, 2021. https://coast.noaa.gov/states/texas.html.

Nofal, O. M., and J. W. van de Lindt. 2020a. "Understanding flood risk in the

context of community resilience modeling for the built environment: research needs and trends." Sustain. Resilient Infrastruct., 00 (00): 1–17. Taylor & Francis. https://doi.org/10.1080/23789689.2020.1722546.

Nofal, O. M., and J. W. van de Lindt. 2020b. "High-resolution approach to quantify the impact of building-level flood risk mitigation and adaptation measures on flood losses at the community-level." Int. J. Disaster Risk Reduct.

Nofal, O. M., J. W. van de Lindt, and T. Q. Do. 2020. "Multi-variate and single-variable flood fragility and loss approaches for buildings." Reliab. Eng. Syst. Saf., 202 (March): 106971. Elsevier Ltd. https://doi.org/10.1016/j.ress.2020.106971.

de Paor, C., L. Connolly, and A. O'Connor. 2019. "Probabilistic resilience assessment of infrastructure—a review." Life-Cycle Anal. Assess. Civ. Eng. Towar. an Integr. Vis. - Proc. 6th Int. Symp. Life-Cycle Civ. Eng. IALCCE 2018, (October): 947–954.

Patil, C., and I. Baidari. 2019. "Estimating the Optimal Number of Clusters k in a Dataset Using Data Depth." Data Sci. Eng., 4 (2): 132–140. Springer Berlin Heidelberg. https://doi.org/10.1007/s41019-019-0091-y.

Perica, S., S. Pavlovic, M. S. Laurent, C. Trypaluk, D. Unruh, and O. Wilhite. 2018. Precipitation-Frequency Atlas of the United States Volume 11 Version 2.0:

Texas.

Reclamation. 2013. “Downscaled CMIP3 and CMIP5 Climate Projections.” Tech. Serv. Center, Bur. Reclamation, US Dep. Inter. Denver, CO, 1 (May): 1–47.

Reclamation. 2014. “Downscaled CMIP3 and CMIP5 Hydrology Climate Projections: Release of Hydrology Projections, Comparison with Preceding Information, and Summary of User Needs.” US Bur. Reclam., (July): 111.

Rodrigues, M., and J. De la Riva. 2014. “An insight into machine-learning algorithms to model human-caused wildfire occurrence.” Environ. Model. Softw., 57: 192–201. Elsevier Ltd. https://doi.org/10.1016/j.envsoft.2014.03.003.

Rözer, V., A. Peche, S. Berkhahn, Y. Feng, L. Fuchs, T. Graf, U. Haberlandt, H. Kreibich, R. Sämann, M. Sester, B. Shehu, J. Wahl, and I. Neuweiler. 2021. “Impact-Based Forecasting for Pluvial Floods.” Earth’s Futur., 9 (2). https://doi.org/10.1029/2020EF001851.

Rufat, S., E. Tate, C. G. Burton, and A. S. Maroof. 2015. “Social vulnerability to floods: Review of case studies and implications for measurement.” Int. J. Disaster Risk Reduct., 14: 470–486. Elsevier Ltd. https://doi.org/10.1016/j.ijdrr.2015.09.013.

Salem, S., A. Siam, W. El-Dakhakhni, and M. Tait. 2020. "Probabilistic Resilience-Guided Infrastructure Risk Management." J. Manag. Eng., 36 (6): 04020073. https://doi.org/10.1061/(asce)me.1943-5479.0000818.

Sen, M. K., S. Dutta, and G. Kabir. 2020. "Housing Infrastructure Resilience Framework Development for Sustainable Future." 2020 Int. Conf. Decis. Aid Sci. Appl. DASA 2020, (January): 519–525. https://doi.org/10.1109/DASA51403.2020.9317137.

Shafizadeh-Moghadam, H., R. Valavi, H. Shahabi, K. Chapi, and A. Shirzadi. 2018. "Novel forecasting approaches using combination of machine learning and statistical models for flood susceptibility mapping." J. Environ. Manage., 217: 1–11. https://doi.org/10.1016/j.jenvman.2018.03.089.

da Silva, J., S. Kernaghan, and A. Luque. 2012. "A systems approach to meeting the challenges of urban climate change." Int. J. Urban Sustain. Dev., 4 (2): 125–145. https://doi.org/10.1080/19463138.2012.718279.

Singh, H. 2018. "Understanding Gradient Boosting Machines | by Harshdeep Singh | Towards Data Science." Accessed May 12, 2021. https://towardsdatascience.com/understanding-gradient-boosting-machines-9be756fe76ab.

Stocker, T. F., Q. Dahe, G.-K. Plattner, M. M. B. Tignor, S. K. Allen, J. Boschung,

A. Nauels, Y. Xia, V. Bex, and P. M. Vincent. 2013. Climate change 2013: The Physical Science Basis.

Sweet, W. V, G. Dusek, G. Carbin, J. Marra, D. Marcy, and S. Simon. 2020. "2019 State of U.S. High Tide Flooding and a 2020 Outlook." NOAA Tech. Rep., NOS CO-OPS (July): 1–12.

Thomas, V., J. R. G. Albert, and C. Hepburn. 2014. "Contributors to the frequency of intense climate disasters in Asia-Pacific countries." Clim. Change, 126 (3–4): 381–398. https://doi.org/10.1007/s10584-014-1232-y.

Trenberth, K. E., L. Cheng, P. Jacobs, Y. Zhang, and J. Fasullo. 2018. "Hurricane Harvey Links to Ocean Heat Content and Climate Change Adaptation." Earth's Futur., 6 (5): 730–744. https://doi.org/10.1029/2018EF000825.

Vano, J., J. Hamman, E. Gutmann, A. Wood, N. Mizukami, M. Clark, D. W. Pierce, D. R. Cayan, C. Wobus, K. Nowak, and J. Arnold. 2020. "Comparing Downscaled LOCA and BCSD CMIP5 Climate and Hydrology Projections - Release of Downscaled LOCA CMIP5 Hydrology." 96.

Wilby, R. L., K. J. Beven, and N. S. Reynard. 2007. "Climate change and fluvial flood risk in the UK: more of the same?" Hydrol. Process., 2309 (December 2007): 2300–2309. https://doi.org/10.1002/hyp.

Wing, O. E. J., W. Lehman, P. D. Bates, C. C. Sampson, N. Quinn, A. M. Smith, J. C. Neal, J. R. Porter, and C. Kousky. 2022. “Inequitable patterns of US flood risk in the Anthropocene.” Nat. Clim. Chang., 12 (2): 156–162. Springer US. https://doi.org/10.1038/s41558-021-01265-6.

Wood, A. W., L. R. Leung, V. Sridhar, and D. P. Lettenmaier. 2004. “Hydrologic implications of dynamical and statistical approaches to downscaling climate model outputs.” Clim. Change, 62 (1–3): 189–216. https://doi.org/10.1023/B:CLIM.0000013685.99609.9e.

World Economic Forum. 2019. The Global Risks Report 2019 14th Edition.

Wu, T. F., C. J. Lin, and R. C. Weng. 2004. “Probability estimates for multi-class classification by pairwise coupling.” J. Mach. Learn. Res., 5: 975–1005.

Yagci, K., I. S. Dolinskaya, K. Smilowitz, and R. Bank. 2018. “Incomplete information imputation in limited data environments with application to disaster response.” Eur. J. Oper. Res., 269 (2): 466–485. Elsevier B.V. https://doi.org/10.1016/j.ejor.2018.02.016.

Chapter 5

MULTI-LEVEL ANALYSIS FOR BRIDGE MANAGEMENT SYSTEM UNDER CLIMATE-INDUCED SCOUR RISK

ABSTRACT

As scour risk remain one of the main contributors to bridge failures, the associated impacts, and losses, whether direct or indirect macro-economic, remain a significant expense for infrastructure asset owners, and impacts the functionality of the interdependent critical infrastructure networks. Given the current need to increase the resilience of our communities to the climate change and the associated hazards, and there is yet to be a framework, of proper utilization, for effective resilience-informed risk management strategies that implement cost-effective periodic monitoring and maintenance. As such, this study introduces a high-order multi-layer framework for scour risk management, aiming at calculating a scour risk score that prioritizes individual bridges within the transport network given their scour risk susceptibility, and overall criticality in the whole network. This approach accounts for different layers of interdependent factors contributing to the formation of scour, such as Structural soundness, water action, peak flow, flood risk, geological riverbed properties, and climate change impact. To showcase the utilization of the novel framework presented herein, the multi-layer framework was applied on different GIS datasets collected from multiple sources on the railway bridges in southeast England to calculate the new comprehensive scour risk score. The updated score showed that the criticality of scour-susceptible bridges has changed, increasing the priorities of some bridges compared to their existing scores,

ultimately improving the decision making for resources allocation, and identifying the more critical assets for detailed inspection and monitoring at later stages.

KEYWORDS: Transport Networks; Climate Resilience; Asset Management; Bridges; Scour Risk; Infrastructure; Decision Making.

A Manuscript based on the work in this chapter is currently in final stages of drafting and preparation for submission in the journal: "*Transportation Research Part D: Transport and Environment*":

Abdel-mooty, Moustafa Naiem, Sasidharan, Manu; Herrera, Manuel; Parlikad, Ajith Kumar; Schooling, Jennifer; El-Dakhakhni, Wael; and Coulibaly, Paulin. "Multi-Level Analysis for Bridge Management System Under Climate Induced Scour Risk"

5.1. INTRODUCTION

Bridges are strategic connections within the transport network which are interconnected with other infrastructure networks. The loss of functionality of a bridge can significantly impact businesses and society's functioning. Bridge restoration is costly and often much more complicated than that for other transport infrastructure assets. They are exposed to numerous natural and artificial hazards during their life cycle. Flooding is a significant natural hazard that may cause considerable damage due to scour; identified as one of the most significant hazards for bridges worldwide. Damage usually occurs when the flowing water removes the material around the piers and abutments causing loss of foundation support (Kerenyi and Flora 2019). The increasing urbanization of watersheds has also led to a growing number of scour-related failures of bridges throughout the UK, Europe and the United States (Argyroudis and Mitoulis 2021). For instance, Storm Desmond (2015) caused widespread damage to masonry bridges in Cumbria (UK) and Storm Irene (2011) resulted in Vermont (USA) losing 26 bridges. While a significant variability exists between different asset owners on the approaches adopted for managing bridge scour (Pregnolato et al. 2020) there is a general consensus that risk-based methods are appropriate. This has been supported by academic research that has developed conceptual frameworks and approaches for risk-based bridge management (Bento et al. 2020; Mondoro et al. 2018; Sasidharan

et al. 2021; Yang and Frangopol 2020a). Studies have also developed approaches to assess how flood conditions might affect bridge performance due to the resulting increase in scour risks (Devendiran et al. 2021; Dikanski et al. 2017; Kallias and Imam 2016; Yang and Frangopol 2020b). The probability of scour formation is linked to structural, hydraulic, geological, environmental, and human-induced factors. A significant body of academic literature has also focused on predicting scour formation (Froehlich 1988; Link et al. 2017, 2020; Melville 1997; Richardson and Davis 2001; Roca et al. 2021a) and assessing the risk of scour-related bridge failures (Argyroudis and Mitoulis 2020; Bento et al. 2020; Panici et al. 2020; Wang et al. 2020; Zhu and Frangopol 2016).

Infrastructure authorities are required to understand and manage a variety of risks to enable efficient bridge scour management. Bridges deteriorate with time and need intermittent inspections to ensure that they can carry traffic without excessive risks. Asset owners and operators use various approaches to rank and prioritize structures using the available data (e.g., UK's BD97/12 and EX2502 standards for road and railway bridges respectively; USA's HEC-18 standard). They often employ risk assessment methodologies based on empirical relationships that estimate the maximum scour depths based on various parameters including flow velocity, river geometry, bed material and component shape. Infrequent inspections and unavailability of data on the foundation depth often result in uncertainties

within the scour risk assessments. Divers are often employed to inspect the condition of the underwater structures and to measure the scour depth using basic instrumentation. Such an approach is particularly at disadvantage for bridge piers as the water around them is often turbulent and murky such that little can be seen.

Current design standards assume that bridges must be designed to cope with a prefixed flood return period, typically within 100 to 200 years. But such an approach does not consider the variability in the frequency of floods induced by climate change (Briaud et al. 2014). The recent allowance of 20% applied to the design peak flow to account for climate change effects (Maroni et al. 2019) does not account for any particular time horizon or regional differences. To this end, technical changes have also been introduced to bridge design and management manuals to provide climate change allowances and guidelines to scour risk assessment and protection (Takano and Pooley 2021). Such efforts also need to jointly consider the revamping of strategic and operational practices within the network (Sasidharan et al. 2022b). While the strategic practices might involve prioritizing bridges for monitoring, maintenance and installation of flood defenses and scour protection measures, the operational practices could inform bridge closures and traffic rerouting. Setting priorities for maintenance and rehabilitation consumes most of the available funding for bridges and requires evaluation at both the network level (i.e. which bridge within the network to maintain) and the bridge

level (i.e. identifying how to manage a given bridge). These decisions are largely governed by multiple performance indicators such as the structural health of the bridge, the safety of users and workers, and the environmental impact (Allah Bukhsh et al. 2019; Yavuz et al. 2017). Infrastructure owners are increasingly considering river level monitoring to provide early warning decision support of potential scour incidents (Roca et al. 2021b). Hitherto, the trigger levels for operational interventions such as bridge closures or weight restrictions are based on weather/flood alerts for the region and do not consider the local situation at the individual bridge sites (Azhari and Loh 2020). Recent research into event-based classification (Maroni et al. 2019) offers a promising direction for scour management by predicting the risk of scour formation at unmonitored bridges based on information from the monitored ones on the same watercourse. An early warning of scour formation could be beneficial to intervene before it presents itself at a significant level that can cause severe damage. The most cost-efficient intervention point needs to be determined and a decision made on whether it is worthwhile proactively monitoring and repairing vulnerable bridges before they reach a point where extensive repairs or reactive interventions are necessitated. The real-time monitoring of every bridge with sensors remains unachievable due to the large associated costs and budget constraints. Moreover, inspecting a network of bridges at regular intervals without considering issues related to bridge characteristics,

functionality and significance is not advisable since this can result in unnecessary spending on more reliable bridges, while some bridges are potentially at higher risk levels. Whilst the current asset management plans employed by the infrastructure authorities provide great insight into the condition of bridges, it presents a list of tasks that are challenging to deliver with budget crunches, timescales and resource constraints. Critical to this will be prioritizing structures for investments and identifying maintenance strategies that can avoid the risk and cost of repeated work while considering the internal and external factors that make the structures vulnerable, the motivation of this study. Enhancing the resilience of transport bridges, this framework can also add value to the current scour risk assessment processes that dictate bridge management. The developed approach is applied to a case study of railway bridges in the Southeastern England. The results are discussed in Section 5.3, and conclusions are drawn in Section 5.4.

5.2. STRATEGIC RISK ASSESSMENT FOR CLIMATE INDUCED SCOUR RISK

Given the value of railway bridges as critical infrastructure, there has been great effort in the development of comprehensive asset management frameworks that integrate risk assessment practices. While such efforts are characterized by a great disparity, most of which have enough maturity for utilization, but none has

been comprehensive enough for a holistic high-level analysis and consideration of multi-layer factors affecting the imposed risk. Infrastructure asset management is a set of sequential activities that are set to maintain and manage the performance of the assets according to levels set by authorities (i.e., budget, service levels, risk) over its lifecycle (Sasidharan et al. 2022a; Usman et al. 2021). These constraints impose the need for targeted resourcing for managing different assets, or a network of infrastructure assets like railway bridges. As such, identifying the most critical bridges is key in effective asset management planning. While this criticality comes from the condition of the assets themselves, it is also dictated by the imposed risks at different levels to this interdependent network of assets. This requires a clear understanding of the different risks the assets are exposed to, and the potential impact (cascading or otherwise) this risk may cause on them. This understanding is also imperative in the development of resilience-informed risk management plans.

Risk assessment studies, and the general concept of risk and risk management, have now been applied in many fields (e.g., technical applications, finance industry, project management, civil protection, and urban planning) (Zebisch et al. 2017). While in infrastructure asset management literature, the widely accepted definition of Risk is that of the ISO Norm 31,000 (ISO 2009), however, the IPCC 2014 report defines climate risk as a combination of hazard, vulnerability, and is generally defined by the multiplication of the probability of occurrence by the consequence

of event (IPCC 2014). While it is imperative that the macroeconomic cost of bridge failures or operation disruptions are considered, including them in the risk-informed asset management is challenging. To that end, this paper introduces a climate-guided high-level Resilience-informed risk assessment conceptual framework (See Figure 5-1).

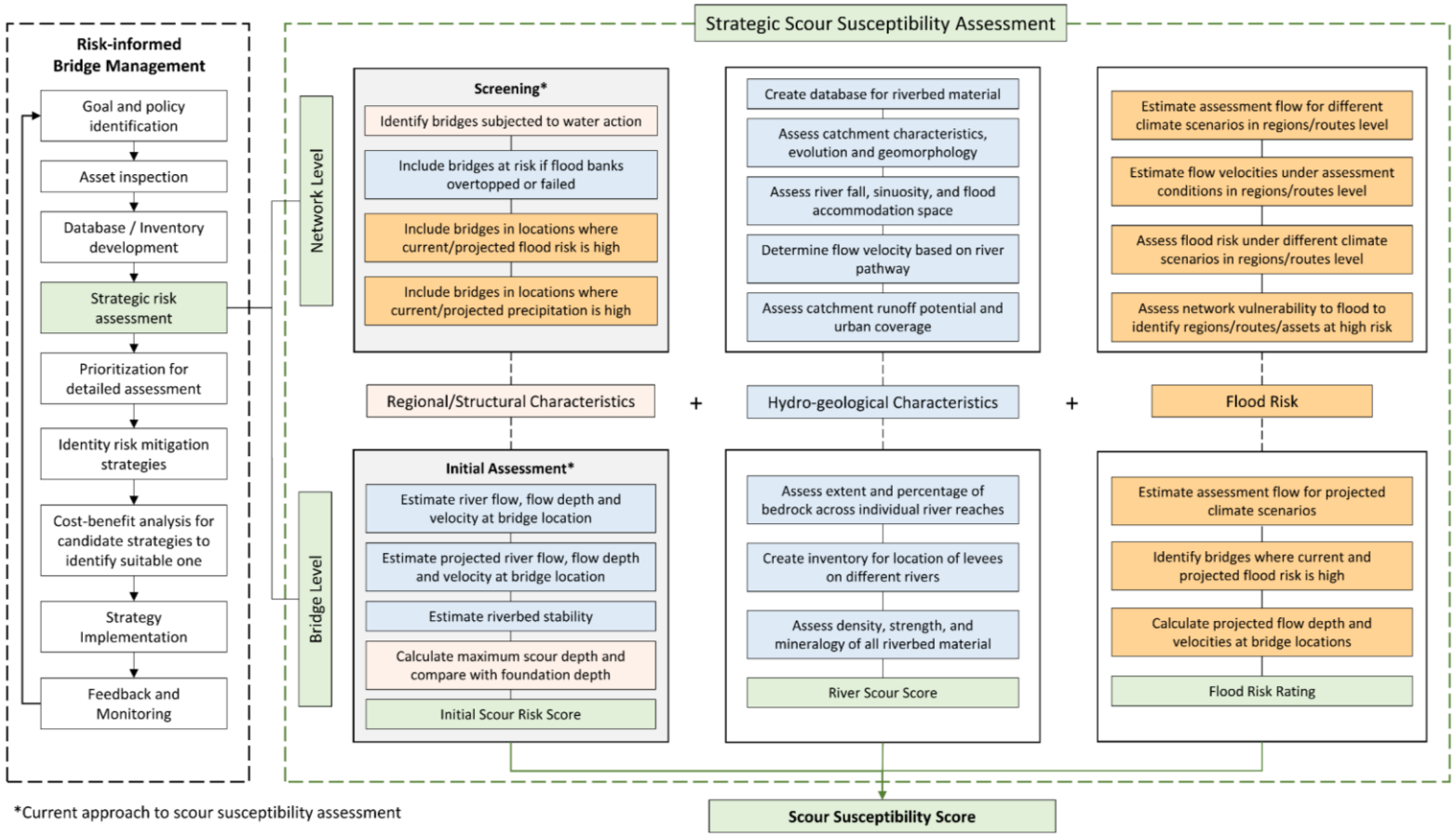

Figure 5-1: High-Level bridge scour risk-informed asset management framework

This framework introduces a novel multi-level approach for how risk management and climate change, along with multiple information layers, can affect the existing scour risk management methodologies in literature. This framework focuses on the strategic risk assessment step of Risk-Informed asset management cycle, where strategy sets the standards for how the policies are translated into actionable items, operations, and lead to decisions which align with the policies set by the stakeholders, given different constraints. This strategic risk assessment is employable on both, network level, and individual asset level (i.e., bridge). The strategic risk assessment is usually employed to determine the level of scour risk, where high scour risk translate to immediate need for scour monitoring, protection, and mitigation as necessary. While medium or lower risk assets might only need monitoring for changes at that level for any changes in the conditions affecting scour risk.

This scour risk is determined by multiplying the severity (consequence) of scour risk by the probability of occurrence (likelihood). While the consequence is determined based on the post-effect of scour failure, it is dependent on multitude of factors, albeit safety (i.e., injuries, fatalities, damage) or loss of functionality, whether partial or complete. It also depends on the needed interventions to remedy these consequences, such that if the failure is local, the recovery can be less disruptive than if the asset was central or critical, such that the entire network is

disrupted. This would depend on the criticality of each asset within its network, and the interconnection of the infrastructure network of networks. The severity in this case would be dependent on level of failure cascading through the networks, and the costs of recovery, whether directly (i.e., cost of repair, etc.) or indirect (i.e., pollution, opportunity cost, disruption to livelihood, increased travel time, etc.). On the other hand, the probability of occurrence (likelihood) of scour risk, depend on multiple factors such as: Structural information, Environmental factors, Natural and manmade components around assets, geotechnical information about the asset, etc. The resulting scour risk influences the strategic direction of stakeholders when choosing a risk management plan, where with the quantification of the scour risk of individual assets, the allocation of resources (i.e., investment) can be targeted to the assets at highest risk - failure probability and collective severity of failure at component or network level - such that the stakeholders' spending would remain within the available resources. To that end, numerous works have been done to assess the likelihood of scour risk, summarizing the contributing factors affecting it to 5 different factors: Bridge age and geometry, Bridge location, Foundation type and level, type of bed material, changes to river flow, with multiple contributors within each factor (Barbetta et al. 2017; Bridge et al. 2017; Lamb et al. 2017; Pizarro et al. 2020; Sasidharan et al. 2021).

While scour risk has been studied extensively in literature, with numerous frameworks and methodologies developed to accurately quantify it, none have included different information layers in a way that could comprehensively capture the effect of geological attributes of the river, and the effect of climate change on different layers of the strategic risk assessment process. Different asset owners and authorities have developed their methodologies for calculating scour risk score (e.g., Highways England in the UK(DMRB 2012), FHWA in the USA (Govindasamy et al. 2008), and Network Rail Britain for railway bridges (Dikanski et al. 2018), with more details on different practices found in the study by Sasidharan et al, 2021 (Sasidharan et al. 2021)). To that end, the objective of the framework proposed herein is the development of a high order scour risk assessment methodology that factors in the effect of in-depth geological information, as well as the effect of climate change on the different layers (i.e., how climate change affects the behavior of river hydrology, flood risk, and future changes in all factors contributing to the formation of scour) to calculate a Comprehensive Scour Risk Score (CSRS), by factoring the initial scour score (ISS), and adding factored scores for river characteristics score (*RCS*), the flood risk (*CCI*) and the Criticality score (*CS*) of the individual bridge within the overall network, in terms of flow and centrality, as seen in Eq(5-1).

$$CSRS = (ISS \times F_1) + (RCS \times F_2) + (CCI \times F_3) + (CS \times F_4) \qquad \text{Eq. (5-1)}$$

The framework introduced in Figure 5-1 shows the Risk-Informed asset management cycle that starts by the objective identification, followed by data collection and assets inspection to facilitate the development of databases and inventory necessary for the completion of the strategic risk assessment. Said assessment is then used for the development of detailed comprehensive assessment at a detailed level for the prioritized assets, facilitating the development of cost-benefit analyses necessary for strategy and policy implementation. The focus of this framework is the assessment of the hazard likelihood on both, the component and network levels, while considering the information pertaining to the Asset characteristics, River characteristics (geological information), and Climate Change Impact. For the transport infrastructure asset characteristics, the network level assessment starts by identifying the bridges subjected to water action, followed by identifying the bridges at risk of flooding if overtopped, and the bridges in location of increasing flood risk, and high precipitation rates. This can be done at "current situation" scenario, or "future scenario" accounting for the effect of climate change on the precipitation rates, and projected flood risk given different climate emission scenarios. On the component level, it starts by the assessment of river flow rate, flow depth, and velocity at the location of the selected bridges, followed by the estimation of the projected future values of river flow and flow depth given different

climate emission scenarios, and the estimation of riverbed stability. Using this information, the initial scour score (*ISS*) is calculated.

As for the River Characteristics score, the proposed process starts by creating a database for all riverbed material for the selected location, assess the catchment characteristics and evolution of geomorphology of the area, the river fall and accommodation space, flow velocity, and potential runoff. Once the individual assets befalling this area are identified, a detailed analysis starts by assessing the extent and percentage of bedrock across different river reaches, identify location of levees on the rivers, and assess the density, strength, and mineralogy of the riverbed material. This information would then be used to develop the scour susceptibility given the river characteristics and can be used to assess the River Characteristics Score (*RCS*). The final layer of information is the effect of climate change, where it starts by the estimating the river flow for multiple climate change emission scenarios, followed by estimating the flow velocity for said scenarios, and ultimately assessing the projected flood risk for the entire catchment under consideration to determine the network vulnerability to flood risk. Once the individual bridges are identified, the flow is calculated at each bridge pier or abutment, identifying the locations with higher flood risk, and calculating the scour score based on projected flood risk (*CCI*).

However, for effective employability of the proposed framework, the quality of information used in its adoption is paramount, highlighting the need for data quality management, and the alignment with international standards for data acquisition and usage. Numerous standards have been set to achieve such a goal, most notably the concept of Information Quality levels set by The world Bank, where different data requirements were set for different levels of strategic importance (Paterson and Scullion 1990) that has been applied to managing bridges, roads and railways assets. This concept ensures the reduction of irrelevant data with its associated costs and increases the overall quality of the infrastructure asset management process. Among the challenges associated with data quality is the probabilistic nature of some of the factors affecting the risk of scour. Some of the factors include, but not limited to: *i*) the lack of frequent inspections, there is uncertainty in the scour related information (e.g., foundation depth, structural conditions, hydrogeologic factors affecting scour formation, etc.), *ii*) Climate change induced uncertainty, where its effect on flood risk and river flow is probabilistic by nature, and heavily dependent on the global intervention towards a certain emission scenario (Abdel-mooty et al. 2022). While these sources of uncertainty have been gaining the traction of the academic community in recent years (Abdel-Mooty et al. 2021; Dikanski et al. 2017; Dong and Frangopol 2016; Yang and Frangopol 2020a), it is yet to remain a challenge for accurate prediction

of scour risk (Sasidharan et al. 2022b). The framework presented herein is adaptable to the uncertainty associated with scour risk prediction, where the probabilistic nature of the layer-specific risk scores can be considered in its probabilistic nature to calculate the final risk score, and the scour risk score associated with different emission scenarios' effect on flood risk and other relevant information can also be considered. While this framework focuses on calculating the likelihood of scour failure, the methodologies upon which each factor is calculated can differ from one infrastructure to another, depending on the standards set for calculating certain factors, and the quality and sparsity of information for the calculation of said factors. However, this can still be accommodated within the framework by adopting different methodology for each of the individual layers of information factoring in the *CSRS.*

To demonstrate the applicability of the proposed framework, the following case study was applied to develop a comprehensive Scour Risk Score for railway bridges in Southeast England region (counties of Kent, Wessex and Essex), that are owned are managed by Network Rail (NR). The region consists of the counties of Kent, Wessex and Essex utilizing different datasets and information provided by different authorities in England, namely: Network Rail Britain (*NR*), British Geological Survey (*BGS*), and United Kingdom Climate Projections (*UKCP 18*). The application presented herein utilizes geospatial information for layering

different datasets and data sources for the development of the *CSRS* and conduct a comparative analysis on the resulting scour ratings for asset prioritization.

5.3. CASE STUDY

With the large number of railway bridges, where over 8,800 of which are built across rivers, the exposure to scour risk becomes more prominent (Lamb et al. 2019; Sasidharan et al. 2022b). Over the past years, there has been a significant increase in precipitation rates across England, and more specifically in the Southeast (Met Office 2022). To that end, the three counties of Essex, Wessex, and Kent were chosen to employ the multilayer framework proposed earlier in this study. Figure 5-2 presents the methodology of applying the framework, where the information layers were converted to spatial datasets, all used to create a multilayer map of the different information layers used to create the final comprehensive scour risk score. It is worth noting that the authors were restricted by the quality and quantity of available data, where for a complete application to the framework presented in earlier section, the authors would need data pertaining to a wide range of datasets (e.g., all railway assets and their information, hydrologic and hydraulic information for the rivers, precipitation patters, flood risk information, future flood risk projections, etc.).

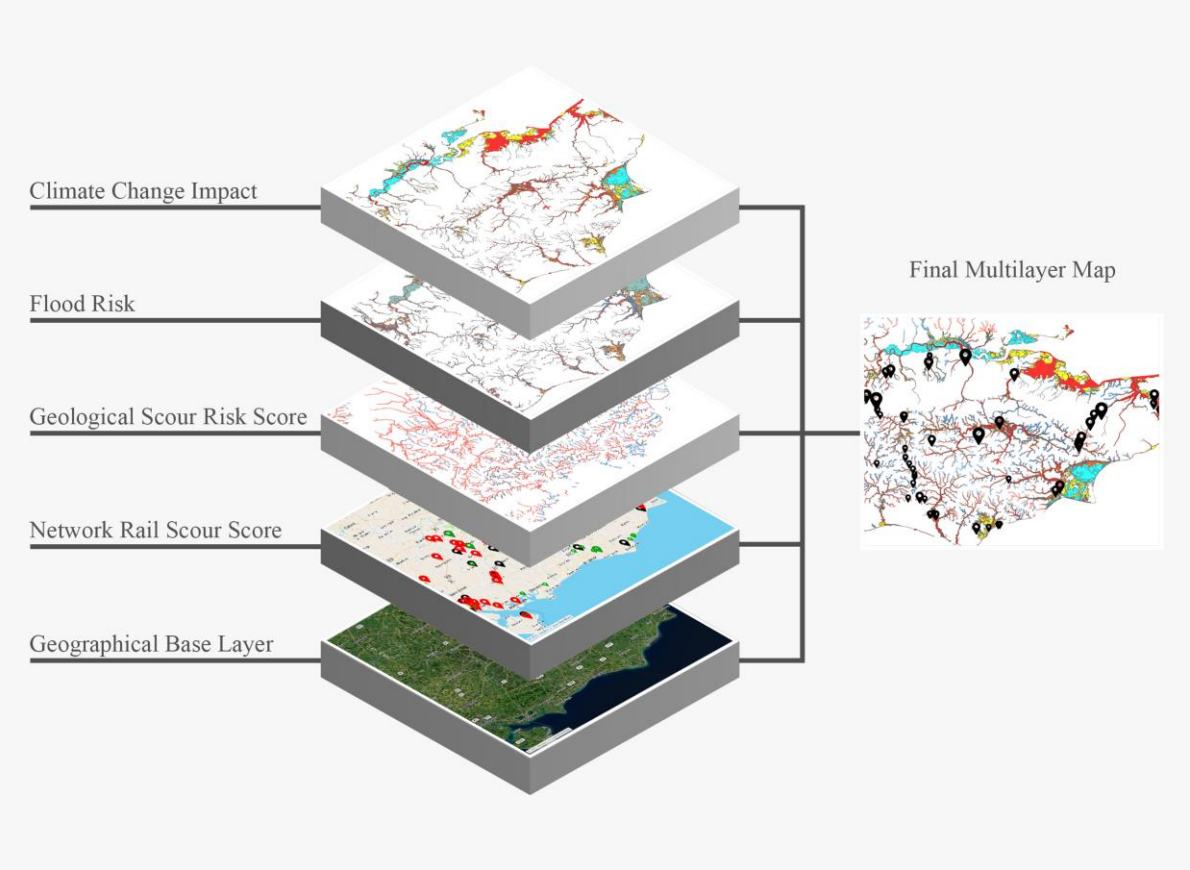

Figure 5-2: Multi-layer information mapping for high-order scour risk assessment

5.3.1. LAYER 1: RAILWAY BRIDGES' SCOUR INFORMATION – NETWORK RAIL BRITAIN

Network Rail (NR) is Britain's railway infrastructure owners, responsible for all asset management plans, creating and maintain the databases, and develop all policies and protocols for sour risk management and maintenance(Lamb et al. 2019). The scour risk assessment policy for Network Rail is comprised of two

stages. Stage 1 is the preliminary analysis, where all railway bridges are assigned a scour score, translated to priority rating, as shown in table 5-1, dictating which assets are at low risk, which at medium risk, and which are at high risk. This scoring scheme is then used to initiate stage 2 analysis, which includes a more rigorous and detailed assessment, including hydrological and hydraulic assessments (Dikanski et al. 2018; Sasidharan et al. 2022a). For stage 1 of Network Rail's approach, the priority rating is assigned as a ratio between the foundation depth, and the predicted scour depth, making this stage pivotal in identifying the critical assets, and accordingly assign resources or priorities maintenance, to commence stage 2. Given the high importance of stage 1 for resource allocation, the information used to develop this priority score needs to be accurate, of quality, and comprehensive enough by including all aspects contributing to the formation of scour. However, in the established methodology, this analysis is done at a base-level, taking into account information only pertaining to the asset under investigation, such as: i) Angle of attack for piers subjected to water action, ii) Foundation depth, iii) Shape of pier, iv) velocity of water flow, v) potential debris in the river, and vi) channel geometry (Sasidharan et al. 2022a).

Table 5-1: Scour Scores and Priority Ratings by Network Rail

Scour rating	Priority Score	Category
17.00 – 21.00	Priority 1	**High**
16.00 – 16.99	Priority 2	
15.00 – 15.99	Priority 3	**Medium**
14.00 – 14.99	Priority 4	
13.00 – 13.99	Priority 5	**Low**
10.00 – 12.99	Priority 6	

The dataset used in this study was provided by Network Rail offers the location of all railway bridges located within the three counties in the southeast of England, as shown in Figure 5-3. There are 262 railway bridges included in this dataset, with scour rating for each pier or abutment facing water action. However, if one component failed (i.e., pier or abutment), the entire asset is considered at a failed state, hence, the maximum scour rating and category for all piers of each railway bridge was taken as the score for that particular bridge. Figure 5-3 shows the location of the railway bridges, and the scour score associated with each bridge, indicated as the size of the marker for that bridge, with the colour showing the priority category.

Figure 5-3: Network Rail Dataset, showing the Scour Ratings and Priority Category of Each railway bridge in Southeast England.

5.3.2. LAYER 2: GEOLOGICAL PROPERTIES CONTRIBUTING TO SCOUR RISK – BRITISH GEOLOGICAL SURVEY DATA

The licensed data provided by the British Geological Survey(Lee et al. 2021) provided information on three different tiers, intended for different uses by different stakeholders. The motivation behind the development of this dataset was to track, model, and document the properties of the catchments of the rivers along Great Britain. Scour risk is dependent on the landscape morphology and topology, which are geological features in nature, and often ignore by other scour risk assessment

methodologies. The river processes are intrinsically influencing the susceptibility of the riverbed and banks to erosion and influences the amount of water going through a stream, and the power of that water streams' flow. In our analysis, Tier 3 dataset was used, where the data provide detailed information on the riverine, with a baseline geological context for river scour development based on common information to be incorporated into comprehensive scour modelling. This tier provides information on the material mineralogy, strength, density of riverbed material, as well as river fall sinuosity and flood accommodation space for each catchment.

The dataset provided by the British Geological Survey developed 3 different scenarios for scour susceptibility throughout all the river reaches, namely: Best-case scenario, average-case scenario, and worst-case scenario. These layers identify the main properties that influence the potential formation of scour, and they include the following variables: Riverbed material density, strength, and mineralogy, as defined by the technical engineering terminology report BS5930:2015 (BSI Standards Publication 2015; Lee et al. 2021).

In the study presented herein, the final scour susceptibility score was utilized using the three provided scenarios. In the best-case scenario, only the materials strength values were used in the calculation of river scour susceptibility score, without adding the information pertaining to the density of the riverbed materials.

For the average-case scenario, the average between the density and strength values were used in the development of the scour susceptibility score. While for the worst-case scenario, only the density values of the riverbed materials were used in calculating the scores to be incorporated in the dataset. This is to indicate that the strength of the materials dictates the behavior of the river reach towards scouring, where the materials which are classified as "Strong" are well consolidated, with greater resistance to scouring. While in catchments with low durability rocks, the river valleys tend to form on a wider area, broadening the flood plains. With that, transient flow would occur through the river flow, and scouring would be highly variable, temporally, and spatially (Lee et al. 2021).

5.3.3. LAYER 3: FLOOD RISK – UNITED KINGDOM ENVIRONMENT AGENCY

The dataset used to determine the flood risk for the area under investigation was obtained from Environment Agency of the United Kingdom. In this dataset, the flood risk is the probability of flooding for all rivers and seas presented at 4 different likelihood categories, accounting for the condition of flood defense measures put in place (EA - Environment Agency 2020; Environment Agency 2022). The modelling was done by using local ground levels, water levels, and flood defense information to ascertain the flood risk based on a 40-levels likelihood

spectrum. The results are then grouped into the final 4 categories and validated by using expert opinion for the development of the final dataset based on the modeling's findings. The dataset is in the form of geospatial data, where in the analysis presented herein, the flood risk categories were first mapped for the area under investigation, then mapped on top of the base geographical data, as shown in Figure 5-4. The geospatial data is of a 50 x 50 m resolution, showing the flood risk for all floodplains in rivers and river reaches, and extending to the surrounding areas, and the coastal areas by the seashores. The 4 categories of flood risk in this analysis are: i) High: There is a yearly chance of flooding greater than 3.3%, ii) Medium: There is a yearly chance of flooding between 1% and 3.3%, iii) Low: There is a yearly chance of flooding between 0.1% and 1%, and finally, iv) Very low: There is a yearly chance of flooding less than 0.1%.

This data is considered reliable and suitable for use in bridge flood risk studies, given its high resolution, quality of information, and validation with local experts and authorities. Further information on the development of this dataset can be found on United Kingdom Environment Agency's website (EA - Environment Agency 2020; Environment Agency 2019, 2022).

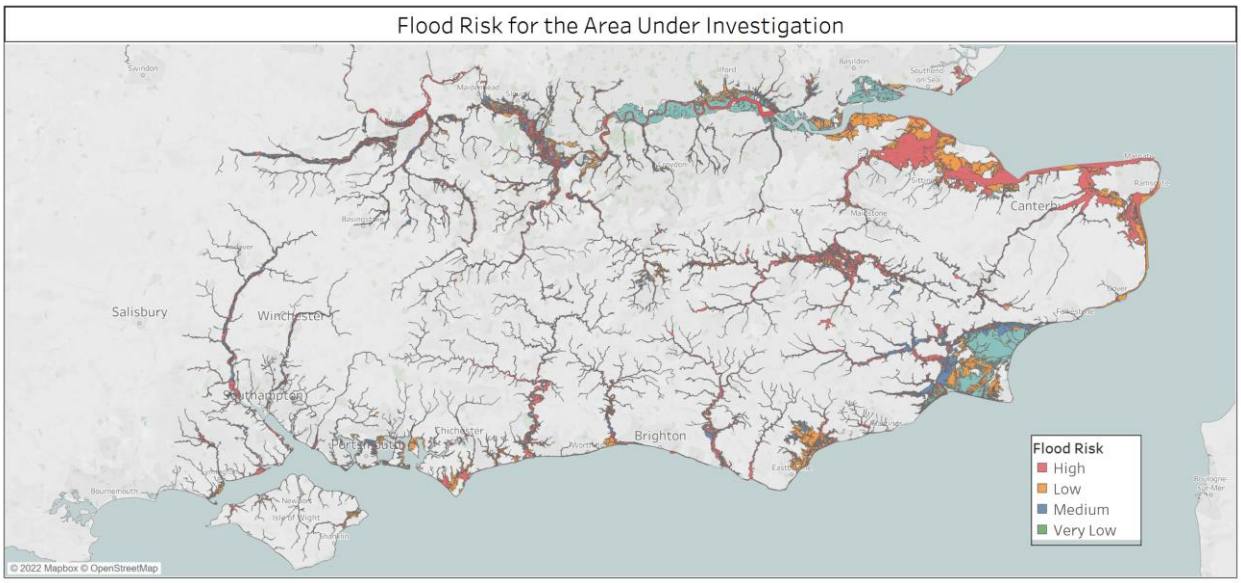

Figure 5-4: Flood Risk Map for the area under investigation showing the likelihood of flooding based on the 4-category-based system

5.3.4. RESULTS

For the high-order strategic risk assessment framework application presented herein, the aforementioned information layers were mapped to assess the following:

- Location of all river-crossing railway bridges for the area under investigation (i.e., Kent, Essex, and Wessex in southeast of England.
- Determine the scour risk score provided by Network Rail for each of the railway bridges, and its subsequent priority category, and map it over the locations of the identified assets.

- Map the geological scour data provided by the British Geological Survey to determine the risk of scouring at the locations of each of the identified railway bridges.
- Mapping the flood risk for the area under investigation to determine the Flood risk category as identified by the Environment Agency.

Figure 5-5 shows the final analysis, where Figure 5-5(a) is the location of the study under investigation where all the layers overlap with one another, 5-5(i) is the layered information where the best-case scour susceptibility score of the BGS dataset is used, 5-5(ii) is the average-case scour susceptibility score, and 5-5(iii) is the worst-case scour susceptibility score. In this case study, the worst-case susceptibility score for the BGS dataset will be utilized for more meaningful and impactful results. It is also worth noting that climate projections for the flood risk maps are yet to be developed for the next decades. These projections were to be used for predicting future changes in scour risk given multiple climate change emission scenarios (i.e., RCP 2.6, RCP 4.5, RCP 6.0, and RCP 8.5) and would help identifying the climate-vulnerability of these railway assets, and the subsequent scour protection investment needs.

Figure 5-6 shows the focus of the analysis in this study, where the worst-case BGS scenario is mapped over flood risk, and multiple NR scour information to be

used in the application of [Eq (5-1)] in this manuscript. For the factors in Eq(5-2), the Initial Scour Score (ISS), the scour risk score provided by Network Rail would suffice, where it contains all information pertaining to the structural properties of the bridge, the hydraulic properties of the water action associated with this bridge, and the maintenance condition of the bridge, along with information on the criticality of the route of the bridge, which can compensate for the criticality score (CS) factor in the equation. For the River Characteristics Score (RCS), the scour susceptibility score provided by BGS is to be used, since it already has all the flow information of the river reach, and the detailed properties of the riverbed materials (e.g., sinuosity, mineralogy, density, and strength) associated with the locations of the brides under investigation. The information provided by Environment Agency is sufficient to be used to calculate the flood risk score in the calculation of the comprehensive scour risk score, while this dataset has information pertaining to the current state of flood risk, it is lacking the future changes on the risk categories. To that end, the final equation to be used in the case study herein to:

$$CSRS = (ISS \times F_1) + (RCS \times F_2) + (FRS \times F_3) \qquad \text{Eq. (5-2)}$$

Where: ISS: Initial scour score, RCS: river characteristics score, and FRS: flood risk score, where F1, F2, and F3, are the factors to be calculated for the ISS, RCS, and FRS, respectively. For the Calculation of the factors for the final calculation of CSRS, Analytical Hierarchical Process was used, where the factors

are determined based on the relative importance of each factor in influencing the final score.

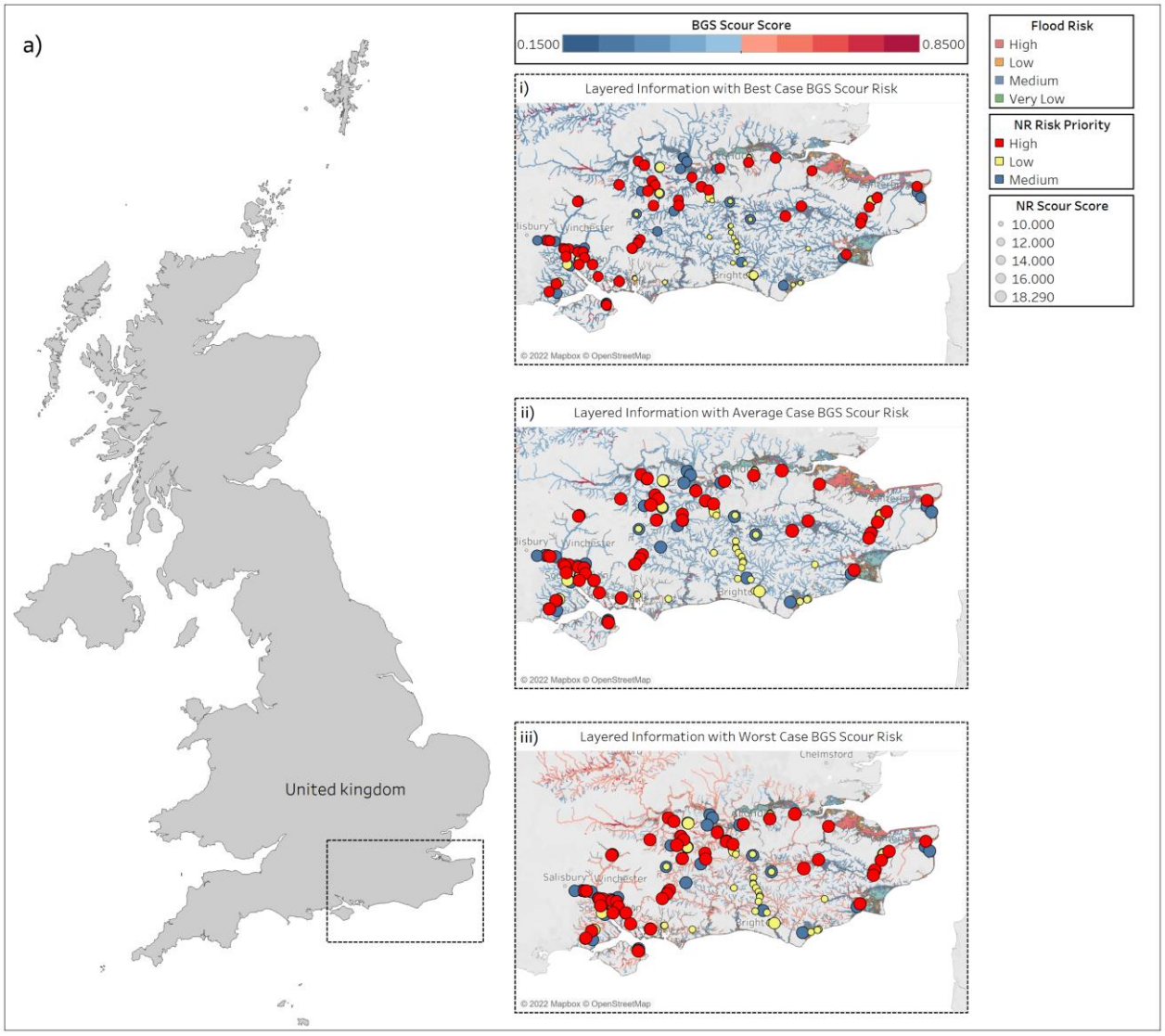

Figure 5-5: Final layered results of the multi-layer analysis where: a) overlap location of the case study, i) layered information with BGS best-case scenario, ii)

layered information with BGS average-case scenario, iii) layered information with BGS worst-case scenario

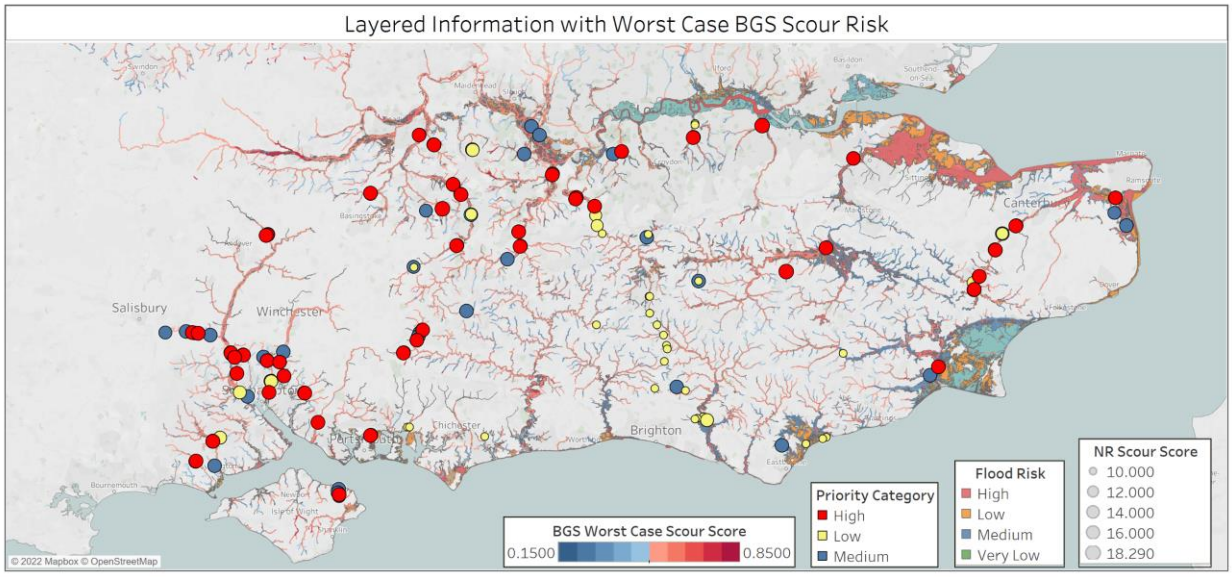

Figure 5-6: Final multilayer analysis for final scour score calculation.

Analytical Hierarchical Process (AHP): AHP is a decision analysis approach that is flexible, robust, and can operate within a multi-criteria space. Formulating the decision hierarchy is a first step in evaluating the different alternatives and goals that are part of a decision variable (Mustafa and Al-Bahar 1991). Due to its flexible nature, it has been adopted in numerous studies, and mostly in risk analysis studies (Lamb et al. 2017; Mustafa and Al-Bahar 1991; Tee et al. 2017; Vargas 2010). In the study presented herein, AHP will be applied to determine the weightage factors in Eq (2) to calculate the final comprehensive score. The process starts by

conducting a quantitative pairwise comparison that uses a scale of importance between the different criteria involved in the decision. The linear scale proposed by Saaty (Saaty 2008) is adopted in this study, and shown in Table 5-2.

Table 5-2: Relative Importance of scale factors involved in AHP

Scale of Importance	Meaning
1	Equally Preferred
3	Mildly Preferred
5	Moderately Preferred
7	Greatly Preferred
9	Always Preferred

For the determination of the scale of importance in the pairwise comparison, the field study survey conducted by Lamb et al. 2017 was adopted as a guide, where a workshop with a wide and diverse group of experts in scour risk determination and analysis was conducted, and a weightages of different factors affecting scour risk was developed (Lamb et al. 2017). The resulting weightages were then validated with a group of scour risk management expert in Network Rail Britain authority. The resulting pairwise comparison were qualitatively determined as shown in Table 5-3.

Table 5-3: Pairwise comparison Matrix

	NR Score	**BGS Score**	**Flood Risk Score**
NR Score	1	5	7
BGS Score	1/5	1	3
Flood Risk Score	1/7	1/3	1

The pairwise matrix is then used to calculate the total comparison score for each column, then all the elements of that column are divided by the total of that column, then adding the resulting rows to calculate the final factors. The eigenvectors of the pairwise matrix was used in calculating the consistency score and compare it with the random consistency index for 3 variables to get the consistency ratio, which was 6.3%, less than the desired 10%, thus falling within an acceptable range. The resulting factors, as shown in table 5-4, reflect the true intrinsic behavior of scour formation, where the structural parameters and the information included in the calculation of the network rail scour score is of most importance, followed by the information pertaining to the geological information and their contribution in the formation of scour, followed by that of flood risk.

Table 5-4: Final factors in each variable

Factors	Weights
NR Scour Score	0.72
BGS Score	0.19
Flood Risk	0.09

The Final equation to be used in the determination of the comprehensive scour score is now shown in Eq. (5-3).

$$CSRS = (ISS \times 0.72) + (RCS \times 0.19) + (FRS \times 0.09) \quad \text{Eq. (5-3)}$$

To calculate the final CSRS for all bridges, all factors in the equation were normalized to have a maximum of 1. As such, in the ISS, the Network Rail priority category was used, from 1 being least risk, to 6 being of most risk, and normalized to have a maximum of 1. For the RCS, the BGS susceptibility score was used, which has a maximum of 0.85, and was accordingly adjusted to have a maximum of 1, and the FRS was already normalized as given. These normalized factors were all used in the calculation of the final CSRS, which is also at a scale of 0-1, with 1 being at most risk of scour given all the contributing factors included in this study.

Figure 5-7 shows the results of the new CSRS for all railway bridges in the study area, where a) is the normalized initial scour score provided by network rail, and b) is the final CRSC calculated using Eq (5-3). As can be seen in Figure 5-7, the scour risk increased for 62% of the bridges in the case study, with an average

of 9% increase than the initial NR Score used in their asset prioritization, and a maximum of 19% increase, completely changing the landscape of the critical assets within the study area. Figure 5-8 shows the difference between the CSRS and the ISS for all railway bridges in this study, identified by their element's ID, and it shows that while the majority of the bridges increase in the CSRS, the average decrease is 3.8%, and the maximum change is 8%. This decrease was attributed to the structural condition of the bridge, and the stronger geological properties of the riverbed that had more weight in the final score than when the initial score was calculated by NR. However, the majority of increase in the final CSRS was associated to the structural material of the bridges, where the 70% of the bridges with increased scour risk were Masonry bridges. In addition, over 78% of the bridges with higher scour risk were associated with a BGS score higher than 0.5, indicating that detailed geological information increased the overall scour risk of the bridges. These two factors would ultimately change the critical bridges identified in preliminary analysis in scour prediction practice by Network Rail Authorities, and hence impacting the allocation of resources in later stages of scour risk asset management.

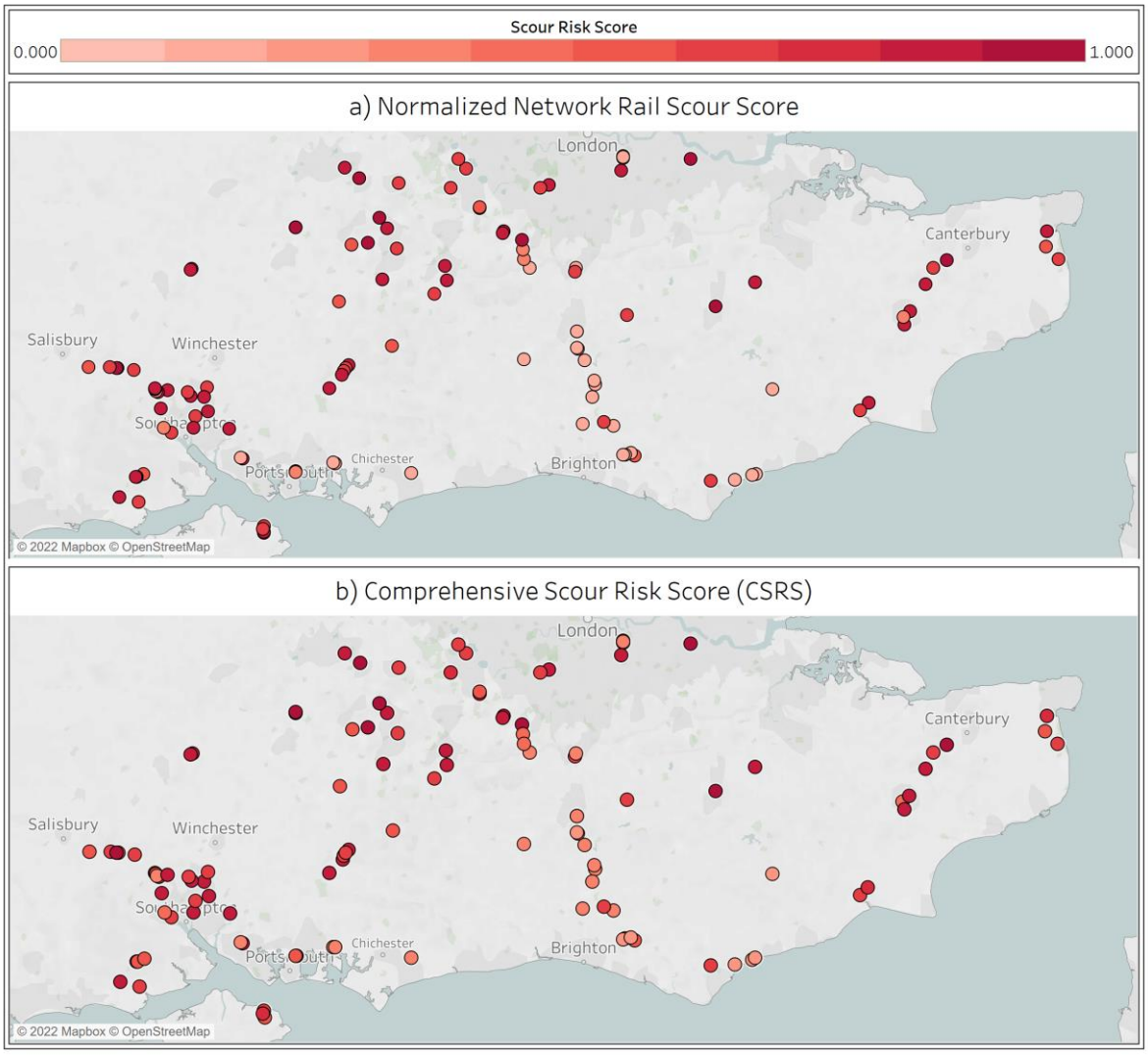

Figure 5-7: Comparative analysis for Scour risk of Railway bridges, such that: a) is the normalized Network Rail initial scour risk score, and b) is the comprehensive scour risk score developed in this study.

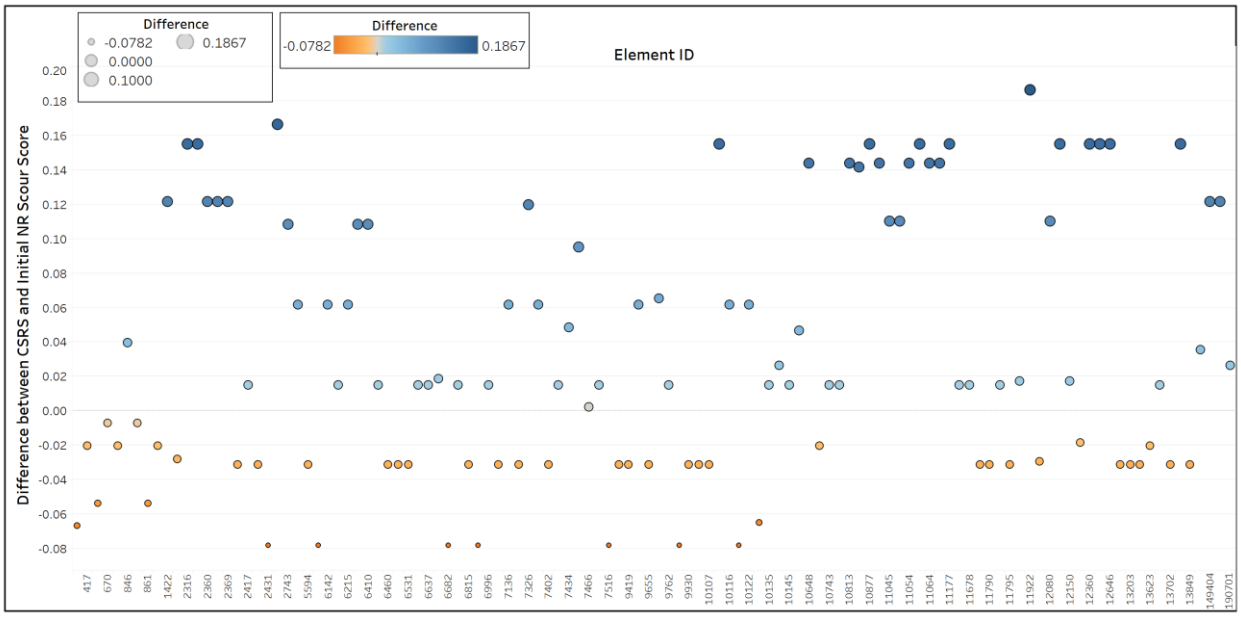

Figure 5-8: Difference between normalized network rail initial score and final comprehensive scour risk score for each railway bridge identified by its element ID.

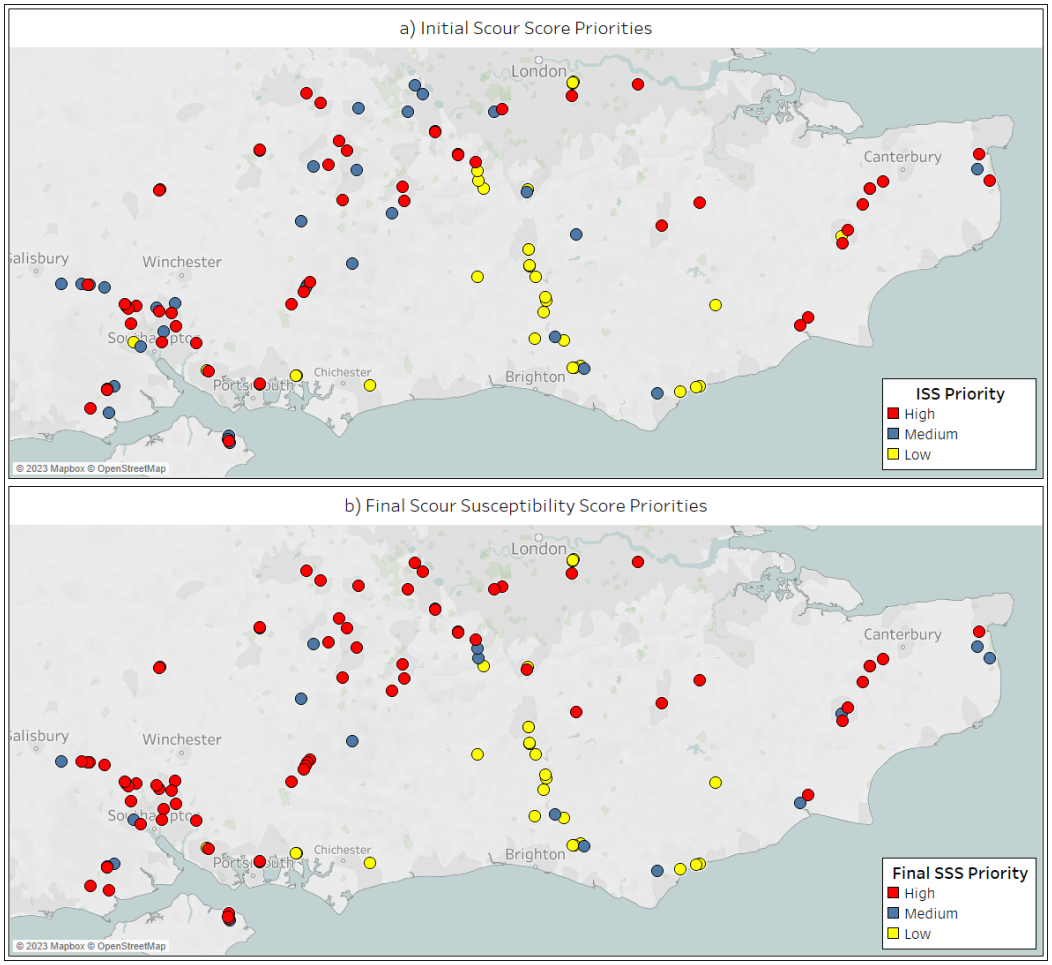

Figure 5-9: Comparative analysis for Scour risk Priorities of Railway bridges, such that: a) is the Initial Scour Score Priorities employed by Network Rail, and b) is the Priority based on Final Scour Risk Score

5.4. DISCUSSION AND CONCLUSION

As the demand on transport networks increase, so does the need for resilience-informed infrastructure risk management strategies. Among the different elements of transport networks, bridges hold a place of high criticality, demanding the need

for more comprehensive, and proactive, management strategies. As authorities and stakeholders are restricted by the available resources (i.e., budgets and manpower) for their asset expenses, it becomes quite challenging to maintain the safety and performance of transport networks through maintenance and other work, let alone improve it. As such, innovative methods become paramount to asset owners and authorities to reduce cost, by automating the monitoring process of asset performance, and selecting high priority assets for intervention and prioritized inspections, facilitating the decision-making process for decisionmakers. This approach would need to be comprehensive enough to capture and incorporate data from various resources, highlighting the need for accurate data gathering and reliable monitoring, to help reach holistic, high-level, resilience-informed decisions. More often than not, the ownership and decision-making process is distributed among different authorities in the UK, resulting in incomplete-knowledge facing the decision makers, forcing them to act upon sub-optimal decisions, compromising the performance of the asset, and the available, already limited, budgets, and the various types of transport assets within the domain of the decision making body (Sasidharan et al. 2021).

While scouring is responsible for the majority of bridge failures, it is extremely important that robust and resilience-informed risk management and monitoring strategies are adopted to predict scour risk and its interdependent implications,

especially that scour risk has higher repair cost, aside from the indirect cost associated with scour failure (i.e., macroeconomic impacts of structure failure, closures, and rerouting). While there exists different guidelines and standards for the risk assessment of scour risk, none has been comprehensive enough to account for high-level multi-layer factors contributing to scour formation, resulting in a continuous scour-related failures within the transport networks, with no mean to change the rate of failure and increase the overall resilience of the network. Additionally, scour formation and related failures are occurring at an increasing rate, attributing that fact to climate-change related hazards (e.g., extreme rainfall, increased frequency and magnitude of floods), and its impact on the different aspects of environment that interacts with the network, and influences the formation of scour (e.g., geological properties of riverbed). To that end, developing frameworks and practices that evaluates the formation of scour given such disparity between different information sources, the manner in which this information is gathered and stored, and the authorities gathering the data, is gaining more traction in the research community, resulting in numerous works in that area. While these different methodologies are of different maturity and utilization levels, there is still a need for resilience-informed proactive risk management approach that predicts the scour formation. This approach would need to take into account the compound effect of climate change, whether on the existing environment by changing the

geological and hydrological properties of rivers and their catchments, or the resulting natural hazards that exacerbate the formation of scour and its associated failures.

Climate change has seemingly limited impact on the scour design dept, since variations in temperature and precipitation does not always lead to an equivalent increase in river flow, however, it develops more frequent flood events with more frequent peak flow events, the main contributor in the formation scour. Thus, incorporating individual catchment's changes in peak flow given different climate change scenarios (i.e., different Greenhouse gas emission scenarios; RCP 4.5, RCP 6.0, RCP 8.5) is paramount in enhancing the overall resilience of the transport network, both on the individual asset level, and the network level. Despite the disparity in existing methodologies, however, very few studies have addressed the climate-change impact on bridge infrastructure, highlighting the need for the study and framework presented herein.

To that end, this manuscript lays the foundation for a high-order multi-layer framework that accounts for the different layers contributing to the formation of scour into the strategic risk assessment step of the resilience-informed transport infrastructure risk management plan. It also accounts for the different interdependent effect of the environmental impacts, along with hydrological, geological, and meteorological properties contributing to the formation of scour.

This process is used to determine the scour risk of individual bridges, aiding in optimizing the resource allocation for detailed inspection and maintenance for assets at most risk. As such, accurate determination of risk level of individual assets would set the criticality levels within a network, and the criticality of the different networks with one another, which highlights the need for this process to be conducted with high degree of accuracy and confidence.

The current work aims to: 1) develop a comprehensive scour risk score that takes into account the effect of detailed geological information, and their associated influence over different factors contributing to the formation of scour, 2) account for climate change impact on the formation of scour in different aspects contributing to the increase in scour risk, whether through water action, hydrological properties, changes in geological properties, or otherwise, 3) enhance the climate resilience of the existing strategic risk management methodologies without having to disrupt the pre-existing methodologies followed by asset owners and authorities for maximum utilization and impact, 4) lay the foundation for a more proactive predictive capability to identify the high priority bridges within the network before failures occur, whether local (i.e., on the asset level), or global (i.e., on the whole transport network) to help optimize the allocation of resources in the asset management cycle, and finally 5) test the applicability of the proposed framework using different datasets gathered to determine the current prioritization

scores for bridge transport network, and apply the framework to investigate the impact on the changed prioritization scheme to ascertain the utility of the framework presented herein.

In the study, different datasets representing the different information layers as indicated in the framework were utilized: *i*) The dataset from Network Rail Britain: this dataset included all locations, structural condition, and scour risk prioritization. This dataset was also used to determine the initial scour risk score by quantifying the scour risk imposed at all piers and abutments at all railway bridges, and assigning the maximum risk score as the score determining the prioritization of the individual bridge, *ii*) The dataset from British Geological Survey: this dataset had information on the geological factors of the riverbed in all catchments in southeast England, including the information contributing to the formation scour. The dataset also includes a scour susceptibility score, that was used to calculate the scour risk component score pertaining to the geological information surrounding the bridges under investigation, and finally *iii*) The Flood Risk Maps, as provided by the United Kingdom Environment Agency, sets the flood risk for all river reaches, and all river catchments. These datasets were used in the calculation of the updated comprehensive scour risk score, based on the aforementioned risk scores using Analytical Hierarchical Process to determine the weightages of each factor in the final score. The results were mapped in a multi-layer visualization to

identify the changes in the prioritization landscape, and aid in the identification of the critical bridges within the transport network with the factors contributing to that change. The study identified the following insights: (1) Most risk scores were changed, resulting in a changed landscape for prioritization of assets and dictating the update of the current methodology, (2) 62% of the bridges had increased scour risk factor, with a maximum of 19% increase, while the maximum decrease for the bridges included was of only 8%, (3) The increased scour risk was related to the structural material of the bridges included in the study, where over 70% of the bridges with increased score were Masonry bridges, (4) The newly added geological information in the calculation of the comprehensive risk score had the most influence over the increasing scour risk of the investigated bridges, highlighting the importance and impact of this information, necessitating its inclusion in scour risk management, and its pivotal importance in increasing the climate resilience of bridges, and ultimately, the entirety of transport infrastructure network.

Future recommendation: The framework presented herein is a steppingstone towards a more comprehensive scour rating for infrastructure asset owners. As such, while the framework is adaptable to include more information layers, the authors were restricted with the available data presented herein. Future work can include: (a) the effect of different climate change scenarios by running a

probabilistic analysis on the formation of scour given more bridge-related information, should they become accessible, (b) the updated future flood risk maps given different GHG climate change emission scenarios to assess the temporal change in the comprehensive scour score, (c) automate the process with geospatial data to be fed the update precipitation and flood peak flow information, to act as a decision support tool for infrastructure asset owners, as a step towards a more complete digital twin platform for decision making and resource allocation.

5.5. ACKNOWLEDGMENT

The work presented herein is supported by the Vanier Canada Graduate Scholarship (Vanier-CGS) awarded to M. N. Abdel-Mooty, and the Natural Science and Engineering Research Council (NSERC) through the Michael Smith Foreign Study Scholarship (NSERC – MSFSS CGS), and the Mitacs Globalink – United Kingdom Research and Innovation (Globalink – UKRI) awards to M. N. Abdel-Mooty, the Natural Science and Engineering Research Council (NSERC) through the CaNRisk— Collaborative Research and Training Experience (CREATE) program. Additional support through the INViSiONLab and the INTERFACE Institute at McMaster University is also acknowledged.

5.6. DATA AVAILABILITY

In this article, multiple datasets were used for the development of the case study. Network Rail Britain Railway Bridge dataset is provided by Network Rail through contract. The Geological information was provided by British Geological Survey through a License. The flood risk dataset is publicly available through (https://environment.data.gov.uk/).

5.7. CONFLICT OF INTEREST

The authors declare that they have no known competing financial interests or personal relationships that could have appeared to influence the work reported in this paper.

5.8. REFERENCES

Abdel-mooty, M. N., W. El-dakhakhni, and P. Coulibaly. 2022. "Data-Driven Community Flood Resilience Prediction." Water (Switzerland), 14 (13): 2120. https://doi.org/10.3390/w14132120.

Abdel-Mooty, M. N., A. Yosri, W. El-Dakhakhni, and P. Coulibaly. 2021. "Community Flood Resilience Categorization Framework." Int. J. Disaster Risk Reduct., 61 (November 2020): 102349. Elsevier Ltd. https://doi.org/10.1016/j.ijdrr.2021.102349.

Allah Bukhsh, Z., I. Stipanovic, G. Klanker, A. O' Connor, and A. G. Doree. 2019. "Network level bridges maintenance planning using Multi-Attribute Utility Theory." Struct. Infrastruct. Eng., 15 (7): 872–885. Taylor & Francis. https://doi.org/10.1080/15732479.2017.1414858.

Argyroudis, S. A., and S. A. Mitoulis. 2020. "Vulnerability of bridges to individual and multiple hazards- floods and earthquakes." Reliab. Eng. Syst. Saf., 107564. Elsevier Ltd. https://doi.org/10.1016/j.ress.2021.107564.

Argyroudis, S. A., and S. A. Mitoulis. 2021. "Vulnerability of bridges to individual and multiple hazards- floods and earthquakes." Reliab. Eng. Syst. Saf., 210 (January): 107564. Elsevier Ltd. https://doi.org/10.1016/j.ress.2021.107564.

Azhari, F., and K. J. Loh. 2020. "Warning Time–Based Framework for Bridge Scour Monitoring." J. Bridg. Eng., 25 (7): 04020040. https://doi.org/10.1061/(asce)be.1943-5592.0001553.

Barbetta, S., S. Camici, and T. Moramarco. 2017. "A reappraisal of bridge piers scour vulnerability: a case study in the Upper Tiber River basin (central Italy)." J. Flood Risk Manag., 10 (3): 283–300. https://doi.org/10.1111/jfr3.12130.

Bento, A. M., A. Gomes, T. Viseu, L. Couto, and J. P. Pêgo. 2020. "Risk-based methodology for scour analysis at bridge foundations." Eng. Struct., 223 (July): 111115. Elsevier. https://doi.org/10.1016/j.engstruct.2020.111115.

Briaud, J.-L., P. Gardoni, and C. Yao. 2014. “Statistical, Risk, and Reliability Analyses of Bridge Scour.” J. Geotech. Geoenvironmental Eng., 140 (2): 04013011. https://doi.org/10.1061/(asce)gt.1943-5606.0000989.

Bridge, P., H. Bridge, N. Devon, B. Bridge, N. Zealand, T. Bridge, C. Dublin, W. London, P. H. Riberio, N. Zealand, N. Zealand, and J. River. 2017. “Publication C742 Manual on scour at bridges and other hydraulic structures, second edition.” (March): 742.

BSI Standards Publication. 2015. code of practice for site investigations: BS 5930:2015. Br. Stand. Inst.

Devendiran, D. K., S. Banerjee, and A. Mondal. 2021. “Impact of Climate Change on Multihazard Performance of River-Crossing Bridges: Risk, Resilience, and Adaptation.” J. Perform. Constr. Facil., 35 (1): 04020127. https://doi.org/10.1061/(asce)cf.1943-5509.0001538.

Dikanski, H., A. Hagen-Zanker, B. Imam, and K. Avery. 2017. “Climate change impacts on railway structures: Bridge scour.” Proc. Inst. Civ. Eng. Eng. Sustain., 170 (5): 237–248. https://doi.org/10.1680/jensu.15.00021.

Dikanski, H., B. Imam, and A. Hagen-Zanker. 2018. “Effects of uncertain asset stock data on the assessment of climate change risks: A case study of bridge scour

in the UK." Struct. Saf., 71: 1–12. The Author(s). https://doi.org/10.1016/j.strusafe.2017.10.008.

DMRB. 2012. "The Assessment of Scour and Other Hydraulic Actions at Highway Structures (BD97/12)." Des. Man. Roads Bridg., 3 (Part 21).

Dong, Y., and D. M. Frangopol. 2016. "Probabilistic Time-Dependent Multihazard Life-Cycle Assessment and Resilience of Bridges Considering Climate Change." J. Perform. Constr. Facil., 30 (5): 1–12. https://doi.org/10.1061/(asce)cf.1943-5509.0000883.

EA - Environment Agency. 2020. "Environment Agency - GOV.UK." Gov.Uk. Accessed October 10, 2022. https://www.gov.uk/government/organisations/environment-agency.

Environment Agency. 2019. "Defra Data Services Platform." Accessed October 10, 2022. https://environment.data.gov.uk/.

Environment Agency. 2022. "Risk of Flooding from Rivers and Sea."

Froehlich, D. C. 1988. "Analysis of onsite measurements of scour at piers."

Govindasamy, A. V., J.-L. Briaud, H.-C. Chen, J. Delphia, K. Elsbury, P. Gardoni, G. Herrman, D. Kim, C. C. Mathewson, M. McClelland, and F. Olivera. 2008.

"Simplified Method for Estimating Scour at Bridges." 385–393. https://doi.org/10.1061/40971(310)48.

IPCC. 2014. WG III Assessment Report 5. Zhurnal Eksp. i Teor. Fiz.

Kallias, A. N., and B. Imam. 2016. "Probabilistic assessment of local scour in bridge piers under changing environmental conditions." Struct. Infrastruct. Eng., 12 (9): 1228–1241. Taylor & Francis. https://doi.org/10.1080/15732479.2015.1102295.

Kerenyi, K., and K. Flora. 2019. "A hybrid approach to forensic study of bridge scour." Proc. Inst. Civ. Eng. Forensic Eng., 172 (1): 27–38. https://doi.org/10.1680/jfoen.19.00001.

Lamb, R., W. Aspinall, H. Odbert, and T. Wagener. 2017. "Vulnerability of bridges to scour: Insights from an international expert elicitation workshop." Nat. Hazards Earth Syst. Sci., 17 (8): 1393–1409. https://doi.org/10.5194/nhess-17-1393-2017.

Lamb, R., P. Garside, R. Pant, and J. W. Hall. 2019. "A Probabilistic Model of the Economic Risk to Britain's Railway Network from Bridge Scour During Floods." Risk Anal., 39 (11): 2457–2478. https://doi.org/10.1111/risa.13370.

Lee, K. A., S. Cornillion, A. Hulbert, and C. Cartwright. 2021. User Guide for the GeoScour GB V1 dataset. British Geological Survey Open Report, OR/19/042. Nottingham.

Link, O., C. Castillo, A. Pizarro, A. Rojas, B. Ettmer, C. Escauriaza, and S. Manfreda. 2017. "A model of bridge pier scour during flood waves." J. Hydraul. Res. https://doi.org/10.1080/00221686.2016.1252802.

Link, O., M. García, A. Pizarro, H. Alcayaga, and S. Palma. 2020. "Local Scour and Sediment Deposition at Bridge Piers during Floods." J. Hydraul. Eng., 146 (3). https://doi.org/10.1061/(ASCE)HY.1943-7900.0001696.

Maroni, A., E. Tubaldi, D. Val, H. Mcdonald, S. Lothian, O. Riches, and D. Zonta. 2019. "A Decision Support System for Scour Management of Road and Railway Bridges Based on Bayesian Networks." 12th Int. Work. Struct. Heal. Monit. IWSHM 2019.

Melville, B. W. 1997. "Pier and abutment scour: Integrated approach." J. Hydraul. Eng. https://doi.org/10.1061/(ASCE)0733-9429(1997)123:2(125).

Met Office. 2022. Update to UKCP18 probabilistic projections : Maps of projected changes in surface temperature and precipitation.

Mondoro, A., D. M. Frangopol, and L. Liu. 2018. “Bridge Adaptation and Management under Climate Change Uncertainties: A Review.” Nat. Hazards Rev., 19 (1): 1–12. https://doi.org/10.1061/(ASCE)NH.1527-6996.0000270.

Mustafa, M. A., and J. F. Al-Bahar. 1991. Project Risk Assessment Using the Analytic Hierarchy Process. IEEE Trans. Eng. Manag.

Panici, D., P. Kripakaran, S. Djordjević, and K. Dentith. 2020. “A practical method to assess risks from large wood debris accumulations at bridge piers.” Sci. Total Environ., 728: 1–10. https://doi.org/10.1016/j.scitotenv.2020.138575.

Paterson, W. D. O., and T. Scullion. 1990. “Information Systems for Road Management: Draft Guidelines on System Design and Data Issues.” Infrastruct. Urban Dev. Dep. Rep., INU 77 (Washingto): The World Bank.

Pizarro, A., S. Manfreda, and E. Tubaldi. 2020. “The science behind scour at bridge foundations: A review.” Water (Switzerland).

Pregnolato, M., A. O. Winter, D. Mascarenas, A. D. Sen, P. Bates, and R. Michael. 2020. “Assessing flooding impact to riverine bridges : an integrated analysis.” Nat. Hazards Earth Syst. Sci., (December). https://doi.org/https://doi.org/10.5194/nhess-2020-375 Preprint.

Richardson, E. V, and S. R. Davis. 2001. “HEC 18: Evaluating Scour At Bridges Fourth Edition.” Hydraul. Eng. Circ.

Roca, M., A. Kitchen, A. Kirby, and M. Escarameia. 2021a. “Briefing: Scour guidance supporting bridge resilience.” Proc. Inst. Civ. Eng. - Bridg. Eng., 1–4. https://doi.org/10.1680/jbren.21.00053.

Roca, M., A. Kitchen, A. Kirby, and M. Escarameia. 2021b. “Briefing: Scour guidance supporting bridge resilience.” Proc. Inst. Civ. Eng. Bridg. Eng., 1–4. https://doi.org/10.1680/jbren.21.00053.

Saaty, T. L. 2008. “Decision making with the analytic hierarchy process.” Int. J. Serv. Sci., 1 (1): 83–98.

Sasidharan, M., M. P. N. Burrow, G. S. Ghataora, and R. Marathu. 2022a. “A risk-informed decision support tool for the strategic asset management of railway track infrastructure.” Proc. Inst. Mech. Eng. Part F J. Rail Rapid Transit, 236 (2): 183–197. https://doi.org/10.1177/09544097211038373.

Sasidharan, M., A. K. Parlikad, and J. Schooling. 2021. “Risk-informed asset management to tackle scouring on bridges across transport networks.” Struct. Infrastruct. Eng., 0 (0): 1–17. Taylor & Francis. https://doi.org/10.1080/15732479.2021.1899249.

Sasidharan, M., A. K. Parlikad, J. Schooling, and G. M. Hadjidemetriou. 2022b. “A practical bridge scour risk management approach to deal with uncertainties of a climate future.”

Takano, H., and M. Pooley. 2021. “New UK guidance on hydraulic actions on highway structures and bridges.” Proc. Inst. Civ. Eng. - Bridg. Eng., 174 (3): 231–238. https://doi.org/10.1680/jbren.20.00024.

Tee, S. J., Q. Liu, and Z. Wang. 2017. “Insulation condition ranking of transformers through principal component analysis and analytic hierarchy process.” IET Gener. Transm. Distrib., 11 (1). https://doi.org/10.1049/iet-gtd.2016.0589.

Usman, K., M. P. N. Burrow, G. S. Ghataora, and M. Sasidharan. 2021. “Using probabilistic fault tree analysis and monte carlo simulation to examine the likelihood of risks associated with ballasted railway drainage failure.” Transp. Res. Rec., 2675 (6): 70–89. https://doi.org/10.1177/0361198120982310.

Vargas, R. V. 2010. “USING THE ANALYTIC HIERARCHY PROCESS (AHP) TO SELECT AND PRIORITIZE PROJECTS IN A PORTFOLIO.” PMI Glob. Congr. 2010, 1–22.

Wang, T., Z. Qu, Z. Yang, T. Nichol, D. Dimitriu, G. Clarke, D. Bowden, and P. T. Lee. 2020. “Impact analysis of climate change on rail systems for adaptation

planning: A UK case." Transp. Res. Part D Transp. Environ., 83 (April): 102324. Elsevier. https://doi.org/10.1016/j.trd.2020.102324.

Yang, D. Y., and D. M. Frangopol. 2020a. "Risk-based portfolio management of civil infrastructure assets under deep uncertainties associated with climate change: a robust optimisation approach." Struct. Infrastruct. Eng., 16 (4): 531–546. Taylor & Francis. https://doi.org/10.1080/15732479.2019.1639776.

Yang, D. Y., and D. M. Frangopol. 2020b. "Life-cycle management of deteriorating bridge networks with network-level risk bounds and system reliability analysis." Struct. Saf., 83 (January): 101911. Elsevier. https://doi.org/10.1016/j.strusafe.2019.101911.

Yavuz, F., U. Attanayake, and H. Aktan. 2017. "Economic impact on surrounding businessess due to Bridge Construction." Procedia Comput. Sci., 109 (C): 108–115.

Zebisch, M., S. Schneiderbauer, K. Renner, T. Below, M. Brossmann, W. Ederer, and S. Schwan. 2017. "Risk Supplement to the Vulnerability Sourcebook."

Zhu, B., and D. M. Frangopol. 2016. "Time-Dependent Risk Assessment of Bridges Based on Cumulative-Time Failure Probability." J. Bridg. Eng., 21 (12): 1–7. https://doi.org/10.1061/(ASCE)BE.1943-5592.0000977.

Chapter 6

CONCLUSION

6.1. SUMMARY

Climate change is the main drive for all extreme weather events occurring in the last decades, at an increasing frequency and magnitude. The report published by the IPCC in 2021 states that extreme rainfall events are expected to increase even further over the span of the upcoming decade (Herrmann et al. 2020). This thesis investigates the climate change impact on established communities and critical infrastructure networks in an effort to understand, quantify and predict their climate resilience. The thesis also attempts to enhance said climate resilience, by developing policies and resilience-informed risk management plans, especially in the face of the most prevalent risk caused directly by climate change— Flood risk.

For most of this thesis, data science and Machine Learning were utilized and developed to achieve the research goals and objective. In Chapter 2, the quantification of the communities' resilience was achieved by developing an unsupervised machine learning algorithm on a historical dataset containing features of the resilience goals (i.e., robustness and rapidity) and the overall impact of the hazard on the community, along with the community's response. These unsupervised machine learning models were developed and compared for the best-fit-model to decrease disparity between observations grouped into a single cluster. The resulting clusters were then investigated to draw their common features,

resulting in 5-categories system containing all the necessary information on how the different communities respond to their respective hazards. For Chapter 3, numerous supervised machine learning models were developed (i.e., predictive analytics) to introduce climate information onto the developed categories. The different models were tested with historical dataset, and their validity confirmed, paving the way for Chapter 4. In Chapter 4, global climate models were introduced to the prediction algorithm, this step successfully predicts the change in the resilience of the communities' features and responses to climate change induced hazard into the year 2050, acting as a vital step in the development of resilience-informed management plans and policies. To continue the investigation of the impact of climate change induced flood hazard onto the critical infrastructure systems and the established communities, Chapter 5 takes a closer look at the climate resilience of individual critical infrastructure networks to assess its climate resilience. The chapter investigates and evaluates the current practice and methodologies for evaluating the scour risk resulting from the increased climate-change related flood hazards. Specific conclusions, results, and recommendations for future work are presented in the following sections.

6.2. CONTRIBUTIONS AND CONCLUSION

Chapter 2

This chapter provides a summary on community resilience, starting by defining resilience within the context of this thesis, identifying it by the two resilience goals (i.e., *Robustness and Rapidity*), and the two means of resilience to achieve said goals (i.e., *Rapidity and Redundancy*). The chapter then aims at achieving the following: 1) quantify the resilience of the exposed communities by developing a categorization framework, using unbiased unsupervised Machine Learning algorithms that explain different aspects of resilience of the community, 2) utilize this categorization to identify vulnerabilities by developing a comparative spatial analysis, 3) identify the validity of the framework by testing it using real-life data in the development of the indices. The framework developed in Chapter 2 is then applied on the historical disaster dataset developed by the National Weather Service (NWS), a subagency under National Oceanic and Atmospheric Association (NOAA). Three unsupervised ML models were developed, namely: K-means clustering, Self Organizing Maps – Artificial Neural Networks, and Model-Based Clustering technique, where their results compared, and the model with the best variability and diversity was selected.

The model resulted in a 5-category system, identifying the unique features of how each community responds to its corresponding respective hazards, enabling the identification of vulnerabilities within specific communities by applying a comparative spatial analysis. This analysis was applied at the United States mainland states, aggregated to a state-level resolution by calculating the cumulative average index (i.e., category) for each state. Depending on the scale and resolution of the study, the users can identify the vulnerabilities at all scales now that an unbiased categorization framework is developed, acting as a decision support tool for stakeholders to allocate their resources. In this study, the comparative analysis identified the state of Oregon as the state with the highest resilience index value (translating to a lower resilience), identifying it as the most vulnerable state in terms of flood impact on their established community, and how they respond to said hazards.

Chapter 3

In Chapter 3, we introduced the concept of introducing climate information to the developed indices for the development of a prediction framework. This study builds on the results of the categorization used in Chapter 2, where these indices were used and coupled with historical climate information from the year 1996 to the end of 2019. The climate information dataset was synchronized with the

historical disaster dataset, such that each data point would contain the resilience category as the independent variable, and the climate information as the independent variables for this datapoint. The state of Texas was chosen as the test location for the application of the developed framework, where Texas had the largest number of recorded flood events (datapoints) and suffered the most cumulative monetary damage compared to the other states, making it a better choice for the application of the data-driven framework than the state of Oregon, given its much larger number of recorded flood events, despite its relative higher flood resilience.

Numerous supervised ML models were developed in this study in order to compare their predictive output, namely: Random Forest with 300 trees, Random Forest with 1000 trees, Bagged Decision trees, and Naïve Bayes Classification. The predictive capability of these developed algorithms, while varying in their capabilities, all resulted in comparable predictive accuracy, and to objectively assess their performances, the Precision, Recall, and F1-score were used to test the performance of all the employed models. To that end, the Bagged Decision trees were the model with highest overall performance.

Chapter 4

Chapter 4 builds on the frameworks presented in Chapters 2 and 3, by incorporating climate change impact with the developed resilience indices. The study presented in chapter 4 employs GCMs for different emission scenarios in 45 different locations within the state of Texas. The chosen spatial resolution was county based, where 16 GCMs were used for each emission scenario, for each of the test locations selected in the study. The GCMs are a result of the CMIP 5 project, where the scenarios under consideration are RCP 6.0 and RCP 8.5. The study also used multiple interpretability techniques to draw relations between the input-outputs of the ML models, in an effort to understand how each variables interact and influence one another. The study concluded that the Temperature (whether daily maximum or minimum) are the most influential over the increase in resilience index (i.e., increase vulnerability), that the windspeed is most impactful around the 6 m/s speed, while its impact on the resilience decreases as the speed increases, and finally, that beyond the 200 mm threshold, precipitation ceases to have an impact on the overall increase of resilience index of the community under consideration.

The prediction algorithm developed a spatiotemporal analysis into the resilience (represented by the index of each location) up until the year 2050,

identifying the expected losses (monetary and otherwise) from climate change-induced flood hazards, and the current state of the community under consideration. These results act as an employable decision support tool for policy holders and decision makers, where it aids in the allocation of resources within their areas of increased predicted vulnerability, ultimately mitigating the effect of climate change on their assets, saving millions of dollars of taxpayers' money, and improve the quality of life for their residents.

Chapter 5

Chapter 5 takes the concept of climate resilience a step further, by focusing its lens on a single critical infrastructure network. In this case, that network is transport network, with a focus on Railway Bridges subjected to climate-induced scour risk. This chapter introduces a high-order multi-layer framework that accounts for different factors, albeit interdependent factors, that contribute to the formation of scour. This chapter works at enhancing the asset management process for infrastructure asset owners and decision makers by developing a resilience-informed strategic risk assessment step within the asset management cycle. In this step, a comprehensive scour risk score for prioritization of assets is developed, but instead of revamping the whole process, the proposed approach builds upon the existing methodologies and strategies set in place by adding more layers to it. The

study introduces more factors into calculating the scour risk score that account for: Geological information, Climate Change and the subsequent flood risk, Hydrological features of water action, and Structural properties of the asset. The study also tests the proposed framework by applying it on all railway bridges in southeast England, in particular, in the counties of Essex, Wessex, and Kent.

The study herein identifies that 62% of the bridges in that area are actually in higher risk than originally determined, with a maximum increase of 19% in risk score, while most of these bridges changed priority from Medium to High priority. This study highlights the importance of the proposed framework, highlighting the need for incorporating climate-resilience within the asset management cycles, along with more information pertaining to the geological properties of riverbed materials, and how they are affected by climate change.

6.3. RECOMMENDATIONS FOR FUTURE RESEARCH

The different chapters in this thesis fall under the umbrella of enhancing community climate resilience, whether through the community as a whole with all its components, or by focusing on the individual critical infrastructure networks. To that end, the study developed, tested, and operationalized multiple frameworks for enhancing communities at multiple levels, quantifying and predicting the community's response to the imposed hazards, and enhance the strategic

management and decision making of the stakeholders and asset owners. However, the following are the limitations, and recommendations for future work to take this research a step further:

- More variables are desirable to be included in the categorization application presented in Chapter 2, where the authors were limited with the available datasets. Should the research community take this framework a step further towards realizing the overarching goal of developing a decision making tool, the dataset used in the development of the unsupervised learning process needs to be comprehensive enough, with more variables pertaining to the socio-economic features of the community (i.e., demographic features of the residents of each community, a more comprehensive recovery time from the moment of failure, more socio-economic information on the indirect losses and impact of the imposed hazard)
- The unsupervised models developed in Chapter 2 can also be further built upon by investigating the use of other data-transformation techniques to unify the data types used in the study, or explore more unsupervised ML models that have better capabilities to deal with mixed-type datasets.
- In Chapter 3, the study was limited to the available climate information, and it is recommended that more variables are to be included in the application

of the developed framework. These variables may include: wind speed, humidity, air pressure, etc.

- The supervised models developed in Chapter 3 can also be further improved by exploring the employability of different ML models on mixed type datasets, and creating larger ensemble models to enhance the overall accuracy of the predictive model.
- The methodology adopted in Chapter 4 can be further developed into a global prediction algorithm, gathering data from all possible locations within a specific test area, whether a full state or a full country, and acts as an early warning system, and ultimately, can be developed into a comprehensive management system for the built environment.
- In Chapter 5, the framework can be adjusted to account for a probabilistic analysis on the formation of scour by utilizing flood fragilities, along with different bridge-related information.
- The study in Chapter 5 can also be further developed with future flood projections (i.e., projected flood risk maps) when such data become available.

6.4. REFERENCES

Herrmann, M., T. Ngo-Duc, and L. Trinh-Tuan. 2020. *Impact of climate change on*

sea surface wind in Southeast Asia, from climatological average to extreme events: results from a dynamical downscaling. *Clim. Dyn.* Springer Berlin Heidelberg.

6.5. ACRONYMS

CMIP	Coupled Model Intercomparison Project
GCMs	Global Climate Models
ML	Machine Learning
NOAA	National Oceanic and Atmospheric Administration
NWS	National Weather Service
RF	Random Forest